OPTIMAL DESIGNS FOR LINEAR AND NONLINEAR PRECODERS AND DECODERS

LI NAN

NATIONAL UNIVERSITY OF SINGAPORE

2006

OPTIMAL DESIGNS FOR LINEAR AND NONLINEAR PRECODERS AND DECODERS

LI NAN

(*B.Eng., Dalian University of Technology, China*)

A THESIS SUBMITTED

FOR THE DEGREE OF MASTER OF ENGINEERING

DEPARTMENT OF ELECTRICAL AND COMPUTER ENGINEERING

NATIONAL UNIVERSITY OF SINGAPORE

2006

Acknowledgment

I must thank my family for all their support, love and care, without which I can never survive.

I would like to express my warmest thanks to those who have consistently been helping me with my research work.

I am grateful to my supervisors, Dr. Abdul Rahim Bin Leyman and Dr. Cheok Adrian David, for their encouragement, support and valuable advice on my research work, all along the way of improving both my skills in research and my attitude to overcome problems. I also would like to express my gratitude to those professors and lecturers who have taught me for their constructive suggestions to my study.

Last but not least, I want to thank sincerely all my colleagues and friends in I^2R for having provided such a great environment to work in.

Contents

List of Figures

List of Tables

Abbreviations

ADSL	Asymmetric Digital Subscriber Line
BPSK	Binary Phase Shift Keying
CDMA	Code Division Multiple Access
CP	Cyclic Prefixed
CSI	Channel State Information
DFE	Decision-Feedback Equalizer
DFT	Discrete Fourier Transform
DMT	Discrete Multitone Modulation
FBF	Feedback Filter
FDD	Frequency Division Duplexing
FFF	Feed-Forward Filter
FIR	Finite Impulse Response
GMSE	Geometric Mean-Squared Error
GPRS	General Packet Radio Service
GSM	Global System Mobile
HDSL	High-bit-rate Digital Subscriber Line
IBI	Interblock Interference
ISP	Internet Service Provider

ISI Intersymbol Interference

LTE Linear Transversal Equalizer

MBER Minimum Bit Error Rate

MIMO Multiple Input Multiple Output

MIR Maximum Information Rate

MMSE Minimum Mean-Squared Error

NADC North American Digital Cellular

OFDM Orthogonal Frequency Division Multiplexing

PDC Pacific Digital Cellular

QPSK Quadrature Phase Shift Keying

SISO Single-Input Single-Output

SNR Signal-to-Noise Ratio

SVD Singular Value Decomposition

TDD Time Division Duplexing

TDMA Time Division Multiple Access

ZF Zero-Forcing

ZP Zero Padding

Summary

Channel precoding and decoding is a new paradigm that is introduced during recent years. It is used to shape the transmitted signal and to introduce the redundancy in order to eliminate the intersymbol interference. In this thesis, we present several linear and nonlinear optimal designs for precoders and decoders.

A lot of research work has been done for designing better performance precoder/decoder pair. Such as minimizing the mean-squared error, maximizing the information rate, minimizing the bit error rate and so on. In this thesis, we introduce a new criterion named weighted information rate criterion for our linear design. This criterion is a generalization of the optimal linear precoder and decoder design. By choosing corresponding weight matrix, we can obtain maximum information rate (MIR) design, minimum mean-squared error (MMSE) design and QoS based design.

For the DFE-based nonlinear precoder and decoder design, we firstly design a precoder which can maximize the information rate, then on the basis of this design, we further improve it by trying to minimize the bit

error rate (MBER) and maximize the information rate together. We are using Lagrangian optimizing method to make the eigenvectors of the precoder matrix match to the eigenvectors of the circulant channel matrix in order to maximize the information rate. And we use discrete fourier transform (DFT) matrix to ensure that the average bit error rate is a convex function and has the minimum value, so by adopting MMSE criterion we can achieve that minimum value. Therefore, the optimal design is obtained.

Various simulation results prove the improvements of our linear and nonlinear optimal precoders and decoders designs. For linear weighted information rate criterion, the results show that we can achieve different kind of designs by choosing the weight matrix properly. The MIR design maximizes the information rate. The MMSE design obtains optimum performance of MSE and the QoS based design allows us to transmit different signals under different subchannel SNR requirements. For DFE-based nonlinear designs, the improvement of the information rate of our MMER-DFE design over the MMSE-DFE design is considerable. Also, our MBER-DFE design always has better BER performance, regardless of the channel frequency selectivity. And the more frequency selective the channel performed, the more obvious the SNR gain we observed of MBER-DFE design.

Chapter 1

Introduction

1.1 Trends on Wireless Communications

Wireless communications is now undergoing its fastest growth period in history. The emergence of wireless cellular communication systems brings about an exciting revolution to the wireless industry in terms of both technologies and applications. The number of worldwide cellular telephone subscribers has exceeded 600 million in late 2001 [1] and the total number of worldwide subscribers to wireless cellular services will exceed 2 billion by 2007, according to a new report from In-Stat/MDR. Most of today's ubiquitous cellular networks use the second generation (2G) technologies which comform to the second generation cellular standards. Unlike the first generation cellular systems that adopted Frequency Division Multiple Access (FDMA), Frequency Division Duplexing (FDD) and analog FM, 2G stan-

dards rely on digital modulation formats and Time Division Multiple Access (TDMA)/FDD and Code Division Multiple Access (CDMA)/FDD multiple access techniques.

Global System Mobile (GSM), North American Digital Cellular (NADC), Pacific Digital Cellular (PDC) and Interim Standard 95 Code Division Multiple Access (IS-95) are four of the 2G standards which are used popularly. GSM supports eight time slotted users for each 200 kHz radio channel. NADC supports three time slotted users for each 30 kHz radio channel while PDC is similar to NADC. IS-95 supports up to 64 users that are orthogonally coded and simultaneously transmitted on each 1.25 MHz channel and is also known as cdmaOne [1].

In order to improve the 2G standards for compatibility with increased throughput data rates on demand, new standards have been developed that can be overlaid upon existing 2G technologies. These new standards are known as the 2.5G technologies. 2.5G systems, such as GPRS, which is a radio technology for GSM networks, boasts of many new features. For instance, it adds packet-switching protocols and requires shorter set-up time for ISP connections, and can even provide up to about 100 Kbps data rate. Many commercial GPRS systems were deployed worldwide at the end of 1990s. Also, IS-95B is an upgrade of IS-95, which can provide high-speed packet and circuit switched data access on a common CDMA radio channel.

At the end of 1990s, the third generation (3G) cellular communication systems were finalized to provide better data service. 3G system allows unparalleled wireless access in ways that have never been possible before.

There are two major 3G technology standards: CDMA2000 and Wideband CDMA (W-CDMA). CDMA2000 are based on the fundamentals of IS-95 and IS-95B technologies and has several variants. W-CDMA is based on the fundamentals of GSM and assures backward compatibility with the second generation GSM. The network structure and bit level packaging of GSM data is retained by W-CDMA, with additional capacity and bandwidth provided by a new CDMA air interface.

Although 3G technologies have improved significantly over the years, it is still inferior in many years, compared to the fixed wire line Internet connection. Most Local Area Networks (LAN) in campus/office support 100 Mbps data rate at very low costs. For high data rate transmission, conventional cellular communication systems are uneconomical since they have to pay attention to covering wide areas, supporting highly mobile users and providing seamless handover. Wireless LAN was hence proposed to address this problem. Compared to cellular communication systems, a wireless LAN cell covers up to several hundreds meters [1], the range of a hot spot, and supports 10 Mbps to 50 Mbps data rate for each user. Currently, the most popular wireless LAN standard is 802.11b, which can support up to 10 Mbps data rate and has been installed at some hot spots, such as airports, hotels, and campus.

At the same time, other wireless technologies are also under intensive study and some are rapidly becoming pervasive in our everyday life. For instance, Bluetooth, Wireless Personal Area Networks (802.15) and Fixed Broadband Wireless Access Standards (802.16).

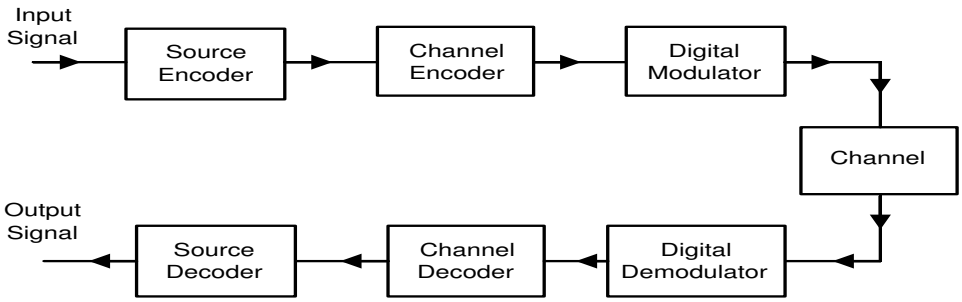

Figure 1.1: Basic Elements of a Digital Communication System

High data transmission rates, low bit error rates over different kinds of wireless channels within the limited radio spectrum are just some of the pre-requisites of the wireless industry today. The need to achieve these requirements, has driven researchers to look for better communication and signal processing technologies. Some techniques, such as modulation, equalization, diversity and coding have been extensively studied during the past decades.

Figure 1.1 shows the basic elements of a digital communication system. Modulation is the process of encoding information from a message source in a manner suitable for transmission. It is generally concerned of translating the baseband message signal to a bandpass signal whose frequencies are very high when compared to the baseband frequency. The baseband message signal is called the modulating signal and the bandpass signal is called the modulated signal. Modulation techniques can be further divided into frequency modulation, amplitude modulation and phase modulation. Frequency modulation is the most popular analog modulation technique used in mobile radio systems. It has better noise immunity and works more ef-

ficiently when compared to amplitude modulation. But it requires a wider frequency band and the equipments used for transmitting and receiving are more complex.

Diversity is another communication technique which is used to compensate for fading channel impairments. It improves the quality of a wireless communications link without increasing the transmitted power or bandwidth. Diversity techniques are often employed at both base station and mobile receivers. The most common diversity technique is spatial diversity. Other diversity techniques include frequency diversity and time diversity.

More recently, linear and nonlinear precoding and decoding techniques have become popular research areas because of their simple closed-form solutions for transmission over frequency-selective multiple-input multiple-output channels. We use precoders and decoders to minimize the bit error rate and eliminate the inter-symbol interferences and they can protect digital data from errors by selectively introducing redundancies in the transmitted data.

In the next section, I will first introduce the fundamentals of channel coding and equalization techniques, followed by a discussion of the research on channel precoding technique. Finally, I will put forth the optimal designs of linear and nonlinear precoders and decoders, and issues on the criterions used in the designs.

1.2 Channel Coding, Equalization and Precoding Techniques

1.2.1 Channel Coding

The channel encoder is a discrete-input, discrete-output device whose usual purpose is seen as providing some error-correction capability for the system [2]. It does this by using a mapping from input sequences to code sequences, which inserts redundancy and utilizes memory. This means that the process of channel coding produces modulator input symbols that are interrelated, introducing a crucial aspect of memory into the signaling process. At the same time, a controlled redundancy is introduced. It is well known [2] that redundancy introduced in the transmitter of a communication system may allow us to overcome serious intersymbol interference (ISI) problems due to highly dispersive channels. The channel decoder exploits the redundancy to decide which message bit was actually transmitted. The reasons for adopting coding are, widely speaking, to achieve highly reliable communication at rates approaching the channel capacity limit defined by the physical channel. Channel coding is useful in virtually every kind of noisy channel transmission problem; some still regard its principal area of application as the unlimited-bandwidth channel, but recently major contributions to practical communications have been made by intelligent coding for band-limited channels. Coding also offers particularly impressive gains on fading and time-varying interference channels. Channel codes that are used

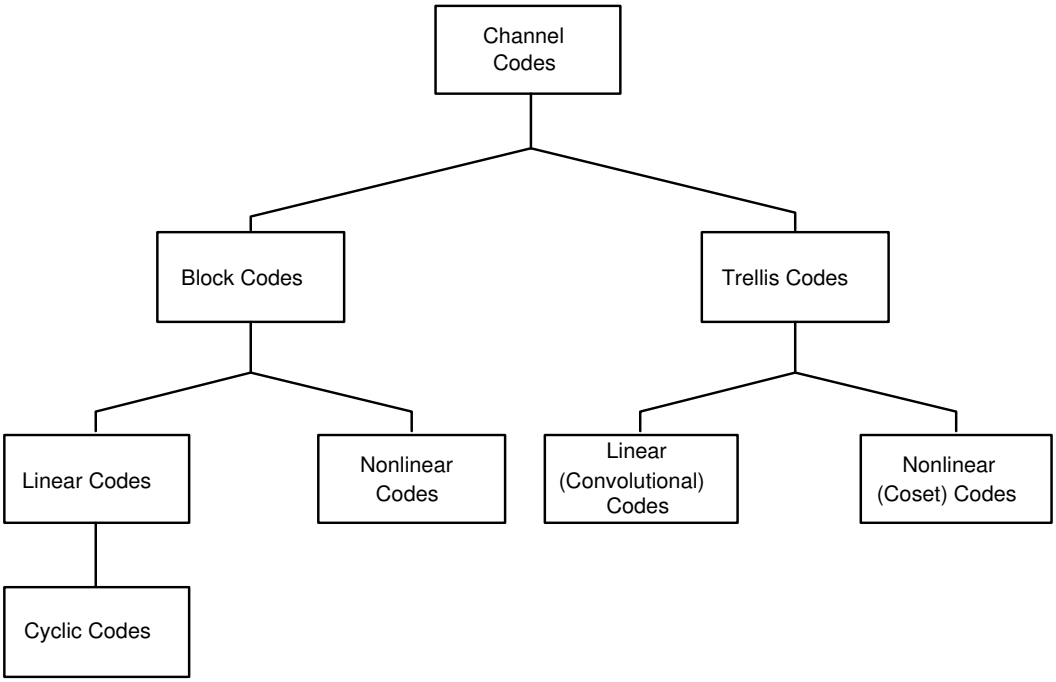

Figure 1.2: Classification of Channel Coding Techniques

to detect errors are called error detection codes, while codes that can detect and correct errors are called error correction codes. The basic purpose of error detection and error correction techniques is to introduce redundancies in the data to improve wireless link performance. The introduction of redundant bits increases the raw data rate used in the link, hence, it increases the bandwidth requirement for a fixed source data rate. This reduces the bandwidth efficiency of the link in high SNR conditions, but provides excellent BER performance at low SNR values. Figure 1.2 [2] shows the classification of channel coding techniques. It is classified based on the structure behind the encoding function, that is, the relation between message symbols and modulator inputs.

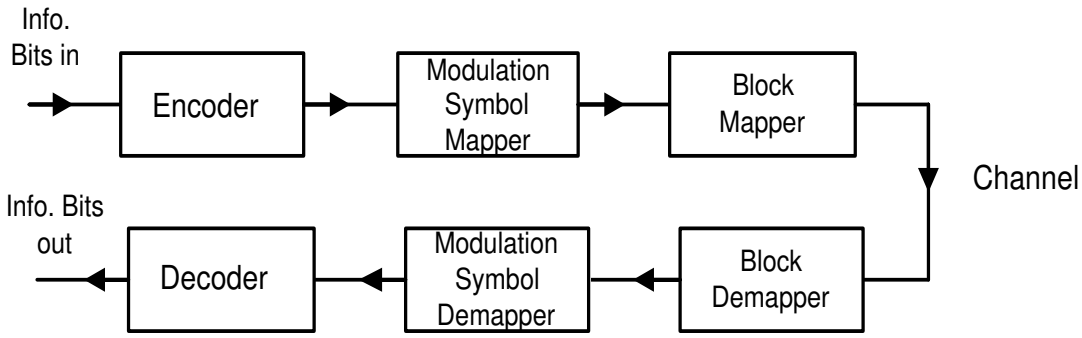

Figure 1.3: Block Coding

1.2.1.1 Block Codes

Figure 1.3 shows a diagram of block coding. Block codes operate in block-by-block manner and each codeword depends only on the current input message block. It may be further categorized as linear and nonlinear codes. Linear block codes are defined by linear mapping from the space of input messages to the space of output messages, and it is ultimately represented by a matrix multiplication. Linear block codes are also known as parity check codes because we can view the codeword as comprised of a message component and parity symbols. The linear block codes are in a more restricted class known as cyclic codes, or at least codes closely related to cyclic codes which are a subset of the class of linear codes that satisfy the cyclic shift property.

The encoder for a block code accepts blocks of k input symbols and produces blocks of n output symbols which is called code word by multiplying a generator matrix. We can create a generator matrix that generate an equivalent code if we permute any rows of the generator matrix and replace

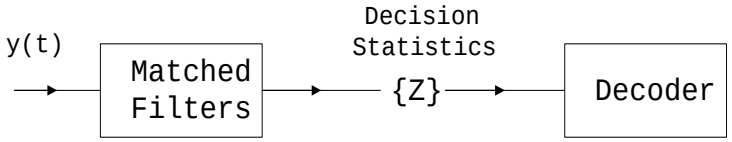

Figure 1.4: Soft Decision

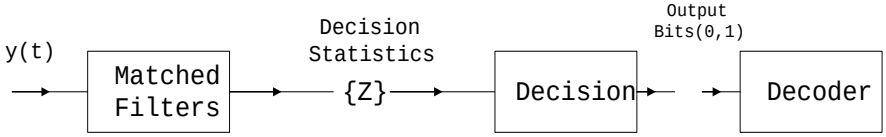

Figure 1.5: Hard Decision

any row of it by a linearly independent combination of rows.

There are two kinds of decoding, one is soft-decision decoding, the other is hard-decision decoding. Soft-decision decoder operates directly on the decision statistics (see Figure 1.4) and hard-decision decoder makes "hard" decisions (0 or 1) on individual bits (see Figure 1.5). In the decoding of a block code for a memoryless channel, we compute the Hamming distance for hard-decision decoding and Euclidean distance for soft-decision decoding between the received code word and all possible code words. Then we select the code word which is closest in distance to the received code word.

The major classes of block codes are: repetition codes, Hamming codes, Golay codes, BCH codes, Reed-Solomon codes, Walsh codes, etc. And these kinds of block codes are widely used in systems, for example, the IS-95 standard employs a rate (64,6) orthogonal code on the reverse link; proposed ETSI standard employs RS codes concatenated with convolutional codes for data communications.

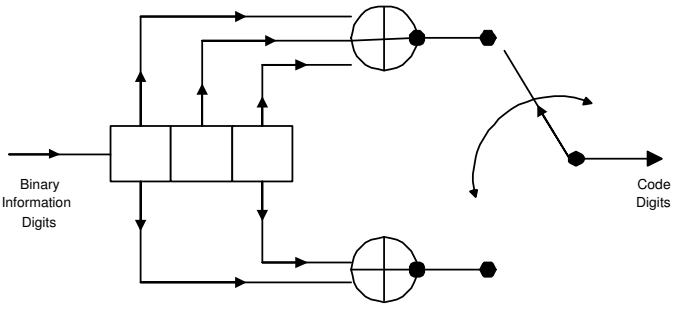

Figure 1.6: Trellis Encoder

1.2.1.2 Trellis Codes

Figure 1.6 shows the typical structure of a trellis encoder. The rectangular box represents one element of a serial register. The content of the shift registers is shifted from left to right. Plus sign represents modulo-2 addition. Trellis codes should be regarded as mapping an arbitrarily long input message sequence to an arbitrarily long code stream without block structure. The reason why we call it trellis codes is because the codewords may be identified with a regular, directed finite-state graph reminiscent of a garden trellis. Trellis codes are also composed of linear codes and nonlinear codes. Linear trellis codes are known as convolutional codes because the original codes were linear mappings from input to output sequences obtained by a discrete-time, finite-alphabet convolution of the input with an encoder's impulse response.

Unlike the block code, optimum decoding of a convolutional code involves a search through the trellis for the most probable sequence. Depending on whether the hard-decision or soft-decision is employed, the corresponding metric in the trellis search may be either a Hamming metric or Euclidean

metric, respectively. The Viterbi algorithm is an optimum decoding method of convolutional codes. It can be used for either hard or soft decision decoding and it is a clever way of implementing maximum likelihood decoding. Convolutional codes are encoded using a finite state machine and the optimal decoder for convolutional codes will find the path through the trellis, which lies at the shortest distance to the received signal.

Convolutional codes are useful for real-time applications because they can be continuously encoded and decoded. We can represent convolutional codes as generators, block diagrams, state diagrams and trellis diagrams.

Also, the convolutional codes are widely used in practice. NASA uses a standard $r = 1/2, K = 7$ convolutional code. IS-54/136 TDMA Cellular Standard uses a $r = 1/2, K = 6$ convolutional code. GSM Cellular Standard uses a $r = 1/2, K = 5$ convolutional code. IS-95 CDMA Cellular Standard uses a $r = 1/2, K = 9$ convolutional code for forward channel and a $r = 1/3, K = 9$ convolutional code for reverse channel.

Both block codes and trellis codes have had their own advocates during these years and both of them have their own advantages in certain applications. For example, most space-time block codes do not provide coding gain. Their key feature is the provision of full diversity with extremely low encoder/decoder complexity. Whereas, space-time trellis codes provide full diversity gain, their key advantage over space-time block codes is the provision of coding gain. Their disadvantage is that they are extremely difficult to design and require a computationally intensive encoder and decoder.

1.2.2 Channel Equalization

Equalization compensates for intersymbol interference (ISI) created by multipath within time dispersive channels. An equalizer within a receiver compensates for the average range of expected channel amplitude and delay characteristics. Equalizer must be adaptive since the channel is generally unknown and time varying. ISI distorts the transmitted signal, resulting in bit errors at the receiver. It has been considered as the major barrier to high speed data transmission over wireless channels. Equalization is one such technique that is used to overcome ISI. Widely speaking, equalization can be used to describe and explain any signal processing operation that minimizes ISI. In a random and time varying channel, equalizers must track the time varying characteristics of the mobile channels, and thus are called adaptive equalizers.

The timespan over which an equalizer converges is a function of the equalizer algorithm, the equalizer structure and the time rate of change of the multipath radio channel. An equalizer is usually implemented at baseband in a receiver, because the baseband complex envelope expression can be used to represent bandpass waveforms.

As can be seen from Figure 1.7, equalization techniques can be divided into two general categories, linear and nonlinear equalizations [1]. These two categories determine how the output of an adaptive equalizer is used for subsequent control of the equalizer. Linear transversal equalizer (LTE) is the most ordinary form of equalizer structure. A linear transversal filter is made up of tapped delay lines, with the tappings spaced a symbol period

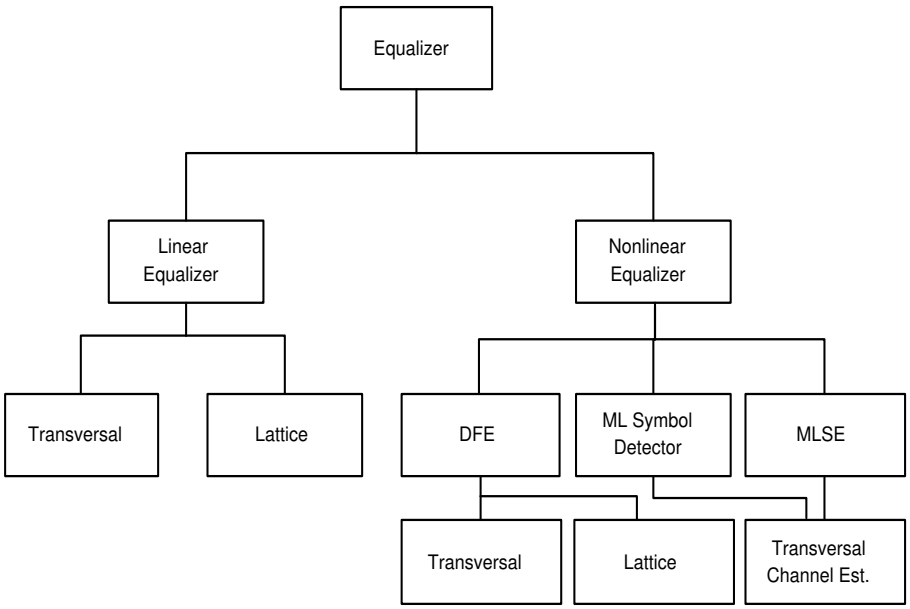

Figure 1.7: Classification of Equalizers

apart. A linear equalizer can be implemented as an FIR filter, otherwise known as the transversal filter. Nonlinear equalizers are used in applications where the channel distortion is too severe for a linear equalizer to handle and are commonplace in practical wireless systems. There are three effective nonlinear methods that have been developed which offer improvements over linear equalization techniques and are used in most 2G and 3G systems [11].

1. Decision Feedback Equalization (DFE)
2. Maximum Likelihood Symbol Detection
3. Maximum Likelihood Sequence Estimation (MLSE)

The basic notion behind DFE is that once an information symbol has been detected and decided upon, the ISI that induces on future symbols can be estimated and subtracted out before detection of subsequent symbols

[21]. The DFE consists of a feed-forward filter (FFF) and a feedback filter (FBF). The FBF is driven by decisions on the output of the detector, and its coefficients can be adjusted to cancel the ISI on the current symbol from past detected symbols. DFE is nonlinear because the FBF contains d_k, which is the previous decision made on the detected signal.(See Figure 1.8) The equalizer has $N_1 + N_2 + 1$ taps in the feed-forward filter and N_3 taps in the feedback filter, and its output can be expressed as:

$$\hat{d_k} = \sum_{n=-N_1}^{N_2} c_n^* y_{k-n} + \sum_{i=1}^{N_3} F_i d_{k-i} \tag{1.1}$$

where c_n^* and y_n are tap gains and the inputs, respectively, to the forward filter, F_i^* are tap gains for the feedback filter, and $d_i (i < k)$ is the previous decision made on the detected signal. It means, once $\hat{d_k}$ is obtained from Eqn.(1.1), d_k is confirmed from it. Then d_k along with previous decisions $d_{k-1}, d_{k-2}, ...$ are fed back into the equalizer and then $\hat{d}_{k+1}$ is obtained using Eqn.(1.1) again. Figure 1.8 shows the direct form of DFE. Both the peak distortion criterion and the MSE criterion result in a mathematically tractable optimization of the equalizer coefficients.

1.2.3 Channel Precoding

During the recent years, a new paradigm for the design of space-time coding that is referred as precoding is being introduced. The process of shaping the transmit signal and/or introducing redundancy based on the knowledge of the channel is known as precoding, while the reverse process

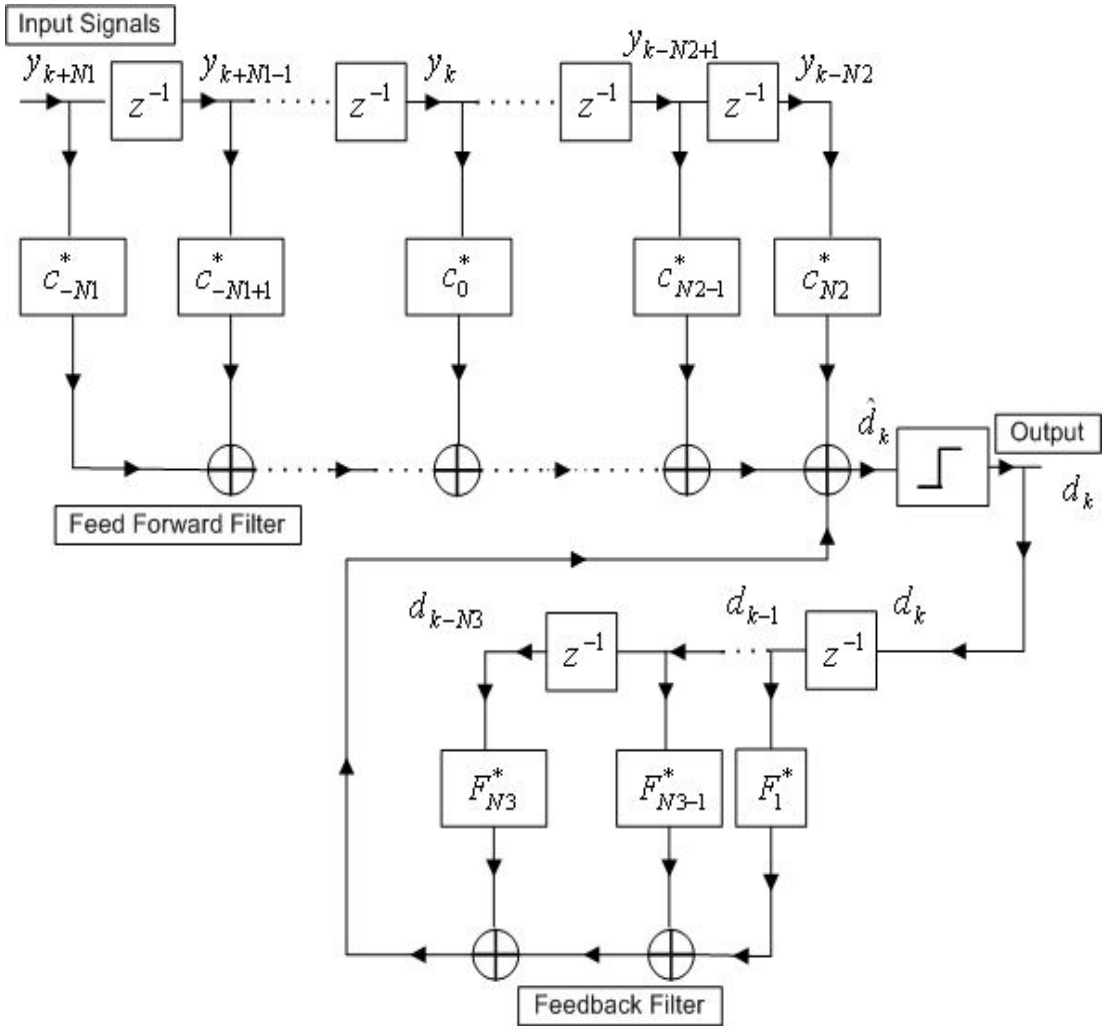

Figure 1.8: Decision Feedback Equalizer (DFE)

is called decoding. Precoding technique is used just before the transmitted symbols pass through the channel and that's why we call it ***pre***coding.

Both channel coding and precoding are used to introduce redundancies in order to improve the rate of information transfer and detect or correct the errors. However, they carry the same point by adopting different methods. Channel coding uses different kind of code words to add redundancies which has been mentioned in the previous section and channel precoding technique uses different pairs of precoder and decoder matrices which are more intuitionistic and convenient to compute and handle. Comparing with channel coding, the main advantage of using precoding technique is that the impairment of ISI due to multipath propagation on the transmission performance can be mitigated without increasing the complexity of the receiver. In addition, channel precoding can lead to simple closed-form solutions for transmission which are scalable with respect to the number of antennas, size of the coding block and transmit average/peak power. The scheme operates as a block transmission system in which vectors of symbols are encoded and modulated through a linear or nonlinear mapping operating jointly in the space and time dimension. In order to achieve the high information rate, we need proper precoding and modulation techniques. Orthogonal frequency division multiplexing (OFDM) system [4] [9] and discrete multitone modulation (DMT) [5] [8] are two modulation schemes that are widely used. OFDM has been selected as the standard modulation scheme for terrestrial digital audio and video broadcasting in Europe. DMT has been adopted for high-bit-rate digital subscriber line (HDSL) and asymmetric digital subscriber line

(ADSL) systems. Lately, a new linear block-by-block transmission scheme, which includes OFDM and DMT as special cases, has been studied in [10], [6] and [12]. The precoding techniques are divided into two main approaches. The first one without knowing the channel state information (CSI), maps the information symbols in space and time at the transmitter and with low complexity at the receiver to obtain full diversity gains [13], [17], [14], [25]. The second one assumes CSI is available at both the transmitter and the receiver sides and illuminates the optimization of the information rate in the case of flat fading [15], [29], [16] and frequency-selective channels [18], [20].

Precoding leads to simple closed-form solutions for transmission over multiple-input multiple-output (MIMO) channels. The solutions are shown to convert the frequency selective MIMO channel into a set of parallel flat fading subchannels.

Designs of the block transceivers, which are optimal in the sense of maximum information rate, minimum mean-squared error (MMSE) or minimum bit error rate (MBER), have been of great interest recently. The purpose of adopting block transmission is to transmit data in the way of block-by-block and to eliminate the interference between the blocks. We have already known that OFDM and DMT are two prevalent illustrations of block transmission.

Linear and nonlinear precoders and decoders make good use of block-by-block transmission. Linear precoder/decoder such as zero-forcing (ZF) and minimum mean-squared error (MMSE) precoder/decoder are easy to implement as compared to nonlinear schemes. However, results have established that nonlinear precoder/decoder such as zero-forcing decision-feedback

equalizer (ZF-DFE) and MMSE decision-feedback equalizer (MMSE-DFE) have better BER performance [32]. In [33] Al-Dhahir and Cioffi derived a quasi-stationary approximation to the optimal nonstationary input covariance process and showed that by properly choosing the eigenvectors of the input symbols, the mutual information rate can be improved significantly. In linear schemes, maximizing information rate has been extensively studied. In [7] Scaglione studied the use of filterbank transceivers to optimize the information rate over dispersive channel. The same technique and theory as in [33] were adopted by Dhahir and Cioffi. In addition, they developed two loading algorithms to distribute transmit power and number of bits across the usable subchannels. With the aim of maximizing the information rate, the ZF and MMSE receiver filterbanks were derived, and the purposed transceivers outperform DMT for small-size blocks transmitted through highly frequency selective channels.

Also, minimizing the mean-squared error (MSE) is another aspect of research. [27] presented MMSE designs for linear precoders and decoders subject to transmit power constraint and maximum eigenvalue constraint for MIMO transmission systems with finite memory. The solutions were to convert the MIMO channel with memory into a set of parallel flat fading subchannels. The channel was eigendecomposed in constructing the optimal precoder and decoder matrix and different kind of optimal precoder/decoder pair was obtained. Alfred Mertins in his work [28] studied the MMSE design of precoders under the condition of arbitrary channel lengths and yielded near-optimal solutions for the transmit filters. The proposed design method

considered the optimal receive filters for given transmit filters and channel, but during transmitter optimization, it used an approximation for simplifying the objective function. And it could be considered as an extension of the work in [10] from block transmission to overlapped block transmission.

Moreover, the design of minimizing the bit error rate becomes another popular research area recently. The works in [3] and [30] achieved the minimum bound of the bit error rate of zero-forcing equalizer and MMSE equalizer, respectively. Both of them obtained the cyclic prefixed minimum bit error rate (BER) precoder by replacing the diagonal water-filling power loading with a full matrix consisting of a diagonal minimum mean-squared error power loading matrix, and also were post-multiplied by a discrete Fourier transform (DFT) matrix. While in nonlinear schemes, Stamoulis in his paper [22] studied to minimize the geometric mean-squared error (GMSE) by joint optimizing both the transmit and receive filters in order to maximize the information rate because the information rate was a monotonic decreasing function of the GMSE. Two different conditions were studied. One was without inter-block interference (IBI) and the other was with IBI. The optimal DFE receivers were derived and it showed that the BER performance was better than that of the linear schemes. [23] converted the frequency fading channel into a set of independent flat fading subchannels and increased the information rate by using the transmit filterbank as precoder (pre-equalizer) and the receive DFE as the post-equalizer. The MMSE-DFE can perform significantly better than a ZF-DFE, particularly at moderate-to-low SNR's and on severe-ISI channels [31]. [19] studied the MMSE-DFE with different

selections of precoder matrix such as Hadamard precoder, OFDM precoder and optimum ZF precoder. In [19], Stamoulis derived closed form solutions for the FIR nonlinear decision-feedback receivers. The block channel estimation method was used to enable a self-recovering framework. Nevertheless, none of the existing papers have tried to maximize the information rate and at the same time minimize the bit error rate. Therefore, minimizing the bit error rate together with maximizing the information rate has become one of the major challenges and hence motivates us to do more research work in this area.

1.3 Motivation and Contribution of The Thesis

The demand for high data rate transmission contributes to the ceaseless research for optimizing the design of linear and nonlinear precoder and decoder. Ways of optimizing the information rate in linear schemes has been widely studied and the maximum information rate has been obtained. However, in nonlinear schemes, the maximum value of the information rate has not been completely acquired. In this thesis, we try to make use of the ideas, which are acquired from linear precoder design and apply them to maximize the information rate of nonlinear precoder/decoder pair by employing the Lagrangian method according to the transmit power constraint. In addition, we attempt to generalize the linear precoder and decoder designs for MIMO

channels using the weighted information rate criterion. By choosing different weight matrix of the information rate, we can obtain different kind of designs such as maximum information rate design, minimum mean-squared error (MMSE) design and QoS based design.

Since the precoding techniques are developing very fast, it is not sufficient to simply obtain the maximum information rate. While trying to maximize the information rate at the same moment, we also attempt to minimize the bit error rate (BER) in nonlinear schemes according to the MMSE criterion and simultaneously add Discrete Fourier Transform (DFT) matrices at both the transmitter and the receiver sides. Hence, our transceiver becomes a DFT-based transceiver. Therefore, all of these ensure that the bit error rates are being minimized and information rates are maximized. The SNR gain of our purposed design over other designs can be several decibels.

Therefore, the contributions of this thesis can be enumerated as follows:

First, we present a new criterion: weighted information rate criterion, which generalizes the optimal linear precoder and decoder designs.

Secondly, we present the maximum information rate design for nonlinear precoders and decoders. The transmission information rate is maximized by using Lagrangian method together with a matched precoder matrix.

Thirdly, we minimize the bit error rate and at the same time maximize the information rate for nonlinear precoders and decoders by using a matched precoder matrix together with a DFT matrix.

Comparing to those existing work, we manage to achieve various opti-

mal precoder and decoder designs through a different way, and also try to generalize these designs using uniform precoder and decoder equations. That is our weighted information rate design. Moreover, we notice that no work of nonlinear precoder and decoder has been done before, while in this thesis, we obtain the nonlinear designs of precoder and decoder which can maximize the information rate and minimize the bit error rate simultaneously. The simulation results show the performance of our designs.

1.4 Organization of The Thesis

The thesis is organized as follows:

Chapter 2 introduces the background preliminaries, including the transmission method that we will adopt in the thesis and some criterions of precoder and decoder design.

In Chapter 3, we show the linear precoder and decoder design. The system model is described. We also present the linear weighted information rate criterion; by choosing different weight matrix, we can obtain maximum information rate design, minimum mean-squared error design and QoS based design. This criterion generalizes different linear precoder and decoder applications.

Nonlinear precoder and decoder designs which can maximize the information rate and minimize the bit error rate are presented in Chapter 4. For the system model, we assume that the channel state information is available at both the transmitter and the receiver sides. This usually results in the

optimal solution for nonlinear precoder and decoder designs as they take advantage of the channel state information appropriately and utilize resources at their best while maintaining a reasonable complexity. We decompose the channel into several eigen subchannels and load the power on the subchannels appropriately. Then we try to maximize the information rate of nonlinear precoder/decoder. Towards the end, on the basis of maximizing the information rate, we move on to minimize the bit error rate and introduce our MBER-DFE design.

In Chapter 5, numerical results are presented to analyze the performance of our linear and nonlinear precoder and decoder designs. We conduct simulations and choose FIR channels with different tap coefficients to verify our analysis. The results show that we can generalize the linear optimal designs and for nonlinear scheme, we can both maximize the information rate and minimize the bit error rate at the same time.

Chapter 6 summarizes the whole thesis.

Chapter 2

Background Preliminaries

For transmissions over wireless dispersive media, channel induced inter-symbol interference (ISI) is a major performance limiting factor. To mitigate such a time-domain dispersive effect that gives rise to frequency selectivity, it has been proved useful to transmit the information-bearing chips in blocks. To eliminate the inter-block interference (IBI), it is necessary to use the cyclic prefixed (CP) transmission method to adopt in our work. In addition, zero padding (ZP) transmission method is an alternative way to get rid of IBI. In this chapter, we will introduce and review the basic principles of these two methods, then briefly present the works that have been done on CP and ZP, and make comparisons between them. We will also present a few optimal designs of precoders and decoders, such as minimum mean-squared error design, maximum output SNR design and maximum information rate design. The design criteria will be derived. The advantages and drawbacks

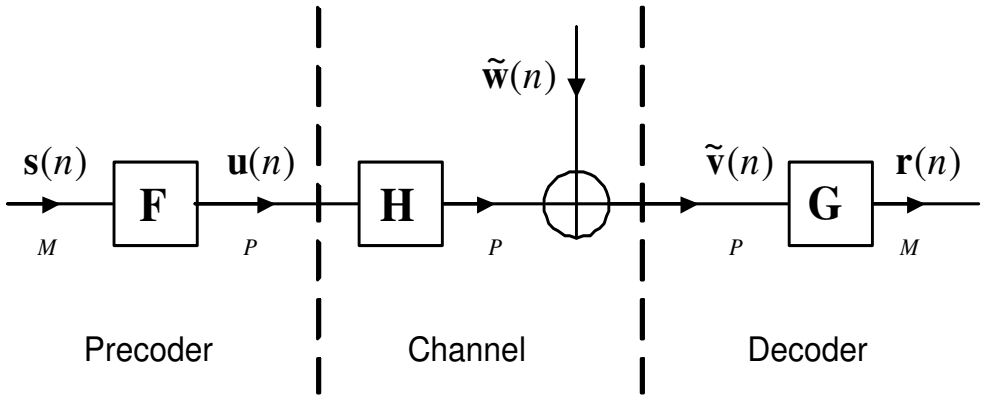

Figure 2.1: Block Transmission System Model

of these designs will be discussed and these discussions will be useful in the following chapters of the thesis.

2.1 Cyclic Prefixed and Zero Padding Transmission Method

2.1.1 Cyclic Prefixed

CP transmission method is a traditional method to ensure symbol recovery. It consists of redundant symbols replicated at the beginning of each transmitted block. To eliminate IBI, the redundant part of each block is chosen greater than the channel length and is discarded at the decoder side. The basic CP-based transmission system model is shown in the above Figure 2.1. $\mathbf{s}(n)$ denotes the n^{th} block of data that contains M data symbols to be transmitted, where $n = 0, 1, 2....$ The data is then transformed to form $\mathbf{u}(n)$

where the n^{th} transmitted block $\mathbf{u}(n)$ is now given as

$$\mathbf{u}(n) \triangleq [u(nP)\ u(nP+1)\ ...\ u(nP+P-1)]^T \triangleq \mathbf{Fs}(n) \tag{2.1}$$

where $\mathbf{F}$ is a $P \times M$ precoder matrix. P is the number of symbols that are transmitted across the channel. Redundancy is introduced in this transformation, where $P > M$ symbols are transmitted across the channel. This redundancy is key to eliminate IBI at the decoder side, as we will see later. At the decoder, the output $\mathbf{r}(n)$ can be written in vector form as

$$\mathbf{r}(n) = \mathbf{G} \sum_{l=-\infty}^{\infty} \mathbf{HFs}(n-l) + \mathbf{G}\tilde{\mathbf{w}}(n) \tag{2.2}$$

where $\tilde{\mathbf{w}}(n)$ denotes the additive noise. $\mathbf{G}$ is the $M \times P$ decoder matrix. The $P \times P$ matrix $\mathbf{H}$ is defined as

$$\mathbf{H} \triangleq \begin{bmatrix} h(lP) & h(lP-1) & \dots & h(lP-P+1) \\ h(lP+1) & h(lP) & \ddots & h(lP-P+2) \\ \vdots & \ddots & \ddots & \vdots \\ h(lP+P-1) & h(lP+P-2) & \dots & h(lP) \end{bmatrix} \tag{2.3}$$

Eqn.(2.2) can be simplified by the judicious choice of the block size and redundancy, as is well known in the special case of cyclic prefixed-based transceivers (see e.g., [12]). To state this formally, we define the following assumptions in order to set up the cyclic prefixed theory clearly and easily:

A1. The channel is an L^{th} order finite impulse response (FIR) channel with impulse response $h(n) = 0$, when $n < 0$ and $n > L$.

A2. The length of the block of transmitted symbols $P \geq M + L$ and $P > 2L$.

Therefore, invoking these two assumptions $A1$, $A2$ and Eqn.(2.3), Eqn.(2.2) can be obtained as

$$\mathbf{r}(n) = \mathbf{G}\mathbf{H}_0\mathbf{F}\mathbf{s}(n) + \mathbf{G}\mathbf{H}_{IBI}\mathbf{F}\mathbf{s}(n-1) + \mathbf{G}\tilde{\mathbf{w}}(n) \tag{2.4}$$

where $\mathbf{H}_0$ and $\mathbf{H}_{IBI}$ are $P \times P$ matrices and can be defined as follows, respectively.

$$\mathbf{H}_0 \stackrel{\triangle}{=} \begin{bmatrix} h(0) & 0 & 0 & \dots & 0 \\ \vdots & h(0) & 0 & \dots & 0 \\ h(L) & \dots & \ddots & \dots & \vdots \\ \vdots & \ddots & \dots & \dots & 0 \\ 0 & \dots & h(L) & \dots & h(0) \end{bmatrix} \tag{2.5}$$

$$\mathbf{H}_{IBI} \stackrel{\triangle}{=} \begin{bmatrix} 0 & \dots & h(L) & \dots & h(1) \\ \vdots & \ddots & 0 & \ddots & \vdots \\ 0 & \dots & \ddots & \dots & h(L) \\ \vdots & \vdots & \vdots & \ddots & \vdots \\ 0 & \dots & 0 & \dots & 0 \end{bmatrix} \tag{2.6}$$

From Eqn.(2.4) we can easily see that the interblock interference now only arises between successive blocks which is denoted by $\mathbf{G}\mathbf{H}_{IBI}\mathbf{F}\mathbf{s}(n-1)$, and IBI of the n^{th} block of received symbols now only comes from the previous

block. To understand this IBI, we can see from Eqn.(2.6) that $\mathbf{H}_{IBI}$ has nonzero elements only in its $L \times L$ top right submatrix. Therefore, it is shown in [30] that IBI can be eliminated, irrespective of the actual impulse response of the channel, if we impose a structure on $\mathbf{F}$ and $\mathbf{G}$ so that $\mathbf{G}\mathbf{H}_{IBI}\mathbf{F} = \mathbf{0}$.

We begin defining the decoder matrix $\mathbf{G}$ as

$$\mathbf{G} \stackrel{\triangle}{=} \mathbf{G}_{cp} = \begin{bmatrix} \mathbf{0}_{M\times L} & \mathbf{I}_{M\times M} \end{bmatrix}_{M\times P} \tag{2.7}$$

Since $\mathbf{H}_{IBI}$ has nonzero elements only in its $L \times L$ top right matrix, therefore, we can see $\mathbf{G}_{cp}\mathbf{H}_{IBI} = \mathbf{0}$ and thus $\mathbf{G}_{cp}\mathbf{H}_{IBI}\mathbf{F}\mathbf{s}(n-1)$ becomes zero. Hence the IBI is eliminated and Eqn.(2.4) can be written as

$$\mathbf{r}(n) = \mathbf{G}_{cp}\mathbf{H}_0\mathbf{F}\mathbf{s}(n) + \mathbf{G}_{cp}\tilde{\mathbf{w}}(n) \tag{2.8}$$

2.1.2 Zero Padding

Zero padding(ZP) is another option to let us obtain an IBI-free transmissions and was recently proposed to replace the traditional CP method. It zero-pads the transmitted block $\mathbf{s}(n)$ with L trailing zeros [13] by appropriately choosing the precoder matrix $\mathbf{F}$. Specifically, in each block of the ZP transmission, zero symbols are appended after the precoded information symbols. If the number of zero symbols equals the CP length, then ZP and CP transmission methods have the same spectral efficiency. Unlike CP and without bandwidth-consuming channel coding, ZP guarantees symbol recov-

ery and assures FIR equalization of FIR channels regardless of the channel zero locations [39].

The only difference of ZP from CP is that the CP is replaced by L trailing zeros that padded at each precoded block. Note that if $\mathbf{F}$ in Eqn.(2.4) is chosen such that $\mathbf{H}_{IBI}\mathbf{F} = \mathbf{0}$, then consequently $\mathbf{G}\mathbf{H}_{IBI}\mathbf{F}\mathbf{s}(n-1) = \mathbf{0}$ and IBI is therefore eliminated. This corresponds to zero padding block transmissions [13]. In order to achieve this zero padding, we have to set the precoder matrix $\mathbf{F}$ as

$$\mathbf{F} \triangleq \mathbf{F}_{zp} = \left[\mathbf{I}_M^T \;\; \mathbf{0}_{L\times M}^T\right]_{P\times M}^T \tag{2.9}$$

which amounts to setting the last L rows of $\mathbf{F}$ to zero, since only the last L columns of $\mathbf{H}_{IBI}$ are nonzero, from Eqn.(2.9) and Eqn.(2.6) we can obtain $\mathbf{H}_{IBI}\mathbf{F}_{zp} = \mathbf{0}$, which is equal to zero padding the IBI matrix $\mathbf{H}_{IBI}$. Accordingly, $\mathbf{G}\mathbf{H}_{IBI}\mathbf{F}_{zp}\mathbf{s}(n-1) = \mathbf{0}$ and the IBI is eliminated. If we make the decoder matrix $\mathbf{G}$ as

$$\mathbf{G} \triangleq \mathbf{G}_{zp} = \left[\mathbf{I}_M \;\; \hat{\mathbf{I}}_{M\times L}\right]_{M\times P} \tag{2.10}$$

where $\hat{\mathbf{I}}_{M\times L}$ consists of the first L columns of an $M \times M$ identity matrix. Premultiplying a matrix or a vector by $\mathbf{G}_{zp}$ adds the last L rows to the first L columns. Then using Eqn.(2.5), Eqn.(2.9) and Eqn.(2.10), the channel

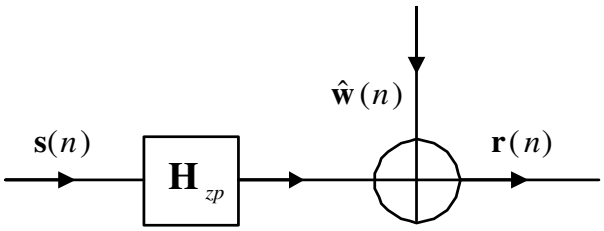

Figure 2.2: Block Transmission with Zero Padding Method

matrix $\mathbf{H}_{zp}$ can now be defined as

$$\mathbf{H}_{zp} \triangleq \mathbf{G}_{zp}\mathbf{H}_0\mathbf{F}_{zp} = \begin{bmatrix} h(0) & 0 & \dots & 0 \\ \vdots & \ddots & \ddots & \vdots \\ h(L) & \vdots & \vdots & 0 \\ 0 & \vdots & \vdots & h(0) \\ \vdots & \ddots & \ddots & \vdots \\ 0 & \ddots & 0 & h(L) \end{bmatrix} \tag{2.11}$$

Finally, the received block $\mathbf{r}(n)$ can be written as

$$\mathbf{r}(n) = \mathbf{H}_{zp}\mathbf{s}(n) + \hat{\mathbf{w}}(n) \tag{2.12}$$

where $\hat{\mathbf{w}}(n) \triangleq \mathbf{G}_{zp} \cdot \tilde{\mathbf{w}}(n)$ is the aliased noise. Therefore, we can see the IBI introduced by $\mathbf{s}(n-1)$ is eliminated, and the system model shown in Figure 2.1 simplifies to Figure 2.2.

2.1.3 Comparisons Between CP and ZP

We first summarize the following results of CP and ZP methods.

1. Blocking and IBI suppression with cyclic prefixed: By inserting a CP of length L to the transmitted block $\mathbf{u}(n)$ through the matrix $\mathbf{F}_{cp}$ and then descarding the first L samples of each received block using the matrix $\mathbf{G}_{cp}$, we can convert the serial ISI channel $h(l)$ of order L to an IBI-free circular-convolution-based block system as in Eqn.(2.8).

2. Blocking and IBI suppression with zero padding: By zero padding each transmitted block $\mathbf{u}(n)$ with L trailing zeros, we can achieve IBI-free linear-convolution-based block transmission. By appropriate time aliasing through $\mathbf{G}_{zp}$, we can obtain the final circular-convolution-based block transmission system as in Eqn.(2.12).

While CP enables simple equalization of multipath channels, ZP offers guaranteed symbol recovery regardless of where channel fades may appear. In addition, a ZP transmission can be recast as a CP transmission by appropriately overlapping and adding successive blocks at the receiver. Therefore, ZP appears to be more flexible than CP: it can trade off equalization complexity with symbol detectability.

Besides allowing individual data symbols to be transmitted over independent sub-channels, the CP transmission method enables one to deal easily with IBI channels by simply taking into account the scalar channel attenuations. It also prevents an exponential growth of errors regardless of the phase

of the channel. In fact, the key property of the cyclic prefixed is that its performance is invariant to the phase of the channel spectrum, and moreover, it keeps this property regardless of what other linear operations are performed prior to adding the cyclic prefixed. Note too that a cyclic prefixed method is the most efficient way of attaining the phase invariance property because a necessary condition for the inverse to exist is for the precoder to introduce at least $L-1$ redundant symbols. However, it has the obvious drawback that the symbol transmitted cannot be recovered when it is hit by a channel zero (e.g., $h(l)=0$). This limitation leads to a loss in frequency diversity and can be overcome by the zero padding (ZP) transmission method [12].

Zero padding introduces the same amount of redundancy as cyclic prefixed method and thus results in the same bit rate loss. Interestingly, ZP assures channel irrespective retrieval of the transmitted symbol blocks even when a channel zero is located on a subcarrier which is not possible with the CP method. The merits of zero padding over cyclic prefixed for wireless applications are channel irrespective linear equalizability and guaranteed symbol recovery [39].

ZP method also has its own defect. In terms of power amplifier-induced clipping effects, ZP introduces slightly more nonlinear distortions leading to a larger SNR of operation, and therefore, needs slightly increased power backoff than CP.

Concerning with wireless applications, where the channel state information is not available at the precoder side, Muquet [39] introduces CP and compares it with ZP in terms of nonlinear amplifier effects.

It is well known that power amplifier introduces nonlinear distortions, which destroy orthogonality between the carriers and deteriorate the overall system performance by introducing intercarrier interference. Thus, for a given clipping ratio(number of clipped symbols divided by the total number of transmitted symbols), the mean transmitted power by ZP is smaller compared to CP. It is shown in [39] that clipping effects alone entail excess SNR incurred by the CP relative to that required by ZP as high as $0.96dB$. However, this degradation may be compensated by some particular properties of ZP such as the existence of the specific subspace channel estimation method. This results in a better performance for CP when transmitting small bursts. However, with long bursts ZP is to be preferred because it has better channel tracking capabilities than CP method.

2.2 Optimal Designs for Precoders and Decoders

Redundancy at the precoder builds diversity in the input of digital communication systems and is well motivated for designing the error correcting codes [21]. However, especially with block transmissions, where the data stream is divided into consecutive equal-size blocks [36], the redundancy added to each block provides also a powerful tool for removing interblock interference by making use of cyclic prefixed or zero padding methods which are presented in the previous section.

Besides the mitigation of IBI and noise, the information rate and/or diversity gain afforded by the increased hardware complexity requires appropriate precoding and decoding techniques. Two main approaches emerged from the effort of defining such effective transmission strategies: One uses appropriate mappings of the information symbols in space and time so that without channel state information (CSI) at the precoder and with low complexity at the decoder, full diversity gains become possible [17]. The second one addresses specifically the optimization of the information rate in the case of flat fading [15] and frequency-selective channels [18], assuming that CSI is available at both the precoder and decoder sides. Optimal designs developed in the past, which were based on multi-input multi-output (MIMO) models such as [37], gained importance because of the new interest in joint transmit-receive diversity schemes. Scaglione has done a lot of research work on optimal precoders and decoders designs. She presents the design paradigm which is based on an optimal pair of linear transformations $\mathbf{F}$ and $\mathbf{G}$ of blocks of the transmit symbols and receive samples, respectively, that operate jointly on the time and space dimensions. $\mathbf{F}$ and $\mathbf{G}$ are named as precoder and decoder, respectively. The designs target different criteria of optimality and constraints, assuming the channel is known at the decoder as well as the precoder end. CSI can be acquired at the precoder either if a feedback channel is present or when the precoder and decoder operate in time division duplex so that the time-invariant MIMO channel transfer function is the same in both ways. The optimal solutions [27] can appropriately take advantage of CSI and utilize resources at best while maintaining a reasonable complexity.

In [27], Scaglione presents the minimum mean-squared error design. Assuming the white transmit symbols $\mathbf{s}(n), n = 1, 2, ...$ are transmitted and $\mathbf{R}_{ss} \triangleq \sigma_{ss}^2\mathbf{I}$(See Figure 2.1). The noise $\tilde{\mathbf{w}}(n)$ is additive Gaussian noise (AGN) with covariance $\mathbf{R}_{\tilde{w}\tilde{w}}$, $\mathbf{R}_{\tilde{w}\tilde{w}}$ is positive definite, and is uncorrelated with the transmit symbols. The system model can be written as

$$\mathbf{r}(n) \triangleq \mathbf{GHFs}(n) + \mathbf{G}\tilde{\mathbf{w}}(n) \tag{2.13}$$

A reasonable criterion to design a decoder $\mathbf{G}$, for given $\mathbf{F}$ and $\mathbf{H}$, is to minimize the mean-squared error (MSE) matrix that is given by

$$\mathrm{MSE}(\mathbf{F}, \mathbf{G}) \triangleq \mathrm{E}\left(\Big(\mathbf{r}(n) - \mathbf{s}(n)\Big)\Big(\mathbf{r}(n) - \mathbf{s}(n)\Big)^H \right) \tag{2.14}$$

where $\mathrm{E}(x)$ is the mathematical expression of x. Referring to the system model, the MSE matrix in Eqn.(2.14) can be written as

$$\mathrm{MSE}(\mathbf{F}, \mathbf{G}) = tr\Big((\mathbf{GHF} - \mathbf{I})\mathbf{R}_{ss}(\mathbf{GHF} - \mathbf{I})^H\Big) + tr\Big(\mathbf{GR}_{\tilde{w}\tilde{w}}\mathbf{G}^H\Big) \tag{2.15}$$

The cumulative MSE of the estimation of $\mathbf{s}(n)$ is $tr(\mathrm{MSE}(\mathbf{F}, \mathbf{G}))$, where $tr(\mathbf{A})$ denotes the trace of matrix $\mathbf{A}$. We adopt Lagrangian method to differentiate Eqn.(2.15) with respect to $\mathbf{F}$, subject to the transmit power constraint, then the optimum decoder $\mathbf{G}_{MMSE}$ that minimize the whole $\mathrm{MSE}(\mathbf{F}, \mathbf{G})$ matrix is given by

$$\mathbf{G}_{MMSE} = \mathbf{F}^H\mathbf{H}^H(\mathbf{HFF}^H\mathbf{H}^H + \mathbf{R}_{\tilde{w}\tilde{w}}\sigma_{ss}^{-2})^{-1} \tag{2.16}$$

Then the determination of precoder matrix $\mathbf{F}$ will be based on different performance measures. Scaglione [27] also introduces the eigenvalue decomposition of $\mathbf{H}^H\mathbf{R}_{\tilde{w}\tilde{w}}^{-1}\mathbf{H}$ in her work, which is defined as

$$\mathbf{H}^H\mathbf{R}_{\tilde{w}\tilde{w}}^{-1}\mathbf{H} \triangleq \mathbf{V}\mathbf{\Lambda}\mathbf{V}^H \tag{2.17}$$

where $\mathbf{V}$ is the unitary matrix whose columns are formed by the corresponding eigenvectors. $\mathbf{\Lambda}$ is a diagonal matrix which contains the non-null eigenvalues λ_{ii} of $\mathbf{H}^H\mathbf{R}_{\tilde{w}\tilde{w}}^{-1}\mathbf{H}$ arranged in decreasing order.

The MMSE design minimizes the $tr(\text{MSE}(\mathbf{F},\mathbf{G}))$ jointly with respect to $\mathbf{G}$ and $\mathbf{F}$ under the transmit power constraint. The solution of the optimization problem

$$\mathbf{F}_{MMSE} = \arg \min_{\mathbf{F},\mathbf{G}} tr(\text{MSE}(\mathbf{F},\mathbf{G})), \quad tr(\mathbf{F}_{MMSE}\mathbf{F}_{MMSE}^H)\sigma_{ss}^2 = p_0 \tag{2.18}$$

is given by $\mathbf{F}_{MMSE} = \mathbf{V}\mathbf{\Phi}$, where $\mathbf{\Phi}$ is a diagonal matrix with the following (i,i) entry

$$|\phi_{ii}|^2 = \Big(\frac{p_0 + tr(\mathbf{\Lambda}^{-1})}{\sigma_{ss}^2 tr(\mathbf{\Lambda}^{-1/2})}\lambda_{ii}^{-1/2} - \frac{1}{\lambda_{ii}}\sigma_{ss}^2\Big)_+ \tag{2.19}$$

where p_0 is the transmit power, $(x)_+ \triangleq \max(x,0)$. And $\mathbf{G}_{MMSE}$ can be obtained by replacing $\mathbf{F}$ with $\mathbf{F}_{MMSE}$ in Eqn.(2.16). It is interesting to see that the minimization of the determinant, in lieu of the trace, of the $\text{MSE}(\mathbf{F},\mathbf{G})$ matrix with respect to $\mathbf{F}$ is equivalent to maximizing the information rate. The capacity of a MIMO channel was derived for the multi-antenna and flat fading case, in [15] and [16]. In [18], the authors generalize the discrete multi-

tone (DMT) scheme for the MIMO frequency selective case. Compared with these works, the approach of Scaglione's [27] has the following advantages.

1. It jointly optimizes the precoder and decoder explicitly.
2. It does not treat the frequency-selective and flat-fading cases separately and includes the time-varying case as well.
3. It links together the MSE metric with the maximum information rate criterion.

The dimensionless signal-to-noise ratio (SNR) is a standard quality measure for digital communications system performance. Therefore, the required SNR can be considered as a metric that characterizes the performance of one system versus another. Maximum output SNR criterion is used to achieve higher signal-to-noise ratio and thus more transmission power can be obtained. The optimum precoder/decoder $(\mathbf{F}, \mathbf{G})$ pair which maximize the output signal-to-noise ratio (SNR) subject to the zero-forcing (ZF) constraint is presented in [10]. Scaglione [10] introduces this criterion in her work to design a pair of precoder and decoder. Since the maximum output SNR criterion tends to transmit more power at the frequencies where the channel attenuation is higher, it can also accommodate interferences appended to the received signal. Also, the design converts transmission over the wideband dispersive channel to transmission over several parallel uncorrelated subchannels. As we know that $\mathbf{s}(n)$ is the transmitted symbols and the additive Gaussian noise vector is $\tilde{\mathbf{w}}(n)$. They are mutually uncorrelated, stationary with known covariance matrix $\mathbf{R}_{ss} \stackrel{\triangle}{=} \sigma_{ss}^2\mathbf{I}$ and $\mathbf{R}_{\tilde{w}\tilde{w}} \stackrel{\triangle}{=} \sigma_{\tilde{w}\tilde{w}}^2\mathbf{I}$. The

precoder and decoder matrices are $\mathbf{F}$ and $\mathbf{G}$, respectively, and the channel matrix is $\mathbf{H}$ (see Figure 2.1). Recalling the system model in Eqn.(2.13), the IBI-free SNR at the decoder output can be expressed as (e.g., [10])

$$\text{SNR} \triangleq \frac{tr(\text{E}\{\mathbf{GHFs}(n)\mathbf{s}^H(n)\mathbf{F}^H\mathbf{H}^H\mathbf{G}^H\})}{tr(\text{E}\{\mathbf{G}\tilde{\mathbf{w}}(n)\tilde{\mathbf{w}}^H(n)\mathbf{G}^H\})} = \frac{tr(\mathbf{GHFR}_{ss}\mathbf{F}^H\mathbf{H}^H\mathbf{G}^H)}{tr(\mathbf{GR}_{\tilde{w}\tilde{w}}\mathbf{G}^H)} \tag{2.20}$$

ZF constraint is used to force the samples of the combined channel and equalizer impulse response to zero. That means $\mathbf{G} = (\mathbf{HF})^\dagger$, where $(\mathbf{A})^\dagger$ denotes the pseudo-inverse of matrix $\mathbf{A}$. It has the disadvantage that the inverse filter may excessively amplify noise at frequencies where the folded channel spectrum has high attenuation. The ZF constraint thus neglects the effect of noise altogether, and is not often used for wireless links. However, it performs well for static channels with high SNR. Assuming the transmit-amplification gain to be unity and the ZF constraint can be expressed as

$$\mathbf{GHF} \triangleq \mathbf{I} \tag{2.21}$$

where $\mathbf{I}$ is the $M \times M$ identity matrix. We need to use the ZF constraint, otherwise the decoder matrix $\mathbf{G}$ will become to infinity by maximizing the SNR. By substituting Eqn.(2.21) into Eqn.(2.20) we obtain

$$\text{SNR} = \frac{tr(\mathbf{R}_{ss})}{tr(\mathbf{GR}_{\tilde{w}\tilde{w}}\mathbf{G}^H)} \tag{2.22}$$

Therefore, the maximum output SNR criterion can be viewed as

$$\arg \max_{\mathbf{G},\mathbf{F}}: \quad \text{SNR} = \frac{tr(\mathbf{R}_{ss})}{tr(\mathbf{G}\mathbf{R}_{\tilde{w}\tilde{w}}\mathbf{G}^H)} \tag{2.23}$$

subject to

$$\mathbf{GHF} = \mathbf{I} \tag{2.24}$$

Since $\mathbf{R}_{ss} = \sigma_{ss}^2\mathbf{I}$ is the known covariance matrix, $tr(\mathbf{R}_{ss})$ can be considered as a constant, hence, in order to get the optimum precoder $\mathbf{F}$ and decoder $\mathbf{G}$, we maximize the SNR. It is equal to minimizing $tr(\mathbf{G}\mathbf{R}_{\tilde{w}\tilde{w}}\mathbf{G}^H)$. Therefore, invoking the mathematical induction in [10], we minimize $tr(\mathbf{G}\mathbf{R}_{\tilde{w}\tilde{w}}\mathbf{G}^H)$ subject to ZF constraint, the Lagrangian equation can be written as

$$\mathcal{L} = tr(\mathbf{G}\mathbf{R}_{\tilde{w}\tilde{w}}\mathbf{G}^H) - \mu(tr(\mathbf{GHF}) - M) \tag{2.25}$$

where μ is the Lagrange multiplier. Differentiating Eqn.(2.25) with respect to $\mathbf{G}$ and letting the result equal to zero, we can see that the SNR is maximized if and only if

$$\mathbf{G} = \mu\mathbf{F}^H\mathbf{H}^H\mathbf{R}_{\tilde{w}\tilde{w}}^{-1} \tag{2.26}$$

since we know that $\mathbf{R}_{\tilde{w}\tilde{w}} = \sigma_{\tilde{w}\tilde{w}}^2\mathbf{I}$ and in order to simplify subsequent expressions, we select $\mu = \sigma_{\tilde{w}\tilde{w}}^2$. Using this choice, then the decoder matrix $\mathbf{G}$ becomes $\mathbf{G} = \mathbf{F}^H\mathbf{H}^H$ and the ZF constraint in Eqn.(2.21) becomes

$$\mathbf{F}^H\mathbf{H}^H\mathbf{HF} = \mathbf{I} \tag{2.27}$$

We perform the singular value decomposition (SVD) to the channel matrix $\mathbf{H}$ to obtain

$$\mathbf{H} = \mathbf{U}_h \mathbf{\Lambda}^{1/2} \mathbf{V_h}^H \tag{2.28}$$

where $\mathbf{U}_h$ and $\mathbf{V_h}$ are unitary matrices which contain the corresponding singular vectors and $\mathbf{\Lambda}$ is the diagonal matrix which contains the singular values of $\mathbf{H}$ on the diagonal. We substitute Eqn.(2.28) into Eqn.(2.26) and Eqn.(2.27) and the final expressions of the optimal precoder and decoder are expressed as

$$\mathbf{F} = \mathbf{V_h} \mathbf{\Lambda}^{-(1/2)}, \quad \mathbf{G} = \mathbf{U}_h^H \tag{2.29}$$

and these expressions are what we require to achieve the maximum SNR criterion.

Maximum output SNR criterion [10] converts transmission over the wideband dispersive channel to transmission over P parallel uncorrelated subchannels. Compared with minimum mean-squared error criterion [27], it has different power distribution across the subchannels and can transmit more power at the frequencies where the channel attenuation is higher. For long distance transmissions where the transmitters have to operate at their maximum power, it is not convenient to use the maximum output SNR criterion because there will be unnecessary waste of power on subchannels experiencing severe attenuation or narrowband interferences. Thus, this can be regarded as the drawback of the maximum output SNR criterion.

In a typical block-based data transmission system, the received output symbols are grouped into equal-size blocks that are buffered prior to being

processed to mitigate the effects of channel impairments such as additive noise and intersymbol interference (ISI). Due to the increasing demand for higher input bit rates, it is important to investigate efficient schemes for transmitting the maximum possible number of bits per input symbol, at an optimized symbol rate, without exceeding capacity limits dictated by fundamental information theoretic principles. This brings out the maximum information rate criterion. It was proved in [33] that maximum information rate with finite-size blocks can be achieved by shaping appropriately the correlation matrix of the transmitted block.

Scaglione [7] designs the precoder and decoder pair $(\mathbf{F}, \mathbf{G})$ that for given $\mathbf{H}$, $\mathbf{R}_{ss}$ and $\mathbf{R}_{\tilde{w}\tilde{w}}$ maximizes that possible information rate, subject to a limited average transmitted power. It is proved that the optimal correlation matrix can be induced exactly [36], irrespective of the non-Toplitz structure of the optimal spectral shaping matrix, using a finite impulse response (FIR) multirate filterbank that introduces minimal redundancy on the input bit stream. The precoding/decoding structure is adopted and the proposed transceivers convert the frequency-selective channel into several independent parallel flat fading subchannels. The decomposition is reached also by [38] in the context of vector coding. However, the solution in [7] stems from maximizing a mutual information criterion and possesses inherent flexibility that yields as special cases zero-forcing and minimum mean-squared error decoders.

The starting point in maximizing the information rate is to express the mutual information between channel input $\mathbf{u}(n)$ and decoder output $\mathbf{r}(n)$ as

a function of matrices $\mathbf{F}$ and $\mathbf{G}$. The result derived in [33] is borrowed and stated without proof in a slightly more general form that allows for colored input and noise vectors. The normalized mutual information $I(\mathbf{u}, \mathbf{r})$ between any block $\mathbf{u}(n)$ of P channel input symbols and the corresponding block $\mathbf{r}(n)$ of M decoder output symbols is maximized when $\mathbf{u}(n)$ is Gaussian, and is given by

$$I(\mathbf{u}, \mathbf{r}) = \frac{1}{P} \log_2 |(\mathbf{R}_{uu}^{\dagger} + \mathbf{H}^H \mathbf{R}_{\tilde{w}\tilde{w}}^{-1} \mathbf{H}) \mathbf{R}_{uu}| \tag{2.30}$$

where $\mathbf{R}_{uu}$ is the correlation matrix of the transmitted symbols $\mathbf{u}(n)$. $\dagger$ denotes the pseudo-inverse. As we can see that spectral shaping of the transmitted blocks $\mathbf{R}_{uu}$ affects mutual information and thus capacity and information rate of our block transmission through the channel. Without specifying the decoder structure and assuming additive white Gaussian noise (AWGN), the mutual information rate can be maximized with respect to $\mathbf{R}_{uu}$. The spectral shaper is the precoder $\mathbf{F}$. It is interesting that $\mathbf{F}$ will turn out to offer the exact spectral shaper leading to the optimum $\mathbf{R}_{uu}$ sought by [33]. Along with the optimum $\mathbf{G}$, the optimum $\mathbf{F}$ will be derived in closed form as a result of maximizing Eqn.(2.30) and will thus achieve the maximum information rate for block transmissions.

Suppose the transmit power $p_0 = tr(\mathbf{F}\mathbf{R}_{ss}\mathbf{F}^H)$, the channel matrix $\mathbf{H}$, the input symbol covariance $\mathbf{R}_{ss}$ and the noise covariance matrix $\mathbf{R}_{\tilde{w}\tilde{w}}$ be given. Denoting by $\mathbf{U}$, $\mathbf{V}$ the unitary matrices which contain the eigenvectors and by $\mathbf{\Delta}$, $\mathbf{\Lambda}$ the diagonal matrices which contain eigenvalues resulting from

the eigen decompositions

$$\mathbf{R}_{ss} \triangleq \mathbf{U}\boldsymbol{\Delta}\mathbf{U}^H, \quad \mathbf{H}^H\mathbf{R}_{\tilde{w}\tilde{w}}^{-1}\mathbf{H} \triangleq \mathbf{V}\boldsymbol{\Lambda}\mathbf{V}^H \tag{2.31}$$

The optimum $(\mathbf{F}, \mathbf{G})$ precoder/decoder pair maximizing the information rate is given by

$$\mathbf{F}_{opt} = \mathbf{V}\boldsymbol{\Phi}\mathbf{U}^H, \quad \mathbf{G}_{opt} = \mathbf{U}\boldsymbol{\Gamma}\boldsymbol{\Lambda}^{-1}\mathbf{V}^H\mathbf{H}^H\mathbf{R}_{\tilde{w}\tilde{w}}^{-1} \tag{2.32}$$

where $\boldsymbol{\Gamma}$ denotes an arbitrary invertible matrix and $\boldsymbol{\Phi}$ is a diagonal matrix with entries

$$\phi_{ii} = \sqrt{\max\left(\frac{p_0 + tr(\boldsymbol{\Lambda}_1^{-1})}{M\delta_{ii}} - \frac{1}{\lambda_{ii}\delta_{ii}}, 0\right)} \tag{2.33}$$

and λ_{ii} and δ_{ii} are the ith diagonal entries of $\boldsymbol{\Lambda}_1$ and $\boldsymbol{\Delta}$.

Note that the optimum pair $(\mathbf{F}_{opt}, \mathbf{G}_{opt})$ is not unique, and matrix $\boldsymbol{\Gamma}$ offers degree of freedom which can be exploited to satisfy added requirements. For example, judicious selections of $\boldsymbol{\Gamma}$ yield the MMSE decoder as

$$\boldsymbol{\Gamma}_{MMSE} = \boldsymbol{\Delta}\boldsymbol{\Phi}^H(\boldsymbol{\Lambda}^{-1} + \boldsymbol{\Phi}^H\boldsymbol{\Delta}\boldsymbol{\Phi})^{-1} \tag{2.34}$$

$$\mathbf{G}_{MMSE} = \mathbf{U}\boldsymbol{\Gamma}_{MMSE}\boldsymbol{\Lambda}^{-1}\mathbf{V}^H\mathbf{H}^H\mathbf{R}_{\tilde{w}\tilde{w}}^{-1} \tag{2.35}$$

Transmission at the maximum information rate in general does not meet the constraint on the bit error rate which has to be lower than a prescribed upper bound dictated by the required quality of services.

Similar to existing precoding schemes, Scaglione [7] also assumes that

the channel is known during her deriving of the maximum information rate precoder/decoder pair. However, channel information may be imperfect due to channel estimation errors and presence of time-varying interference. Therefore, it is important to analyze how sensitive the performance of proposed procoder/decoder pair is obtained from the eigenvectors of the channel matrix. The sensitivity is expected to increase when the channel matrix $\mathbf{H}^H\mathbf{R}_{\tilde{w}\tilde{w}}^{-1}\mathbf{H}$ tends to have multiple eigenvalues.

The relative improvement achieved with the maximum information rate precoder/decoder pair over the discrete multitone (DMT) [35] increases also as the channel's frequency selective increases. DMT avoids transmission over the corresponding subchannels and distributes the available power on the remaining channels. In contrast, depending on the channel's eigen characteristics, the optimal design in [7] reshapes all the transmit filters and this extra flexibility offers the aforementioned improvement over the DMT.

Therefore, we can conclude that in spite of the indisputable interest of asymptotic results, it is clearly important from the application point of view to derive systems leading to the maximum information rate for finite-size block transmissions. Relatively small-size blocks are in fact highly desirable because they avoid excessive decoding delays, storage requirements, and computational load.

2.3 Summary

In this chapter, we have introduced the cyclic prefixed and zero padding transmission methods which can provide an IBI-free transmission. Cyclic prefixed method inserts a CP of length L to the transmitted block and then discards the first L entries in the received block. Zero padding method resorts to zero-pad the transmitted block with L trailing zeros using the transmitted matrix. These are very effective methods to eliminate IBI and will be adopted in the following chapters. We have also introduced several optimal designs for precoders and decoders, including minimum mean-squared error design, maximum output SNR design and maximum information rate design and evaluated their respective characteristics. In the next chapter, we will make use of the minimum mean-squared error criterion and maximum information rate criterion to design our linear precoders and decoders and try to present a generalized form to unify different designs.

Chapter 3

Linear Precoder and Decoder Design

3.1 Introduction

Since the demand for higher transmission information rate is increasing, addressing this problem has been a crucial part for the research of wireless communications. Researchers have studied extensively to obtain the methods which can achieve high information rate. Space-time coding [18] and spatial multiplexing [15] are two conventional methods that are used to achieve high data rates over Multiple-Input-Multiple-Output (MIMO) channels. Spatial multiplexing involves transmitting independent streams of data across multiple antennas to maximize throughput, whereas, space-time coding appropri-

ately maps input symbol streams across space and time for transmit diversity and coding gain at a given data rate. The advantage is that none of them requires channel knowledge at the precoder side. However, when channel knowledge is available at the precoder side, some channel-dependent linear precoder and decoder designs such as minimum mean-squared error (MMSE) design [10], maximum information rate (MIR) design [7] and minimum bit error rate (MBER) design [30] will have good performance in either information rate or bit error rate. All these designs use a pair of linear precoder matrix $\mathbf{F}_0$ and decoder matrix $\mathbf{G}_0$ which operate linearly on the time and space dimensions. However, the objective in high bit rate transmissions is the maximization of the mutual information between precoder and decoder given performance specifications and limited resources. Optimality in the sense of maximizing mutual information was proved theoretically for ideal decision-feedback equalizers (DFE) in [33], assuming PAM signaling, error-free decisions, and infinite-length feed-forward equalizers. An alternative approach is the so-called vector coding (VC), that utilizes a bank of filters whose impulse responses are the eigenvectors of an appropriately defined channel matrix [38]. The VC approach converts size-M block transmission over a frequency-selective channel into transmission over M parallel independent flat fading channels. In this chapter, we derive the generalized linear precoder and decoder that maximize any weighted sum of information rate, assuming total transmit power constraint across all transmit antennas. We summarize now the main result of this chapter:

- We first introduce the system model for our linear block communication

system.

- Then we derive the optimum structure for the linear precoder and decoder, assuming a total transmit power constraint, and we show that they diagonalize the channel into several eigen subchannels, for any set of information rate weights.

- Next, closed-form solutions are derived for the optimum precoder and decoder as functions of information rate weights, transmit power, decoder noise variance and eigenvalues of the channel. We show how to select appropriate information rate weights to obtain: 1) the maximum information rate design; 2) the minimum mean-squared error design and 3) QoS based design(we show how to achieve any set of relative SNRs across the subchannels).

3.2 System Model

Figure 3.1 shows the model of a linear block communication system, where $\mathbf{s}(n) \triangleq [s(nM)\ s(nM+1)\ ...\ s(nM+M-1)]^T$ is the n^{th} block of M transmitted data symbols. After being processed by the precoder $\mathbf{F}_0$, we get a block of P data symbols $\tilde{\mathbf{u}}(n) \triangleq [\tilde{u}(nP)\ \tilde{u}(nP+1)\ ...\ \tilde{u}(nP+P-1)]^T$, which contains the redundancy inserted by the precoder. We define the channel $\mathbf{H}_0$ is an L^{th} order FIR channel with the impulse response $h(n) = 0$, when $n < 0$ and $n > L$ and we let $P = M + L$. At the decoder side, $\mathbf{r}(n)$ denotes the n^{th} block of M data symbols of the decoder output. The $P \times 1$ additive white Gaussian noise vector $\tilde{\mathbf{w}}(n)$ is defined as

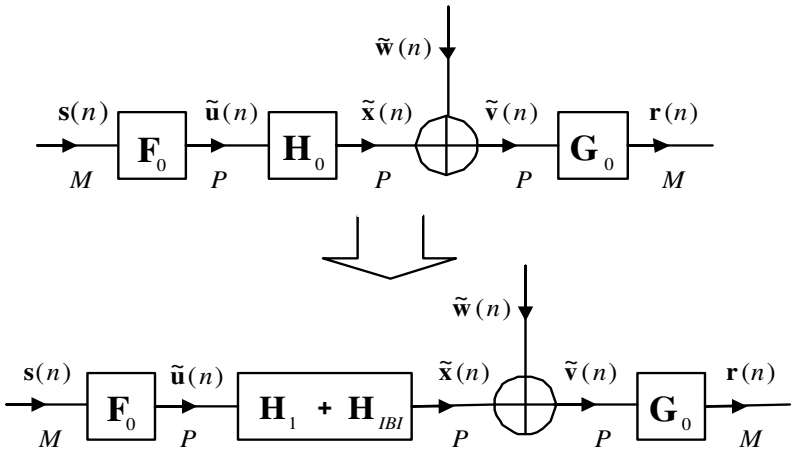

Figure 3.1: Linear Block Transmissions Communication System

$\tilde{\mathbf{w}}(n) \triangleq [\tilde{w}(nP)\ \tilde{w}(nP+1)\ ...\ \tilde{w}(nP+P-1)]^T$, which is independent of the transmitted symbols and has the correlation matrix $\mathbf{R}_{\tilde{w}\tilde{w}}$. We assume the channel $\mathbf{H}_0$ is time invariant and also the channel knowledge is available at both the precoder and the decoder sides apriori. It is important to note that if the channel is time-varying, the assumption of channel knowledge at the precoder side becomes untenable, with the exceptions that the channel can be taken to be time invariant for an enough long interval or it can be designed resorting to some roughly invariant parameters that can be evaluated to predict the channel evolution with sufficient accuracy [26]. We use CP method to eliminate the IBI, this means that we simply discard the first L entries in the block $\tilde{\mathbf{v}}(n)$ as shown in Figure 3.1. Therefore, according to the property of CP and referring to Eqn.(2.15), the precoder $\mathbf{F}_0$ can be defined to have the same structure as $\mathbf{F}_{cp}$ in Chapter 2, which is used to insert a CP of length L to the transmitted block $\mathbf{u}(n)$, thus the precoder matrix can be

expressed as

$$\mathbf{F}_0 \triangleq \left[\begin{array}{cc} [\mathbf{0}_{L\times(M-L)}\ \mathbf{I}_{L\times L}] & \mathbf{F}_{M\times M} \end{array} \right]^T_{P\times M} \tag{3.1}$$

which is a $P \times M$ "tall" matrix and the decoder $\mathbf{G}_0$ can be considered to have the same structure as $\mathbf{G}_{cp}$, which is used to discard the first L rows of the CP which denotes the IBI. We can obtain the expression of $\mathbf{G}_0$ as

$$\mathbf{G}_0 \triangleq \left[\begin{array}{cc} \mathbf{0}_{M\times L} & \mathbf{G}_{M\times M} \end{array} \right]_{M\times P} \tag{3.2}$$

which is an $M \times P$ "fat" matrix, and here $\mathbf{F}$ and $\mathbf{G}$ are both $M \times M$ matrices. They are the simplified precoder and decoder matrices, respectively, which means they only process M entries of the transmitted symbols and the noise vectors. Since both of them have the size of $M \times M$, it is easy to use them to do the transformations of the transmit symbols $\mathbf{s}(n)$ and receive samples $\mathbf{r}(n)$. According to different optimal designs, $\mathbf{F}$ and $\mathbf{G}$ will have different formats, which will be shown in the following.

Since the channel is an L^{th} order FIR channel with the response $h(n) = 0$, when $n < 0$ and $n > L$, and referring to the CP method we mentioned in Chapter 2, the system model can be written as

$$\mathbf{r}(n) \triangleq \mathbf{G}_0\mathbf{H}_0\mathbf{F}_0\mathbf{s}(n)+\mathbf{G}_0\tilde{\mathbf{w}}(n) = \mathbf{G}_0\mathbf{H}_1\mathbf{F}_0\mathbf{s}(n)+\mathbf{G}_0\mathbf{H}_{IBI}\mathbf{F}_0\mathbf{s}(n-1)+\mathbf{G}_0\tilde{\mathbf{w}}(n) \tag{3.3}$$

where $\mathbf{H}_1$ and $\mathbf{H}_{IBI}$ can be defined as

$$\mathbf{H}_1 \triangleq \begin{bmatrix} h(0) & 0 & 0 & \dots & 0 \\ \vdots & h(0) & 0 & \dots & 0 \\ h(L) & \dots & \ddots & \dots & \vdots \\ \vdots & \ddots & \dots & \dots & 0 \\ 0 & \dots & h(L) & \dots & h(0) \end{bmatrix} \tag{3.4}$$

$$\mathbf{H}_{IBI} \triangleq \begin{bmatrix} 0 & \dots & h(L) & \dots & h(1) \\ \vdots & \ddots & 0 & \ddots & \vdots \\ 0 & \dots & \ddots & \dots & h(L) \\ \vdots & \vdots & \vdots & \ddots & \vdots \\ 0 & \dots & 0 & \dots & 0 \end{bmatrix} \tag{3.5}$$

According to the format of $\mathbf{F}_0$ and $\mathbf{G}_0$ in Eqn.(3.1) and Eqn.(3.2), we know that $\mathbf{G}_0\mathbf{H}_{IBI}\mathbf{F}_0 = 0$ and $\mathbf{G}_0\mathbf{H}_1\mathbf{F}_0 = \mathbf{GHF}$, where $\mathbf{H}$ can be defined as

$$\mathbf{H} \triangleq \begin{bmatrix} h(0) & 0 & \dots & h(L) & \dots & h(1) \\ \vdots & h(0) & 0 & 0 & \dots & \vdots \\ h(L) & \vdots & \ddots & \vdots & \dots & h(L) \\ 0 & h(L) & \vdots & \ddots & \dots & 0 \\ \vdots & 0 & \vdots & \vdots & \ddots & \dots \\ 0 & \dots & h(L) & h(L-1) & \dots & h(0) \end{bmatrix} \tag{3.6}$$

which is an $M \times M$ circulant matrix. Also, since $\tilde{\mathbf{w}}(n)$ is a $P \times 1$ additive white Gaussian noise vector, $\mathbf{G}_0\tilde{\mathbf{w}}(n)$ will discard the first L elements of

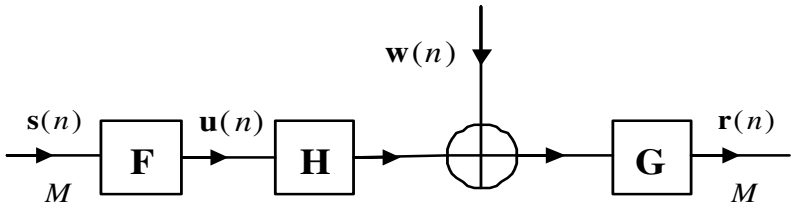

Figure 3.2: Linear Block Transmissions Communication System without IBI

$\tilde{\mathbf{w}}(n)$, hence $\mathbf{G}_0\tilde{\mathbf{w}}(n)$ equals to $\mathbf{G}\mathbf{w}(n)$ where $\mathbf{w}(n)$ holds the last M entries of $\tilde{\mathbf{w}}(n)$ with autocorrelation $\mathbf{R}_{ww} = \sigma^2\mathbf{I}$. Thus, the system model can be rewritten as (See Figure 3.2)

$$\mathbf{r}(n) = \mathbf{GHFs}(n) + \mathbf{Gw}(n) \tag{3.7}$$

In this chapter, we assume that the noise is statistically independent of the transmitted symbols. Hence, $\mathbf{R}_{sw} \triangleq \mathrm{E}(\mathbf{sw}^H) = 0$.

In all of our designs, the paradigm of precoding/decoding exploits the channel eigen-decomposition and transmitted symbol eigen-decomposition in constructing the optimal $\mathbf{F}$, $\mathbf{G}$. The distinct solutions are characterized by how the power is loaded on each channel eigenfunction. Eigenvalue decomposition of the $\mathbf{H}^H\mathbf{R}_{ww}^{-1}\mathbf{H}$ can decouple the channel into M independent eigen-subchannels and load the noise power on each eigen-subchannels. Also, the eigenvalue decomposition of $\mathbf{R}_{ss}$ can load the power of transmitted symbols on every eigen-subchannels. Therefore, we make use of the following

eigenvalue decompositions (EVD)

$$\mathbf{H}^H\mathbf{R}_{ww}^{-1}\mathbf{H} \triangleq \mathbf{X}\mathbf{Y}\mathbf{X}^H \tag{3.8}$$

and

$$\mathbf{R}_{ss} \triangleq \mathbf{U}\mathbf{Z}\mathbf{U}^H \tag{3.9}$$

where $\mathbf{Y}$ and $\mathbf{Z}$ are $M \times M$ diagonal matrices with nonnegative entries y_{ii} and z_{ii}, $1 \leq i \leq M$, arranged in a descending order, which contain the eigenvalues of $\mathbf{H}^H\mathbf{R}_{ww}^{-1}\mathbf{H}$ and $\mathbf{R}_{ss}$ on their diagonals, respectively. $\mathbf{X}$ and $\mathbf{U}$ are $M \times M$ unitary matrices whose columns are formed by the corresponding eigenvectors.

We simplify the objective function by diagonalizing the symmetric matrices involving $\mathbf{R}_{ss}$, $\mathbf{H}$ and $\mathbf{R}_{ww}$, all of which are assumed to be available. Towards this end, we first find the unitary matrices $\mathbf{U}$, $\mathbf{X}$ and the diagonal matrices $\mathbf{Y}$ and $\mathbf{Z}$. Next, with appropriately defined matrices $\mathbf{\Gamma}_f$ and $\mathbf{\Gamma}_g$, we focus on matrices $\mathbf{F}$ and $\mathbf{G}$ that can be decomposed as [10]

$$\mathbf{F} \triangleq \mathbf{X}\mathbf{\Gamma}_f\mathbf{U}^H \tag{3.10}$$

$$\mathbf{G} \triangleq \mathbf{U}\mathbf{\Gamma}_g\mathbf{Y}^{-1}\mathbf{X}^H\mathbf{H}^H\mathbf{R}_{ww}^{-1} \tag{3.11}$$

where both $\mathbf{\Gamma}_f$ and $\mathbf{\Gamma}_g$ are $M \times M$ diagonal matrices with nonnegative entries $\gamma_{f,ii}$ and $\gamma_{g,ii}$. They are not unique and will offer degrees of freedom which can be exploited to satisfy added requirements. For example, the MMSE design

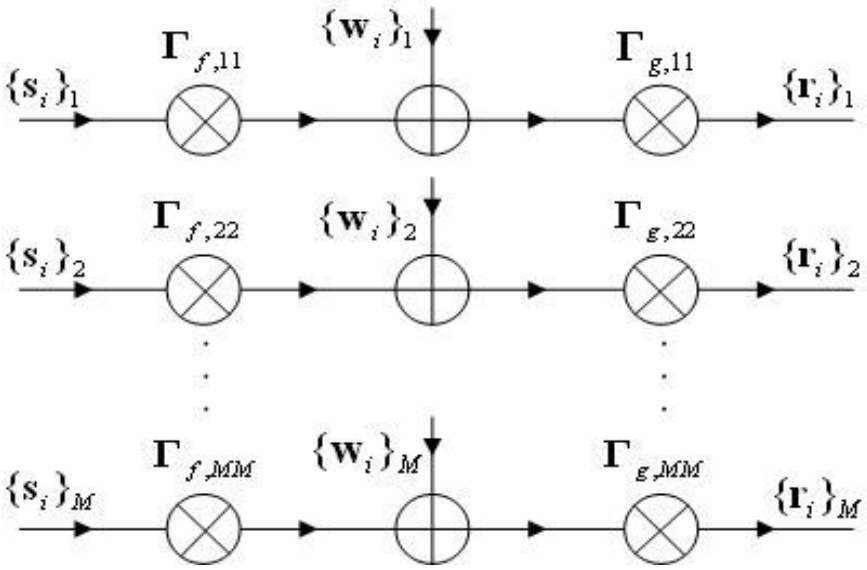

Figure 3.3: Equivalent Subchannels

and maximum information rate design will result in different structures of $\mathbf{\Gamma}_f$ and $\mathbf{\Gamma}_g$ matrices. Thus, the matrix(or block) channel is described by the diagonal transfer matrix $\mathbf{\Gamma}_f$, $\mathbf{\Gamma}_g$ and additive noise. Hence, Figure 3.2 becomes equivalent to Figure 3.3, from which we can see that the precoder and decoder decouple the channel $\mathbf{H}$ into M independent eigen-subchannels, in which case, the flat fading on each of the parallel subchannels corresponds to the diagonal elements of $\mathbf{\Gamma}_g\mathbf{\Gamma}_f$.

3.3 Weighted Information Rate Design

Sampath [24] introduces the concept of weighted MMSE criterion. This criterion gets a better handle on the errors on each eigen subchannel because it is chosen to design a generalized linear precoder and decoder that minimize

any weighted sum of symbol estimation errors. Since a diagonalized weight matrix is presented, the sum of symbol estimation errors on each eigensubchannel can be managed to be minimized. Based on the idea of weighted MMSE, we hereby put forward the weighted information rate criterion which also has a better control on the information rates on each eigen subchannel. Thus, firstly, we derive the expression of information rate equation that will be used in precoder/decoder design.

For linear precoding and decoding matrices $\mathbf{F}$ and $\mathbf{G}$, we first assume the noise symbol $\tilde{\mathbf{w}}(n)$ is to be drawn from a Gaussian distribution. Moreover, it is complex, zero-mean and identically distributed with the correlation matrix $\mathbf{R}_{\tilde{w}\tilde{w}} \stackrel{\triangle}{=} \mathrm{E}(\tilde{\mathbf{w}}\tilde{\mathbf{w}}^H)$. The transmitted symbol $\tilde{\mathbf{u}}(n)$ is also assumed to be complex, zero-mean and independent of the noise with a correlation matrix $\mathbf{R}_{\tilde{u}\tilde{u}} \stackrel{\triangle}{=} \mathrm{E}(\tilde{\mathbf{u}}\tilde{\mathbf{u}}^H)$. From Figure 3.1, we obtain $\tilde{\mathbf{v}}(n) = \mathbf{H}_0\tilde{\mathbf{u}}(n) + \tilde{\mathbf{w}}(n)$, therefore, the output correlation matrix is given by

$$\mathbf{R}_{\tilde{v}\tilde{v}} \stackrel{\triangle}{=} \mathrm{E}(\tilde{\mathbf{v}}\tilde{\mathbf{v}}^H) = \mathbf{H}_0\mathbf{R}_{\tilde{u}\tilde{u}}\mathbf{H}_0^H + \mathbf{R}_{\tilde{w}\tilde{w}} \tag{3.12}$$

and also

$$\mathbf{R}_{\tilde{u}\tilde{v}} \stackrel{\triangle}{=} \mathrm{E}(\tilde{\mathbf{u}}\tilde{\mathbf{v}}^H) = \mathbf{R}_{\tilde{u}\tilde{u}}\mathbf{H}_0^H, \quad \mathbf{R}_{\tilde{v}\tilde{u}} \stackrel{\triangle}{=} \mathrm{E}(\tilde{\mathbf{v}}\tilde{\mathbf{u}}^H) = \mathbf{H}_0\mathbf{R}_{\tilde{u}\tilde{u}} \tag{3.13}$$

It is well known [14] that the normalized information rate between any block

of $\tilde{\mathbf{u}}(n)$ and $\tilde{\mathbf{v}}(n)$ can be written as

$$I(\tilde{\mathbf{u}};\tilde{\mathbf{v}}) \triangleq \frac{1}{M}\Big(C(\tilde{\mathbf{u}}) + C(\tilde{\mathbf{v}}) - C(\tilde{\mathbf{u}};\tilde{\mathbf{v}})\Big) \tag{3.14}$$

where $C(\tilde{\mathbf{u}})$ is the entropy of the random vector $\tilde{\mathbf{u}}$ and can be defined as

$$C(\tilde{\mathbf{u}}) \triangleq -\int f_{\tilde{\mathbf{u}}}(\mathbf{x}) \log_2(f_{\tilde{\mathbf{u}}}(\mathbf{x}))\mathrm{d}\mathbf{x} \tag{3.15}$$

$f_{\tilde{\mathbf{u}}}(\mathbf{x})$ is the probability density function of the complex vector $\tilde{\mathbf{u}}$. It is well known in information theory that $I(\tilde{\mathbf{u}};\tilde{\mathbf{v}})$ is only maximized when $\tilde{\mathbf{u}}$ obeys a Gaussian distribution, for example, if

$$f_{\tilde{\mathbf{u}}}(\mathbf{x}) = \frac{1}{\pi^M |\mathbf{R}_{\tilde{u}\tilde{u}}|} e^{-\mathbf{x}^H \mathbf{R}_{\tilde{u}\tilde{u}}^{-1}\mathbf{x}} \tag{3.16}$$

where $|\mathbf{R}_{\tilde{u}\tilde{u}}|$ is the determinant of matrix $\mathbf{R}_{\tilde{u}\tilde{u}}$, in which case we have

$$C(\tilde{\mathbf{u}}) = \log_2\Big((\pi e)^M |\mathbf{R}_{\tilde{u}\tilde{u}}|\Big) \tag{3.17}$$

Because the noise $\tilde{\mathbf{w}}(n)$ is assumed to be Gaussian, the output vector $\tilde{\mathbf{v}}(n)$ will also be Gaussian with entropy

$$C(\tilde{\mathbf{v}}) = \log_2\Big((\pi e)^M |\mathbf{R}_{\tilde{v}\tilde{v}}|\Big) \tag{3.18}$$

and similarly,

$$C(\tilde{\mathbf{u}};\tilde{\mathbf{v}}) \triangleq \log_2\left((\pi e)^{2M}\left|\begin{array}{cc}\mathbf{R}_{\tilde{u}\tilde{u}} & \mathbf{R}_{\tilde{u}\tilde{v}}\\ \mathbf{R}_{\tilde{v}\tilde{u}} & \mathbf{R}_{\tilde{v}\tilde{v}}\end{array}\right|\right) \tag{3.19}$$

Therefore, according to the definition of the conditional entropy of the transmitted symbol $\tilde{\mathbf{u}}(n)$, given $\tilde{\mathbf{v}}(n)$, and the expressions of $C(\tilde{\mathbf{u}};\tilde{\mathbf{v}})$ and $C(\tilde{\mathbf{v}})$ in Eqn.(3.19) and Eqn.(3.18), respectively, we can express the following conditional entropy as

$$C(\tilde{\mathbf{u}}|\tilde{\mathbf{v}}) \triangleq C(\tilde{\mathbf{u}};\tilde{\mathbf{v}}) - C(\tilde{\mathbf{v}}) = \log_2\left((\pi e)^{2M}\left|\begin{array}{cc}\mathbf{R}_{\tilde{u}\tilde{u}} & \mathbf{R}_{\tilde{u}\tilde{v}}\\ \mathbf{R}_{\tilde{v}\tilde{u}} & \mathbf{R}_{\tilde{v}\tilde{v}}\end{array}\right|\right) - \log_2((\pi e)^M|\mathbf{R}_{\tilde{v}\tilde{v}}|) \tag{3.20}$$

and according to the properties of logarithm and the determinant of a block matrix, which denotes

$$\left|\begin{array}{cc}\mathbf{A} & \mathbf{B}\\ \mathbf{C} & \mathbf{D}\end{array}\right| \triangleq |\mathbf{AD}-\mathbf{BD}^{-1}\mathbf{CD}|, \quad |\mathbf{AB}| \triangleq |\mathbf{A}||\mathbf{B}| \tag{3.21}$$

we can obtain

$$C(\tilde{\mathbf{u}}|\tilde{\mathbf{v}}) = \log_2\left((\pi e)^M\frac{\left|\begin{array}{cc}\mathbf{R}_{\tilde{u}\tilde{u}} & \mathbf{R}_{\tilde{u}\tilde{v}}\\ \mathbf{R}_{\tilde{v}\tilde{u}} & \mathbf{R}_{\tilde{v}\tilde{v}}\end{array}\right|}{|\mathbf{R}_{\tilde{v}\tilde{v}}|}\right) = \log_2\left((\pi e)^M\left|\frac{\mathbf{R}_{\tilde{u}\tilde{u}}\mathbf{R}_{\tilde{v}\tilde{v}}-\mathbf{R}_{\tilde{u}\tilde{v}}\mathbf{R}_{\tilde{v}\tilde{v}}^{-1}\mathbf{R}_{\tilde{v}\tilde{u}}\mathbf{R}_{\tilde{v}\tilde{v}}}{\mathbf{R}_{\tilde{v}\tilde{v}}}\right|\right) \tag{3.22}$$

Thus, the final expression of the conditional entropy $C(\tilde{\mathbf{u}}|\tilde{\mathbf{v}})$ can be shown as

$$C(\tilde{\mathbf{u}}|\tilde{\mathbf{v}}) = \log_2\left((\pi e)^M|\mathbf{R}_{\tilde{u}\tilde{u}}-\mathbf{R}_{\tilde{u}\tilde{v}}\mathbf{R}_{\tilde{v}\tilde{v}}^{-1}\mathbf{R}_{\tilde{v}\tilde{u}}|\right) \tag{3.23}$$

Referring to the equations of $\mathbf{R}_{\tilde{u}\tilde{v}}$, $\mathbf{R}_{\tilde{v}\tilde{v}}$ and $\mathbf{R}_{\tilde{v}\tilde{u}}$ which are expressed in Eqn.(3.12) and Eqn.(3.13), we can see that

$$\mathbf{R}_{\tilde{u}\tilde{u}} - \mathbf{R}_{\tilde{u}\tilde{v}}\mathbf{R}_{\tilde{v}\tilde{v}}^{-1}\mathbf{R}_{\tilde{v}\tilde{u}} = \mathbf{R}_{\tilde{u}\tilde{u}} - \mathbf{R}_{\tilde{u}\tilde{u}}\mathbf{H}_0^H(\mathbf{R}_{\tilde{w}\tilde{w}} + \mathbf{H}_0\mathbf{R}_{\tilde{u}\tilde{u}}\mathbf{H}_0^H)^{-1}\mathbf{H}_0\mathbf{R}_{\tilde{u}\tilde{u}} \quad (3.24)$$

Using the matrix identity theory, which can be expressed as

$$(\mathbf{A} + \mathbf{BCB}^H)^{-1} \triangleq \mathbf{A}^{-1} - \mathbf{A}^{-1}\mathbf{B}(\mathbf{C}^{-1} + \mathbf{B}^H\mathbf{A}^{-1}\mathbf{B})^{-1}\mathbf{B}^H\mathbf{A}^{-1} \quad (3.25)$$

we note that

$$\mathbf{R}_{\tilde{u}\tilde{u}} - \mathbf{R}_{\tilde{u}\tilde{u}}\mathbf{H}_0^H(\mathbf{R}_{\tilde{w}\tilde{w}} + \mathbf{H}_0\mathbf{R}_{\tilde{u}\tilde{u}}\mathbf{H}_0^H)^{-1}\mathbf{H}_0\mathbf{R}_{\tilde{u}\tilde{u}} = (\mathbf{R}_{\tilde{u}\tilde{u}}^{-1} + \mathbf{H}_0^H\mathbf{R}_{\tilde{w}\tilde{w}}^{-1}\mathbf{H}_0)^{-1} \quad (3.26)$$

Using the CP method and referring to Figure 3.2, we note that after discarding the first L elements of the cyclic prefixed, the channel matrix $\mathbf{H}_0$ can be simplified to $\mathbf{H}$ and the correlation matrix $\mathbf{R}_{\tilde{u}\tilde{u}}$; $\mathbf{R}_{\tilde{w}\tilde{w}}$ can be expressed as $\mathbf{R}_{uu}$ and $\mathbf{R}_{ww}$, where $\mathbf{u}(n)$ and $\mathbf{w}(n)$ denote the first M elements of $\tilde{\mathbf{u}}(n)$ and $\tilde{\mathbf{w}}(n)$, respectively. Eqn.(3.26) can be considered as

$$(\mathbf{R}_{\tilde{u}\tilde{u}}^{-1} + \mathbf{H}_0^H\mathbf{R}_{\tilde{w}\tilde{w}}^{-1}\mathbf{H}_0)^{-1} \Rightarrow (\mathbf{R}_{uu}^{-1} + \mathbf{H}^H\mathbf{R}_{ww}^{-1}\mathbf{H})^{-1} \quad (3.27)$$

Then, according to the eigenvalue decomposition of $\mathbf{H}^H\mathbf{R}_{ww}^{-1}\mathbf{H}$ of Eqn.(3.8), Eqn.(3.24) can finally be written as

$$\mathbf{R}_{\tilde{u}\tilde{u}} - \mathbf{R}_{\tilde{u}\tilde{v}}\mathbf{R}_{\tilde{v}\tilde{v}}^{-1}\mathbf{R}_{\tilde{v}\tilde{u}} \Rightarrow (\mathbf{R}_{uu}^{-1} + \mathbf{H}^H\mathbf{R}_{ww}^{-1}\mathbf{H})^{-1} = (\mathbf{R}_{uu}^{-1} + \mathbf{XYX}^H)^{-1} \quad (3.28)$$

Thus, referring to Eqn.(3.28), the $C(\tilde{\mathbf{u}}|\tilde{\mathbf{v}})$ in Eqn.(3.23) can now be written as

$$C(\tilde{\mathbf{u}}|\tilde{\mathbf{v}}) \Rightarrow \log_2\left((\pi e)^M|(\mathbf{R}_{uu}^{-1}+\mathbf{X}\mathbf{Y}\mathbf{X}^H)^{-1}|\right) \tag{3.29}$$

Since $\mathbf{u}(n) = \mathbf{F}\mathbf{s}(n)$ and we assume the transmitted symbols $\mathbf{s}(n)$ are whitened and normalized to unit power, which implies that $\mathbf{R}_{ss} = \mathbf{I}$ and referring to Eqn.(3.10), we can derive Eqn.(3.17) as

$$C(\tilde{\mathbf{u}}) \Rightarrow \log_2\left((\pi e)^M|\mathbf{F}\mathbf{s}\mathbf{s}^H\mathbf{F}^H|\right) = \log_2\left((\pi e)^M|\mathbf{X}\mathbf{\Gamma}_f\mathbf{U}^H\mathbf{U}\mathbf{\Gamma}_f^H\mathbf{X}^H|\right) \tag{3.30}$$

Since $\mathbf{\Gamma}_f$ is the diagonal matrix with diagonal entries $\gamma_{f,ii}$ and $\mathbf{U}$, $\mathbf{X}$ are both unitary matrices, then Eqn.(3.30) can be written as

$$C(\tilde{\mathbf{u}}) \Rightarrow \log_2\left((\pi e)^M|\mathbf{X}\mathbf{\Gamma}_f\mathbf{\Gamma}_f^H\mathbf{X}^H|\right) = \log_2\left((\pi e)^M\prod_{i=1}^{M}|\gamma_{f,ii}|^2\right) \tag{3.31}$$

and based on the same derivation, the expression of $C(\tilde{\mathbf{u}}|\tilde{\mathbf{v}})$ in Eqn.(3.29) can be written as

$$C(\tilde{\mathbf{u}}|\tilde{\mathbf{v}}) \Rightarrow -\log_2\left((\pi e)^{-M}\prod_{i=1}^{M}(|\gamma_{f,ii}|^{-2}+y_{ii})\right) \tag{3.32}$$

Referring to Eqn.(3.20), we substitute Eqn.(3.31) and Eqn.(3.32) into Eqn.(3.14), and obtain

$$I = \frac{1}{M}\log_2\left(\prod_{i=1}^{M}(1+y_{ii}|\gamma_{f,ii}|^2)\right) = \frac{1}{M}\sum_{i=1}^{M}\log_2(1+y_{ii}|\gamma_{f,ii}|^2) \tag{3.33}$$

which expresses the information rate.

Eqn.(3.33) is the well known equation of normalized information rate [26]. Subsequently, we are going to introduce how to make use of the equation of the information rate and the weight matrix to acquire the MMSE design, maximum information rate design and QoS based design.

Before we begin to design, we can see from Eqn.(3.33) that if there is no constraint, maximizing the weighted information rate will lead to $\|\mathbf{F}\| = \infty$ because $|\gamma_{f,ii}|$, $i \in [1, M]$ is going to be maximized to infinity. Here, in this section, we consider the transmit power constraint, which can be expressed as: $p_0 \triangleq tr(\mathbf{F}\mathbf{F}^H)$ or $p_0 \triangleq \sum_{i=1}^{M} |\gamma_{f,ii}|^2$ to avoid excessive maximization of $\mathbf{F}$. p_0 is the fixed transmit power. Then our maximum weighted information rate criterion can be written as the following with the transmit power constraint.

$$\arg \max_{|\gamma_{f,ii}|^2} : I_1 = \frac{t_{ii}}{M} \sum_{i=1}^{M} \log_2(1 + y_{ii}|\gamma_{f,ii}|^2) \tag{3.34}$$

subject to

$$\sum_{i=1}^{M} |\gamma_{f,ii}|^2 = p_0 \tag{3.35}$$

$\mathbf{T}$ is the $M \times M$ diagonal positive definite weighted matrix, which contains the information rate weights on its diagonal, i.e. $\mathbf{T} = diag\Big([t_{11}, t_{22}, ..., t_{MM}]\Big)$. According to Eqn.(3.34) and Eqn.(3.35), the Lagrangian equation can now be expressed as

$$\mathcal{L} = \frac{t_{ii}}{M} \sum_{i=1}^{M} \log_2(1 + y_{ii}|\gamma_{f,ii}|^2) - \mu(\sum_{i=1}^{M} |\gamma_{f,ii}|^2 - p_0) \tag{3.36}$$

μ is the Lagrange multiplier and the method of Lagrange multiplier is used to solve the optimization problem of maximum weighted information rate.

Differentiating Eqn.(3.36) with respect to $|\gamma_{f,ii}|^2$ and letting the result equal to zero, we have (Proof, see Appendix C)

$$|\gamma_{f,ii}|^2 = \frac{t_{ii}\log_2 e}{\mu M} - y_{ii}^{-1} \tag{3.37}$$

using to the transmit power constraint, we substitute Eqn.(3.37) into Eqn.(3.35) and obtain that

$$\mu = \frac{tr(\mathbf{T})\log_2 e}{M\Big(p_0 + tr(\mathbf{Y}^{-1})\Big)} \Rightarrow \mu M = \frac{tr(\mathbf{T})\log_2 e}{p_0 + tr(\mathbf{Y}^{-1})} \tag{3.38}$$

By substituting Eqn.(3.38) into Eqn.(3.37) and expressing it in the vector form, we finally get the following expression

$$\mathbf{\Gamma}_f = \left(\sqrt{\frac{p_0 + tr(\mathbf{Y}^{-1})}{tr(\mathbf{T})}\mathbf{T}} - \mathbf{Y}^{-1}\right)_+ \tag{3.39}$$

where $(x)_+$ denotes $\max(x, 0)$. Next, we will show that we can acquire different designs of the precoder/decoder matrices by appropriately choosing the weight matrix $\mathbf{T}$. In the following, we show different designs, namely, MMSE design, maximum information rate design and Qos based design.

3.3.1 Minimum Mean-Squared Error (MMSE) Design

The design of joint precoder and decoder that minimizes the mean-squared error and the expressions of the precoder and decoder matrices are well known in [2]. The MMSE design minimizes the sum of the symbol estimation errors across all subchannels and improves the system performance. By choosing $\mathbf{T} = \mathbf{Y}^{-\frac{1}{2}}$, we can obtain the MMSE solution for the well-known $\mathbf{\Gamma}_f$ matrix, therefore

$$\mathbf{\Gamma}_{f_{MMSE}} = \left(\sqrt{\frac{p_0 + tr(\mathbf{Y}^{-1})}{tr(\mathbf{Y}^{-\frac{1}{2}})} \mathbf{Y}^{-\frac{1}{2}} - \mathbf{Y}^{-1}} \right)_+ \tag{3.40}$$

Accordingly, the precoder and decoder matrices which are used to minimize the mean-squared error can be expressed as

$$\mathbf{F}_{MMSE} = \mathbf{X}\mathbf{\Gamma}_{f_{MMSE}}\mathbf{U}^H \tag{3.41}$$

$$\mathbf{G}_{MMSE} = \mathbf{F}_{MMSE}^H \mathbf{H}^H (\sigma^2 \mathbf{I} + \mathbf{H}\mathbf{F}_{MMSE}\mathbf{F}_{MMSE}^H \mathbf{H}^H)^{-1} \tag{3.42}$$

where the expression of $\mathbf{G}_{MMSE}$ can be obtained from Eqn.(2.25). The MMSE design minimizes the sum of the symbol estimation errors across all subchannels and improves system performance. Furthermore, the MMSE power allocation policy allocates no power to an eigensubchannel, if its gain is less than a certain threshold, i.e., the weakest eigensubchannels are dropped. The power is then redistributed among the remaining eigensubchannels, so that more power is allocated to the weaker eigensubchannels and vice versa.

3.3.2 Maximum Information Rate (MIR) Design

We know that if $\mathbf{\Gamma}_f$ is chosen according to the well-known water-pouring solution [14], the information rate will be maximized, so we choose our weight matrix $\mathbf{T} = \mathbf{I}$ and can obtain the well-known precoder matrix [24] [7] which maximize the information rate. According to Eqn.(3.39) and Eqn.(3.10), the equations of $\mathbf{\Gamma}_f$ and precoder matrix $\mathbf{F}$ can be expressed as

$$\mathbf{\Gamma}_{f_{MIR}} = \left(\sqrt{\frac{p_0 + tr(\mathbf{Y}^{-1})}{M} \mathbf{I} - \mathbf{Y}^{-1}} \right)_+, \quad \mathbf{F}_{MIR} = \mathbf{X}\mathbf{\Gamma}_{f_{MIR}}\mathbf{U}^H \tag{3.43}$$

The decoder $\mathbf{G}$ can be chosen as either an MMSE decoder or a zero-forcing (ZF) decoder because the choice of the decoder will not affect the procedure of designing the diagonal precoder matrix $\mathbf{\Gamma}_f$ since $\mathbf{\Gamma}_g$ has provided the freedom of added requirements and it does not enter in the expression for the maximum information rate given as Eqn.(3.36).

For a zero-forcing decoder, since $\mathbf{GHF} = \mathbf{I}$ should be satisfied, according to Eqn.(3.10) and Eqn.(3.11) which denote the precoder $\mathbf{F}$ and decoder $\mathbf{G}$, respectively, the ZF equation can be expressed as

$$\mathbf{U}\mathbf{\Gamma}_{g_{ZF}}\mathbf{Y}^{-1}\mathbf{X}^H\mathbf{H}^H\mathbf{R}_{ww}^{-1}\mathbf{H}\mathbf{X}\mathbf{\Gamma}_{f_{MIR}}\mathbf{U}^H = \mathbf{U}\mathbf{\Gamma}_{g_{ZF}}\mathbf{\Gamma}_{f_{MIR}}\mathbf{U}^H \tag{3.44}$$

Then we finally obtain $\mathbf{\Gamma}_{g_{ZF}} = \mathbf{\Gamma}_{f_{MIR}}^{-1}$ which denotes the ZF constraint and refer to Eqn.(3.11), the ZF decoder matrix $\mathbf{G}_{ZF}$ can finally be expressed as $\mathbf{G}_{ZF} = \mathbf{U}\mathbf{\Gamma}_{g_{ZF}}\mathbf{Y}^{-1}\mathbf{X}^H\mathbf{H}^H\mathbf{R}_{ww}^{-1}$.

For an MMSE decoder, the error vector $\mathbf{e}(n)$ at the point of the input

of the decision device can be defined as

$$\mathbf{e}(n) \triangleq \mathbf{r}(n) - \mathbf{s}(n) = (\mathbf{GHF} - \mathbf{I})\mathbf{s}(n) + \mathbf{Gw}(n) \tag{3.45}$$

In the previous section, we have assumed that the transmitted symbol correlation matrix $\mathbf{R}_{ss} = \mathbf{I}$ and the noise correlation matrix $\mathbf{R}_{ww} = \sigma^2\mathbf{I}$ and they are independent, therefore, the error covariance matrix can be defined as $\mathbf{R}_{ee} \triangleq \mathrm{E}[\mathbf{ee}^H] = (\mathbf{GHF} - \mathbf{I})(\mathbf{GHF} - \mathbf{I})^H + \sigma^2\mathbf{GG}^H$. Subject to the transmitted power constraint, we can minimize the mean-squared error of the received symbols which is defined as in Eqn.(2.24). We obtain the MMSE optimal design by using Lagrangian method. This equation can be shown as

$$\mathcal{L} \triangleq tr\Big((\mathbf{GHF} - \mathbf{I})(\mathbf{GHF} - \mathbf{I})^H + \sigma^2\mathbf{GG}^H\Big) + \mu_1\Big(tr(\mathbf{FF}^H) - p_0\Big) \tag{3.46}$$

where μ_1 is the Lagrange multiplier for MMSE design. Differentiating Eqn.(3.46) with respect to $\mathbf{G}$ and letting the result equal to zero, we obtain

$$\frac{\partial \mathcal{L}}{\partial \mathbf{G}} = 0 = \mathbf{HF}(\mathbf{GHF})^H - \mathbf{HF} + \sigma^2\mathbf{G}^H \tag{3.47}$$

Pre-multiply Eqn.(3.47) by $\mathbf{G}$, therefore, we have

$$\mathbf{GHF} = \sigma^2\mathbf{GG}^H + (\mathbf{GHF})(\mathbf{GHF})^H \tag{3.48}$$

Substitute Eqn.(3.10) and Eqn.(3.11) into Eqn.(3.48) and we finally obtain

the expression of MMSE decoder

$$\mathbf{\Gamma}_{g_{MMSE}} = \mathbf{\Gamma}_{f_{MIR}}^{H}(\mathbf{Y}^{-1}+\mathbf{\Gamma}_{f_{MIR}}\mathbf{\Gamma}_{f_{MIR}}^{H})^{-1},\ \mathbf{G}_{MMSE} = \mathbf{U}\mathbf{\Gamma}_{g_{MMSE}}\mathbf{Y}^{-1}\mathbf{X}^{H}\mathbf{H}^{H}\mathbf{R}_{ww}^{-1} \tag{3.49}$$

The choice $\mathbf{T} = \mathbf{I}$ in the expression for $\mathbf{\Gamma}_{f_{MIR}}$ obtained from the weighted information rate design results in the well-known water-pouring solution. Hence, the maximum information rate design is just a special case of our generalized design. Also, from the maximum information rate design, we can see that stronger subchannels support higher rates when compared to weaker subchannels. The maximum information rate design finds applications in adaptive modulation systems [40] where more power and higher order modulation are used on subchannels with higher gains to improve data rates.

3.3.3 QoS Based Design

We now consider a multimedia application that has different types of signals and needs to be sent simultaneously on different subchannels, for example, video and audio signals. Usually video signal needs a higher SNR than audio for successful transmission [24]. In such kind of QoS based applications, it is imperative to have subchannels with different SNRs.

From [27] we know that the subchannel SNR matrix can be defined as

$$\mathbf{\Omega} \triangleq \frac{\mathbf{GHFs}(n)\mathbf{s}^{H}(n)\mathbf{F}^{H}\mathbf{H}^{H}\mathbf{G}^{H}}{\mathbf{Gw}(n)\mathbf{w}^{H}(n)\mathbf{G}^{H}} = \mathbf{GHF}(\mathbf{F}^{H}\mathbf{H}^{H}\mathbf{G}^{H})(\mathbf{GR}_{ww}\mathbf{G}^{H})^{-1} \tag{3.50}$$

where $\Omega_{i,i}$ is the i^{th} subchannel SNR. Using $\mathbf{F}$ and $\mathbf{G}$ matrix in Eqn.(3.10) and Eqn.(3.11), the eigenvalue decomposition of $\mathbf{H}\mathbf{R}_{ww}^{-1}\mathbf{H}^H$ and the expression of $|\gamma_{f,ii}|^2$ in Eqn.(3.37), we can simplify the expression of $\mathbf{\Omega}$ as following

$$\mathbf{\Omega} = \mathbf{\Gamma}_f^2\mathbf{Y} = \frac{\log_2 e}{\mu M}\mathbf{T}\mathbf{Y} - \mathbf{I} \tag{3.51}$$

We now demonstrate how to choose the $\mathbf{T}$ matrix to achieve any set of relative SNRs across the subchannels. From Eqn.(3.51), we make the following definition

$$\mathbf{\Omega} = \mathbf{\Gamma}_f^2\mathbf{Y} = \frac{\log_2 e}{\mu M}\mathbf{T}\mathbf{Y} - \mathbf{I} \triangleq \alpha\mathbf{Q} \tag{3.52}$$

where $\mathbf{Q} = diag([q_1, q_2, ...q_M])$ is a diagonal matrix of relative SNRs across subchannels and we assume that $\sum_{i=1}^{M} q_i = 1$, $\alpha > 0$ is a scalar. From Eqn.(3.52) we can compute $\mathbf{T}$ as

$$\mathbf{T} = (\alpha\mathbf{Q} + \mathbf{I})\mathbf{Y}^{-1}\frac{\mu M}{\log_2 e} \tag{3.53}$$

From Eqn.(3.38) we can see that μ is a function of $\mathbf{T}$. Substituting the expression for $\mathbf{T}$ from Eqn.(3.53) into Eqn.(3.38), we obtain

$$\alpha = \frac{p_0}{tr(\mathbf{Y}^{-1}\mathbf{Q})} \tag{3.54}$$

Substituting Eqn.(3.54) into Eqn.(3.53), we finally obtain

$$\mathbf{T} = \Big(\frac{p_0\mathbf{Q}}{tr(\mathbf{Y}^{-1}\mathbf{Q})} + \mathbf{I}\Big)\frac{\mu M}{\log_2 e}\mathbf{Y}^{-1} \tag{3.55}$$

Again, we substitute Eqn.(3.55) into the expression of $\mathbf{\Gamma}_f$ and we can get the precoder and decoder matrix. In addition, we adopt the MMSE decoder, so the precoder and decoder that can provide any set of relative SNRs($\mathbf{\Omega}$) across subchannels are given by

$$\mathbf{F}_{QoS} = \mathbf{X}\mathbf{\Gamma}_{f_{QoS}}\mathbf{U}^H,\ \mathbf{G}_{MMSE} = \mathbf{F}_{QoS}^H\mathbf{H}^H(\sigma^2\mathbf{I} + \mathbf{H}\mathbf{F}_{QoS}\mathbf{F}_{QoS}^H\mathbf{H}^H)^{-1} \quad (3.56)$$

$$\mathbf{\Gamma}_{f_{QoS}} = \left(\frac{p_0}{tr(\mathbf{Q}\mathbf{Y}^{-1})}\right)^{\frac{1}{2}}\mathbf{Q}^{\frac{1}{2}}\mathbf{Y}^{-\frac{1}{2}} \quad (3.57)$$

Thus we have shown that by choosing different weight matrices $\mathbf{T}$, we can obtain MMSE design, MIR design and QoS based design, respectively. Therefore, we see that MMSE design, MIR design and QoS based design are just three special cases of our weighted information rate design. Comparing these three designs, we noticed that MMSE design provides perhaps the best compromise between BER and information rate. The maximum information rate design is useful if the information rate is considered as the most important quality of the performance of a communication system. And as we have mentioned before, the QoS based design is usually used in the multimedia applications which have different types of signals and need to be sent coinstantaneously on different subchannels. However, Neither the maximum information rate design nor the QoS based design considers the bit error rate performance, so their bit error rate performances may be unsatisfactory and are worse than the MMSE design. We will show these simulation results in Chapter 5.

3.4 Summary

In this chapter, we have addressed the problem of linear precoder and decoder design and introduced a new criterion of maximum weighted information rate subject to the transmit power constraint. We have also illustrated the optimum precoder and decoder which diagonalize the channel into M eigen subchannels for any set of information rate weights. We observe that by choosing different weights of information rate appropriately, we can achieve MMSE design, MIR design and QoS based design. However, we can see from these designs that none of them has a optimum performance of bit error rate. Since bit error rate (BER) is a very important quality measure for digital system performance, in the next chapter, we will aim to achieve the minimum bit error rate performance and maximize the information rate simultaneously for nonlinear precoder and decoder.

Chapter 4

Nonlinear DFE-based Precoder/Decoder

4.1 Introduction

The design of the block transceivers, which are optimal in the sense of maximum information rate (MIR), minimum mean-squared error (MMSE) or minimum bit error rate (MBER), has been of great interest. The purpose of adopting block transmission is to transmit data in the way of block-by-block and to eliminate the interference between the blocks. Orthogonal frequency division multiplexing (OFDM) [34] system and discrete multitone modulation (DMT) [35] system are two prevalent illustrations of block transmission.

Linear and non-linear equalizers make good use of the block-by-block

transmission [10] [7] [19] [32]. Linear ones such as zero-forcing (ZF) and MMSE equalizers are easy to implement as compared to non-linear equalizers. However, results have established that nonlinear equalizers such as ZF decision-feedback equalizer (ZF-DFE) and MMSE decision-feedback equalizer (MMSE-DFE) have better BER performance [32]. In linear schemes, maximizing information rate has been studied and gained plenty of attention [7] [24]. Scaglione [7] studied to use filterbank transceivers to optimize the information rate over dispersive channel. Moreover, the design of minimizing the bit error rate becomes another pop research area and Ding [30] achieved the minimum bound of the bit error rate of zero-forcing equalizer. While in non-linear schemes, maximum information rate and minimum bit error rate were obtained, respectively. Stamoulis [22] tried to minimize the geometric mean-squared error (GMSE) in order to maximize the information rate and in Liu's paper [23] a ZF-DFE was proposed and the minimum BER was achieved, however, maximum information rate was not achievable. In this chapter, we focus on nonlinear precoder and decoder designs which make use of the decision-feedback equalizer. It is well know [1] that BER performance of the equalization process depends critically upon the structure of the receiver side and decision-feedback equalizers have been known to exhibit superior bit error rate (BER) performance when compared to linear schemes and under certain circumstances, have the potential to achieve the performance of the maximum likelihood receiver.

The basic limitation of a linear equalizer, such as the MMSE equalizer or ZF equalizer, is that it performs poorly on channels having spectral

nulls [1]. Such channels are usually encountered in cellular mobile radio applications. A decision-feedback equalizer is a nonlinear equalizer that uses previous detector decisions to eliminate the ISI on pulse that are currently being demodulated. The ISI being removed was caused by the tails of previous pulse. In effect, the distortion on a current pulse that was caused by previous pulse is subtracted. The advantage of a DFE implementation is that the feedback filter, which is additionally working to remove ISI, operates on noiseless quantized levels, and thus its output is free of channel noise.

In this chapter, due to the properties of the DFE, we will present a precoder/decoder design, which can acquire the minimum bit error rate and maximum information rate performances simultaneously. We summarize now the main result of this chapter:

- We first introduce the system model for our nonlinear block communication system.
- Then we use the Lagrangian optimizing method and subject to the transmit power constraint to obtain the optimum structure of precoder matrix $\mathbf{F}$ which can maximize the information rate.
- In addition, based on the maximum information rate design, we further present how to minimize the bit error rate by adopting the minimum mean-squared error criterion and add the discrete fourier transform (DFT) matrix at both the precoder and decoder sides. Therefore, our transceiver becomes a DFT-based transceiver. All of these not only ensure that the bit error rate (BER) is minimized, but also guarantee

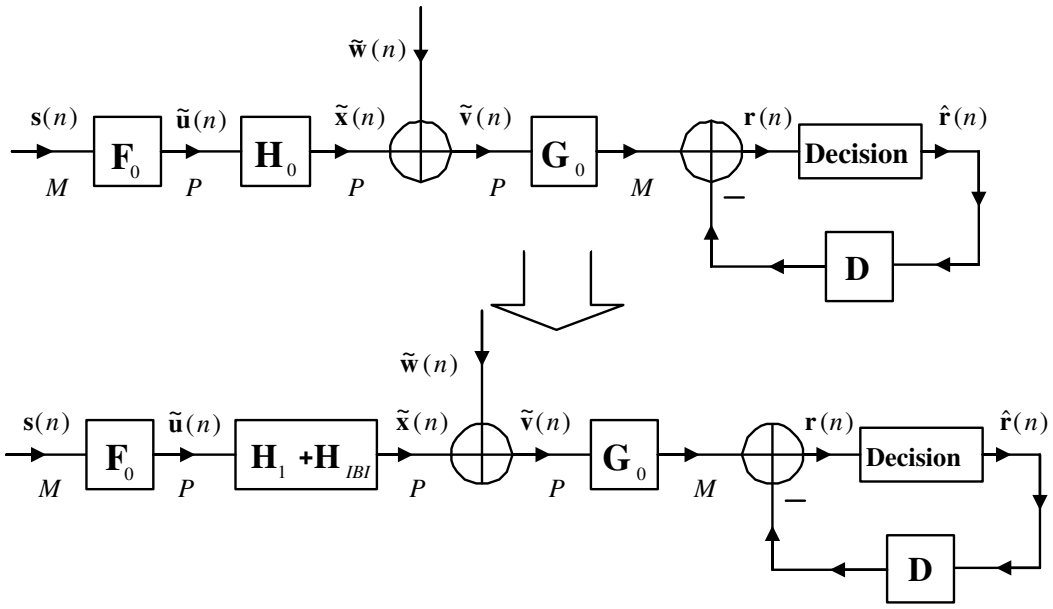

Figure 4.1: Nonlinear Block Transmissions Communication System

that the information rate is maximized.

4.2 System Model

Figure 4.1 depicts a block transmission communication system with M parallel data symbols being precoded to form P parallel channel symbols. In the system, we assume that a block of M data symbols $\mathbf{s}(n) \triangleq [s(nM)\ s(nM+1)\ ...\ s(nM+M-1)]^T$ is transformed to a block of P data symbols $\tilde{\mathbf{u}}(n) \triangleq [\tilde{u}(nP)\ \tilde{u}(nP+1)\ ...\ \tilde{u}(nP+P-1)]^T$ after being inserted the redundancy by the precoder $\mathbf{F}_0$. Subsequently, the data symbols are transmitted across the communication channel $\mathbf{H}_0$, which is an L^{th} order FIR channel with the impulse response $h(n) = 0$, when $n < 0$ and $n > L$,

and we define $P = M + L$. At the decoder side, a block of P data symbols $\tilde{\mathbf{v}}(n) = \tilde{\mathbf{x}}(n) + \tilde{\mathbf{w}}(n) = \mathbf{H}_0\tilde{\mathbf{u}}(n) + \tilde{\mathbf{w}}(n)$ is re-constructed to get the final received block of M data symbols $\mathbf{r}(n)$ where the L cyclic prefix are elinimated by the decoder $\mathbf{G}_0$. The $P \times 1$ additive white Gaussian noise vector $\tilde{\mathbf{w}}(n)$ is defined as $\tilde{\mathbf{w}}(n) \triangleq [\tilde{w}(nP)\ \tilde{w}(nP+1)\ ...\ \tilde{w}(nP+P-1)]^T$. The noise is independent of the transmitted symbols and has the correlation matrix $\mathbf{R}_{\tilde{w}\tilde{w}} \triangleq \mathrm{E}(\tilde{\mathbf{w}}\tilde{\mathbf{w}}^H)$. We assume the channel is time invariant and the channel knowledge is known apriori at both the precoder and the decoder sides. Hence, a cyclic prefixed (CP) transmission method can be used to eliminate the inter-block interference (IBI). CP method simply discards the first L entries in the block $\tilde{\mathbf{v}}(n)$ and gets $\mathbf{v}(n)$. Therefore, according to Chapter 2, we can have the precoder and decoder matrices defined as following

$$\mathbf{F}_0 \triangleq \left[\begin{array}{cc} [\mathbf{0}_{L\times(M-L)}\ \mathbf{I}_{L\times L}] & \mathbf{F}_{M\times M} \end{array} \right]^T_{P\times M} \tag{4.1}$$

which is a $P \times M$ "tall" matrix and the decoder matrix is

$$\mathbf{G}_0 \triangleq \left[\begin{array}{cc} \mathbf{0}_{M\times L} & \mathbf{G}_{M\times M} \end{array} \right]_{M\times P} \tag{4.2}$$

which is an $M \times P$ "fat" matrix. $\mathbf{F}$ and $\mathbf{G}$ are both $M \times M$ matrices as defined in Chapter 3. Using the CP method to eliminate the IBI, the channel matrix, $\mathbf{H}_0$ which is a $P \times P$ matrix, can be divided into two parts. They are $\mathbf{H}_1$ and $\mathbf{H}_{IBI}$, where $\mathbf{H}_1$ and $\mathbf{H}_{IBI}$ are defined in Eqn.(3.4) and Eqn.(3.5).

Then, referring to Figure 4.1, the system model can be written as

$$\mathbf{r}(n) \triangleq \mathbf{G}_0\mathbf{H}_1\mathbf{F}_0\mathbf{s}(n) + \mathbf{G}_0\mathbf{H}_{IBI}\mathbf{F}_0\mathbf{s}(n-1) + \mathbf{G}_0\tilde{\mathbf{w}}(n) - \mathbf{D}\hat{\mathbf{r}}(n) \tag{4.3}$$

where $\mathbf{D}$ is an $M \times M$ matrix denoting the feedback filter. It should be expressed as a strictly upper triangular matrix in order to make the successive cancellation possible. $\hat{\mathbf{r}}(n)$ is a $M \times 1$ vector which denotes the output of the decision device and is defined as $\hat{\mathbf{r}}(n) \triangleq [\hat{r}(nM)\ \hat{r}(nM+1)\ ...\ \hat{r}(nM+M-1)]^T$.

Making use of the structure of $\mathbf{F}_0$ and $\mathbf{G}_0$ in Eqn.(4.1) and Eqn.(4.2), we see that $\mathbf{G}_0\mathbf{H}_{IBI}\mathbf{F}_0 = 0$ and $\mathbf{G}_0\mathbf{H}_1\mathbf{F}_0 = \mathbf{GHF}$, where $\mathbf{H}$ can be defined as

$$\mathbf{H} \triangleq \begin{bmatrix} h(0) & 0 & \dots & h(L) & \dots & h(1) \\ \vdots & h(0) & 0 & 0 & \dots & \vdots \\ h(L) & \vdots & \ddots & \vdots & \dots & h(L) \\ 0 & h(L) & \vdots & \ddots & \dots & 0 \\ \vdots & 0 & \vdots & \vdots & \ddots & \dots \\ 0 & \dots & h(L) & h(L-1) & \dots & h(0) \end{bmatrix} \tag{4.4}$$

Referring to Figure 4.2 and Eqn.(4.3), the system model can thus be written as

$$\mathbf{r}(n) \triangleq \mathbf{GHFs}(n) + \mathbf{Gw}(n) - \mathbf{D}\hat{\mathbf{r}}(n) \tag{4.5}$$

where $\mathbf{v}(n)$ and $\mathbf{w}(n)$ hold the last M entries of $\tilde{\mathbf{v}}(n)$ and $\tilde{\mathbf{w}}(n)$, respectively. Employing the standard assumption of correct past decisions [19], which means the output of the decision device is the same as the system input symbol, we obtain $\hat{\mathbf{r}}(n) = \mathbf{s}(n)$, therefore, the system model can be rewritten

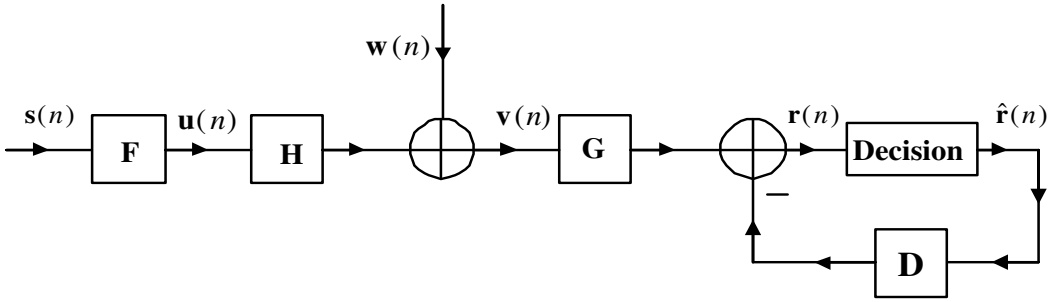

Figure 4.2: Nonlinear Block Transmissions Communication System without IBI

as

$$\mathbf{r}(n) \stackrel{\triangle}{=} (\mathbf{GHF} - \mathbf{D})\mathbf{s}(n) + \mathbf{Gw}(n) \tag{4.6}$$

In this chapter, we assume $\mathbf{w}(n)$ is the additive white Gaussian noise with autocorrelation $\mathbf{R}_{ww} = \sigma^2\mathbf{I}$ and we also assume that the transmitted symbols have been whitened and normalized to unit power, i.e. $\mathbf{R}_{ss} \stackrel{\triangle}{=} \mathrm{E}(\mathbf{ss}^H) = \mathbf{I}$, and the noise is statistically independent of the transmitted symbols.

In order to decouple the channel into M independent eigen-subchannels to handle the power of every eigen-subchannel easily, we need to make use of the eigenvalue decomposition of the channel. With the eigenvalues on the diagonal of a diagonal matrix $\mathbf{Y}$ and the corresponding eigenvectors forming the columns of a matrix $\mathbf{X}$, we introduce the following eigenvalue decomposition: $\mathbf{H}^H\mathbf{R}_{ww}^{-1}\mathbf{H} \stackrel{\triangle}{=} \mathbf{XYX}^H$, where $\mathbf{X}$ is an $M \times M$ unitary matrix, $\mathbf{Y}$ is an $M \times M$ diagonal matrix with nonnegative entries y_{ii}, $1 \leq i \leq M$.

In order to obtain the matrix $\mathbf{D}$ for the feedback filter, which is an upper triangular matrix, we need to introduce the Cholesky factorization. The Cholesky factorization expresses a symmetric matrix as the product of a

triangular matrix and its transpose. Invoking the cholesky factorization [19] of $\mathbf{H}^H\mathbf{R}_{ww}^{-1}\mathbf{H}$, we obtain

$$\mathbf{H}^H\mathbf{R}_{ww}^{-1}\mathbf{H} = \mathbf{B}^H\mathbf{B} \tag{4.7}$$

where $\mathbf{B}$ is an upper triangular matrix with unit diagonal. Since the feedback connection will not affect the precoder and decoder part, the general forms of the precoder and decoder are similar to those in linear scheme. Therefore, the $(\mathbf{F}; \mathbf{G}, \mathbf{D})$ pair is given by

$$\mathbf{F} \triangleq \mathbf{X}\mathbf{\Gamma}_f;\ \mathbf{G} \triangleq \mathbf{\Gamma}_g\mathbf{Y}^{-1}\mathbf{X}^H\mathbf{H}^H\mathbf{R}_{ww}^{-1},\ \mathbf{D} \triangleq \mathbf{B} - \mathbf{I} \tag{4.8}$$

Since $M + L = P$, and we use the power constraint to prevent negative solutions for $\mathbf{\Gamma}_f$ and $\mathbf{\Gamma}_g$, $\mathbf{\Gamma}_f$ and $\mathbf{\Gamma}_g$ are both diagonal matrices with nonnegative entries $\gamma_{f,ii}$ and $\gamma_{g,ii}$. Hence, the optimal precoder and decoder decouple the channel $\mathbf{H}$ into M independent eigen subchannels. Since $\mathbf{B}$ is an upper triangular matrix with unit diagonal and $\mathbf{I}$ is the identity matrix, here, $\mathbf{D} = \mathbf{B} - \mathbf{I}$ is set to a strictly upper triangular matrix which satisfies the definition of matrix $\mathbf{D}$ and makes successive cancellation possible. By successive cancellation we mean that for every block of $\hat{\mathbf{r}}(n)$, firstly, the $(M-1)^{th}$ symbol is recovered, then the estimated $\hat{r}(nM + M - 1)$ is weighted by the last column of $\mathbf{D}$ and is removed from $\mathbf{G}\mathbf{v}(n)$ so that the remaining symbols can be recovered. The $(M-2)^{nd}$ symbol is recovered next, and the estimate $\hat{r}(nM + M - 2)$ is removed from $\mathbf{G}\mathbf{v}(n)$. This procedure is carried out until all the symbols of the current block have been recovered. Therefore, the remaining symbols can be recovered.

4.3 Optimal Design for Non-linear DFE-based Precoders and Decoders

4.3.1 Maximum Information Rate Precoder

In chapter 3, referring to Eqn.(3.33), we have established that the normalized information rate between any transmitted and received block can be written as

$$I \triangleq \frac{1}{M}\sum_{i=1}^{M}\log_2(1+y_{ii}|\gamma_{f,ii}|^2) \tag{4.9}$$

Let $p_0 \triangleq tr(\mathbf{F}\mathbf{F}^H) = \sum_{i=1}^{M}|\gamma_{f,ii}|^2$ be the fixed transmitted power. We now maximize the above information rate subject to the transmitted power constraint. Therefore, we have

$$\max_{|\gamma_{f,ii}|} : I = \frac{1}{M}\sum_{i=1}^{M}\log_2(1+y_{ii}|\gamma_{f,ii}|^2) \tag{4.10}$$

subject to

$$\sum_{i=1}^{M}|\gamma_{f,ii}|^2 = p_0 \tag{4.11}$$

We can now use the Lagrangian optimization method to solve the above problem, the Lagrangian equation can be written as

$$\mathcal{L} = \frac{1}{M}\sum_{i=1}^{M}\log_2(1+y_{ii}|\gamma_{f,ii}|^2) + \mu(p_0 - \sum_{i=1}^{M}|\gamma_{f,ii}|^2) \tag{4.12}$$

where μ is the Lagrangian multiplier. Differentiating Eqn.(4.12) with respect to $|\gamma_{f,ii}|$ and letting the result equal to zero, we have

$$\frac{\partial \mathcal{L}}{\partial |\gamma_{f,ii}|} = 0 = \frac{1}{M} \frac{2 y_{ii} |\gamma_{f,ii}| \log_2 e}{1 + y_{ii} |\gamma_{f,ii}|^2} - 2\mu |\gamma_{f,ii}| \tag{4.13}$$

According to the transmit power constraint, we substitute Eqn.(4.13) into Eqn.(4.11) and we get (Proof, see Appendix D)

$$\mu = \frac{\log_2 e}{p_0 + tr(\mathbf{Y}^{-1})} \tag{4.14}$$

Hence, by substituting Eqn.(4.14) into Eqn.(4.13), we finally obtain

$$\mathbf{\Gamma}_{f_{MIR}} = \left(\sqrt{\frac{p_0 + tr(\mathbf{Y}^{-1})}{M} \mathbf{I} - \mathbf{Y}^{-1}} \right)_+ \tag{4.15}$$

where $(x)_+$ denotes $\max(x, 0)$. The decoder $\mathbf{\Gamma}_g$ can be designed as either a zero-forcing decoder or an MMSE decoder, as we have already known that choosing the type of the decoder will not affect the information rate.

For a zero-forcing decoder, since $\mathbf{GHF} - \mathbf{D} = \mathbf{I}$ should be satisfied, then according to Eqn.(4.8) and the eigenvalue decomposition of $\mathbf{H}^H \mathbf{R}_{ww}^{-1} \mathbf{H}$, we can obtain

$$\mathbf{\Gamma}_g \mathbf{Y}^{-1} \mathbf{X}^H \mathbf{H}^H \mathbf{R}_{ww}^{-1} \mathbf{H} \mathbf{X} \mathbf{\Gamma}_f = \mathbf{B} - \mathbf{I} + \mathbf{I} \tag{4.16}$$

$$\Longrightarrow \mathbf{\Gamma}_{g_{ZF}} = \mathbf{\Gamma}_g = \mathbf{B} \mathbf{\Gamma}_{f_{MIR}}^{-1} \tag{4.17}$$

For an MMSE decoder, it is already known that, the error vector $\mathbf{e}(n)$

at the point of the input of the decision device can be defined as $\mathbf{e}(n) \triangleq \mathbf{r}(n) - \mathbf{s}(n) = (\mathbf{GHF} - \mathbf{D} - \mathbf{I})\mathbf{s}(n) + \mathbf{Gw}(n)$ and $\mathbf{R}_{ee} \triangleq \mathrm{E}(\mathbf{ee}^H)$ is the error covariance matrix. Subject to the transmitted power constraint, we can minimize the mean-squared error of the received symbols, which is defined as

$$\mathrm{MSE} \triangleq \mathrm{E}(tr(\mathbf{ee}^H)) = tr\Big((\mathbf{GHF} - \mathbf{I} - \mathbf{D})(\mathbf{GHF} - \mathbf{I} - \mathbf{D})^H\Big) + \sigma^2 tr(\mathbf{GG}^H) \tag{4.18}$$

Since $\mathbf{GHF} = \mathbf{\Gamma}_g\mathbf{\Gamma}_f$ is a diagonal matrix, and $\mathbf{D}$ is an upper triangular matrix, $tr(\mathbf{GHFD}^H)$, $tr(\mathbf{D}(\mathbf{GHF})^H)$, $tr(\mathbf{D})$ and $tr(\mathbf{D}^H)$ are all equal to zero. Therefore, we obtain the final expression of mean-squared error (MSE)

$$\mathrm{MSE} = tr\Big(\mathbf{GHF}(\mathbf{GHF})^H - \mathbf{GHF} - (\mathbf{GHF})^H + \mathbf{DD}^H + \mathbf{I} + \sigma^2\mathbf{GG}^H\Big) \tag{4.19}$$

We obtain the MMSE optimal design by using Lagrangian method again subject to the transmit power constraint. This results in

$$\mathcal{L} \triangleq \mathrm{MSE} + \mu\Big(tr(\mathbf{FF}^H) - p_0\Big) \tag{4.20}$$

where μ is the Lagrange multiplier. Differentiating Eqn.(4.20) with respect to $\mathbf{G}$ and letting the result equal to zero, we can obtain

$$\frac{\partial\mathcal{L}}{\partial\mathbf{G}} = 0 = \mathbf{HF}(\mathbf{GHF})^H - \mathbf{HF} + \sigma^2\mathbf{G}^H \tag{4.21}$$

Pre-multiply Eqn.(4.21) by $\mathbf{G}$, therefore, we have

$$\mathbf{GHF} = \sigma^2\mathbf{GG}^H + (\mathbf{GHF})(\mathbf{GHF})^H \tag{4.22}$$

Substitute Eqn.(4.8) into Eqn.(4.22) and we finally obtain

$$\mathbf{\Gamma}_{g_{MMSE}} = \mathbf{\Gamma}_{f_{MIR}}(\mathbf{Y}^{-1} + \mathbf{\Gamma}^2_{f_{MIR}})^{-1} \tag{4.23}$$

4.3.2 Minimum Bit Error Rate Decoder

Although the MIR-DFE design maximizes the information rate, it nevertheless cannot guarantee that the average bit error rate (BER) is minimized. In this section, we will attempt to minimize the BER and at the same time ensure the information rate is also maximized. We use the MMSE criterion to minimize the BER. The average BER of the detected signal is the average of the probability of error of each element of the block, therefore, the average BER which is denoted by P_e can be obtained as [21]

$$P_e \triangleq \frac{1}{M}\sum_{m=1}^{M} P_{e,m} \approx \frac{1}{2M}\sum_{m=1}^{M} \text{erfc}\left(\frac{[\mathbf{GHF}-\mathbf{D}]_{mm}}{\sqrt{4[\mathbf{A}]_{mm}}}\right) \tag{4.24}$$

where $P_{e,m}$ is the BER of the m^{th} symbol, $[\mathbf{X}]_{mm}$ denotes the $(m,m)^{th}$ element of a matrix $\mathbf{X}$, $\mathbf{A}$ is the covariance matrix which can be expressed as

$$2[\mathbf{A}]_{mm} \triangleq \sigma^2[\mathbf{GG}^H]_{mm} \tag{4.25}$$

and $\mathrm{erfc}(x) \triangleq \frac{2}{\sqrt{\pi}} \int_x^\infty \exp(-z^2)\mathrm{d}z$ is the complementary error function. Because (**GHF**) and $(\mathbf{GHF})^H$ are diagonal matrices, we can get

$$[(\mathbf{GHF})(\mathbf{GHF})^H]_{mm} = [\mathbf{GHF}]_{mm}[(\mathbf{GHF})^H]_{mm} \tag{4.26}$$

By substituting Eqn.(4.22) into Eqn.(4.25), we can obtain

$$2[\mathbf{A}]_{mm} = [\mathbf{GHF}]_{mm} - [\mathbf{GHF}]_{mm}[(\mathbf{GHF})^H]_{mm} \tag{4.27}$$

Because we know **D** is a strictly upper triangular matrix, Eqn.(4.27) can be rewritten as

$$2[\mathbf{A}]_{mm} = [\mathbf{GHF}-\mathbf{D}]_{mm} - [\mathbf{GHF}-\mathbf{D}]_{mm}[(\mathbf{GHF}-\mathbf{D})^H]_{mm} \tag{4.28}$$

Therefore, substituting Eqn.(4.28) into Eqn.(4.24), we can obtain the following expression

$$P_e \approx \frac{1}{2M}\sum_{m=1}^{M} \mathrm{erfc}\left(\frac{[\mathbf{GHF}-\mathbf{D}]_{mm}}{\sqrt{2[\mathbf{GHF}-\mathbf{D}]_{mm} - 2[\mathbf{GHF}-\mathbf{D}]_{mm}[(\mathbf{GHF}-\mathbf{D})^H]_{mm}}}\right)$$

$$\Longrightarrow P_e \approx \frac{1}{2M}\sum_{m=1}^{M} \mathrm{erfc}\left(\left(\left[\frac{2[\mathbf{I}]_{mm}}{[\mathbf{GHF}-\mathbf{D}]_{mm}}\right] - 2[\mathbf{I}]_{mm}\right)^{-\frac{1}{2}}\right) \tag{4.29}$$

Now, we define $\mathbf{\Phi} \triangleq \Big(diag(\mathbf{GHF}-\mathbf{D})\Big)^{-1}$ and apply Jensen's inequality [14], (proved in Appendix A) thus, Eqn.(4.29) can be expressed as

$$P_e \approx \frac{1}{2M}\sum_{m=1}^{M}\text{erfc}\bigg(\Big(2[\mathbf{\Phi}-\mathbf{I}]_{mm}\Big)^{-\frac{1}{2}}\bigg) \geq \frac{1}{2}\text{erfc}\bigg(\Big(\frac{2}{M}\Big(tr(\mathbf{\Phi})-M\Big)\Big)^{-\frac{1}{2}}\bigg) \tag{4.30}$$

where $diag(\mathbf{GHF}-\mathbf{D})$ is a diagonal matrix whose elements are $(\mathbf{GHF}-\mathbf{D})_{mm}$, $m \in [1, M]$. Because $\text{erfc}(x)$ is a monotonically decreasing function, minimizing P_e is comparable to maximizing $tr\Big(diag(\mathbf{GHF})\Big)$. With regards to Eqn.(4.19) and Eqn.(4.22) and using the properties of getting the trace of a matrix, we can see that minimizing the MSE is equivalent to maximizing the $tr(\mathbf{GHF})$. In other words, minimizing P_e is equivalent to minimizing the MSE. Because we adopt MMSE criterion in this section, the BER can be minimized.

In addition, we must check whether P_e has a minimum value, otherwise, minimizing P_e will become meaningless. We can see that only if P_e is a convex function, it will have a minimum value. Therefore, to prove P_e is a convex function becomes important. Firstly, we can define $f(x) = \text{erfc}\Big(\frac{1}{\sqrt{2x}}\Big)$, $x > 0$ which has the same form as P_e. We can obtain

$$\frac{\partial^2 f}{\partial x^2} = \frac{1}{\sqrt{2\pi}}\exp\Big(-\frac{1}{2x}\Big)x^{-\frac{5}{2}}\Big(\frac{1}{2x}-\frac{3}{2}\Big) \tag{4.31}$$

when $x < \frac{1}{3}$, $\frac{\partial^2 f}{\partial x^2} > 0$ and $f(x)$ becomes a convex function. Thereby, P_e also becomes a convex function when $\Big[(\mathbf{GHF})^{-1}-\mathbf{I}\Big]_{mm} < \frac{1}{3}$. So we finally obtain: if $[\mathbf{GHF}]_{mm} > \frac{3}{4}$, $\forall m \in [1, M]$, P_e will be a convex function and have

a minimum value.

By taking the definition given in Eqn.(4.8), we get

$$\mathbf{GHF} = \mathbf{\Gamma}_g \mathbf{\Gamma}_f \stackrel{\triangle}{=} \mathbf{\Gamma} \tag{4.32}$$

where $\mathbf{\Gamma} \stackrel{\triangle}{=} \mathbf{\Gamma}_g \mathbf{\Gamma}_f$ is a diagonal matrix because both $\mathbf{\Gamma}_g$ and $\mathbf{\Gamma}_f$ are diagonal matrices. Now we only need to ensure that every diagonal element of $\mathbf{\Gamma}$ is greater than $\frac{3}{4}$ in order to guarantee that P_e is a convex function. Referring to Lemma 1 in [30], we can obtain the following:

For an $M \times M$ positive semi-definite(symmetric) matrix $\mathbf{E}$ which can be eigenvalue decomposed as $\mathbf{E} = \mathbf{\Phi T \Phi}^H$, where $\mathbf{T}$ is a diagonal matrix whose diagonal elements are the eigenvalues of $\mathbf{E}$ and $\mathbf{\Phi}$ is the unitary matrix, that is $\mathbf{\Phi \Phi}^H = \mathbf{I}$, which contains the eigenvectors of $\mathbf{E}$, we can get:

$$\max_{\mathbf{V V}^H = \mathbf{I}} \min[\mathbf{V}^H \mathbf{E V}]_{mm} = tr(\mathbf{E})/M \tag{4.33}$$

and the maximum value of Eqn.(4.33) can be achieved by choosing

$$\mathbf{V} = \mathbf{\Phi L} \tag{4.34}$$

where $\mathbf{L}$ denotes the $M \times M$ (normalized) DFT matrix and we can obtain $\mathbf{V}^H \mathbf{E V} = \mathbf{L}^H \mathbf{T L}$. Therefore, we see that if $\mathbf{T}$ is a diagonal matrix, we can find a DFT matrix $\mathbf{L}$ to maximize the minimum diagonal element of $\mathbf{T}$ and make all the diagonal entries of $\mathbf{T}$ equal.

Proof: see Appendix B.

So we can maximize the minimum value of $\mathbf{\Gamma}$ and make all the diagonal entries of $\mathbf{\Gamma}$ equal, mathematically expressed as

$$\max_{\mathbf{L}\mathbf{L}^H=\mathbf{I}} \min[\mathbf{L}^H\mathbf{\Gamma}\mathbf{L}]_{mm} = tr(\mathbf{\Gamma})/M > 3/4 \tag{4.35}$$

The maximum value in Eqn.(4.35) can be achieved by setting $\mathbf{L}$ as a normalized $M \times M$ Discrete Fourier Transform (DFT) matrix, which is obtained from the eigenvalue decomposition of $\mathbf{H} = \mathbf{L}^H\mathbf{\Lambda}\mathbf{L}$, where $\mathbf{\Lambda}$ is the diagonal matrix holding the corresponding eigenvalues of $\mathbf{H}$. Therefore, the system model comes up to concatenate a DFT matrix and an inverse DFT (IDFT) matrix at the precoder and the decoder side, respectively, shown in Figure 4.3. We still make the precoder $\mathbf{\Gamma}_f = \mathbf{\Gamma}_{f_{MIR}}$, $\mathbf{F}_{MIR} = \mathbf{X}\mathbf{\Gamma}_{f_{MIR}}$ which denotes an MIR precoder and the decoder $\mathbf{\Gamma}_{g_{MMSE}} = \mathbf{\Gamma}_{f_{MIR}}(\mathbf{Y}^{-1} + \mathbf{\Gamma}^2_{f_{MIR}})^{-1}$, $\mathbf{G}_{MMSE} = \mathbf{\Gamma}_{g_{MMSE}}\mathbf{Y}^{-1}\mathbf{X}^H\mathbf{H}^H\mathbf{R}_{ww}^{-1}$, which denotes an MMSE decoder. So by employing both the MIR precoder matrix and the MMSE decoder matrix, we can see that the precoder is an MIR precoder and the decoder is an MMSE decoder with specially chosen unitary matrices $\mathbf{L}$ and $\mathbf{L}^H$. Therefore, the information rate is maximized while the bit error rate is also minimized.

4.4 Summary

In this chapter, we have presented a method to design the precoder matrix $\mathbf{F}$ by ensuring that maximum information rate is achieved. By applying

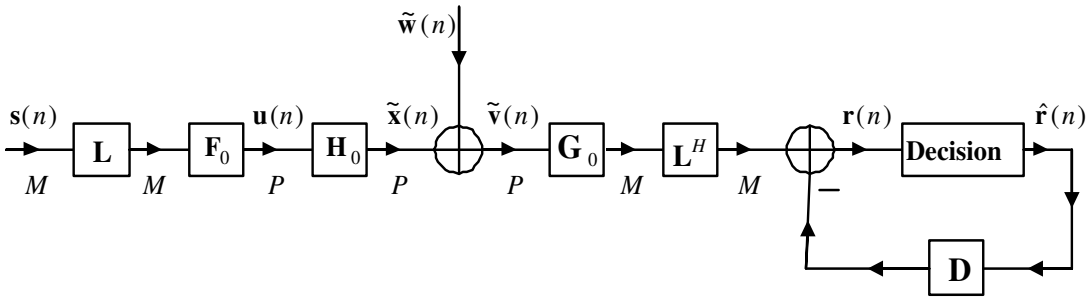

Figure 4.3: Block Transmissions Communication System Concatenated with DFT Matrix

the Lagrangian method subject to the transmit power constraint, we maximize the information rate and achieve it in our design. Moreover, since the error probability P_e is a convex function and has the minimum value, we can make use of the MMSE criterion and DFT matrix to obtain the minimum bit error rate and keep $\mathbf{\Gamma}_f$ the same as which we got from MIR-DFE design to achieve optimum information rate simultaneously. In the next chapter, we will present our simulation results to show the advantages of our various optimal designs and make discussions.

Chapter 5

Simulation Results and Discussions

5.1 Introduction

In this chapter, We will provide some numerical examples that illustrate the performance of our optimal designs under the transmit power constraint. The performance measures include information rate, mean-squared error and bit error rate. As we know from Chapter 3, the information rate can be expressed as

$$I = \frac{1}{M}\log_2\left(\prod_{i=1}^{M}(1+y_{ii}|\gamma_{f,ii}|^2)\right) = \frac{1}{M}\sum_{i=1}^{M}\log_2(1+y_{ii}|\gamma_{f,ii}|^2) \qquad (5.1)$$

which can be used to compute the information rate for different design such as MIR design, MMSE design and MBER design. The MSE equation can be

obtained from Chapter 2 and is expressed as the following

$$\text{MSE} \triangleq \text{E}(tr(\mathbf{e}\mathbf{e}^H)) = tr\Big((\mathbf{GHF}-\mathbf{I})(\mathbf{GHF}-\mathbf{I})^H\Big) + \sigma^2 tr(\mathbf{G}\mathbf{G}^H) \quad (5.2)$$

and it coincides with the cumulative MSE over the M independent subchannels and is given by

$$\text{MSE} = \sum_{i=1}^{M}\left[|\gamma_{g,ii}\gamma_{f,ii}-1|^2 + \frac{|\gamma_{g,ii}|^2}{y_{ii}}\right] \quad (5.3)$$

for the MMSE decoder where $\mathbf{\Gamma}_g = \mathbf{\Gamma}_f(\mathbf{Y}^{-1}+\mathbf{\Gamma}_f^2)^{-1}$, the MSE can be written as

$$\text{MSE} = \sum_{i=1}^{M}\frac{1}{1+|\gamma_{f,ii}|^2 y_{ii}} \quad (5.4)$$

and the BER expression for the nonlinear precoder/decoder design can be shown as

$$P_e \triangleq \frac{1}{2M}\sum_{m=1}^{M}\text{erfc}\left(\frac{[\mathbf{GHF}-\mathbf{D}]_{mm}}{\sqrt{2\sigma^2[\mathbf{G}\mathbf{G}^H]_{mm}}}\right) \quad (5.5)$$

which is obtained from Chapter 4. Relying on these performance measures, we adopt the following channel model.

Channel Model: For most of our simulations, we use the third order FIR channel since it is widely adopted by many research works. The channel order is $L = 3$ for the impulse response samples beyond the 3^{rd} are statistically very small. The channel $\mathbf{H}$ is assumed known at the transmitter and receiver sides with full rank and well conditioned. We normalize the total transmission power $p_0 = 1$. The noise is white Gaussian noise and its autocorrelation is

$\mathbf{R}_{ww} = \sigma^2\mathbf{I}$ and the transmitted symbols have been normalized to unit power, so its autocorrelation matrix should be $\mathbf{R}_{ss} = \mathbf{I}$, the horizontal axis in the plots that follow is the average block SNR (in decibels) which can be defined as

$$\text{SNR} \triangleq \frac{\text{Total transmitted power}}{\text{received noise}} = \frac{tr(\mathbf{F}\mathbf{F}^H)}{\sigma^2} \tag{5.6}$$

5.2 Performances of Linear Schemes

5.2.1 Information Rate Performance

Table 5.1: Comparison of Information Rate between MIR Design and MMSE Design Using Random Generated Channels

SNR(dB)	I_{MMSE_5}	I_{MIR_5}	I_{MMSE_7}	I_{MIR_7}	$I_{MMSE_{10}}$	$I_{MIR_{10}}$
2	0.8395	1.0487	0.9639	1.2063	1.1038	1.3835
4	0.9911	1.2211	1.1305	1.3965	1.2578	1.5417
6	1.1491	1.3579	1.3062	1.5735	1.3884	1.6555
8	1.3932	1.6194	1.5434	1.8187	1.6211	1.9069
10	1.6759	1.9116	1.9038	2.1914	1.9524	2.2385
12	1.9972	2.2378	2.2088	2.4827	2.3184	2.5978
14	2.4348	2.6875	2.6222	2.8872	2.7740	3.0404
16	2.9528	3.2002	3.0698	3.3573	3.2081	3.4925
18	3.4235	3.6609	3.5971	3.8633	3.7536	4.0454
20	3.9822	4.2255	4.2058	4.4633	4.3225	4.5949
22	4.4829	4.7068	4.7443	4.9933	4.9085	5.1937
24	5.1364	5.3628	5.3755	5.6279	5.4686	5.7454

For the weighted information rate design, it is known that if $\mathbf{\Gamma}_f$ is chosen according to the well-known water-pouring solution, the information rate will be maximized. Hence by choosing the weighted matrix $\mathbf{T} = \mathbf{I}$, the maximum information rate design can be obtained. We will analyze the information rate

performance using different channels. Firstly, we consider three randomly generated channels with the data block length $M = 5, 7, 10$, respectively. The complex valued taps of the channels are generated independently from a zero-mean Gaussian distribution with unit variance. The information rate performance curves for MMSE design and MIR design are averaged over 500 channel realizations. And the precoder allocates power on the $M = 5, 7, 10$ eigen subchannels using the water-pouring solution. Using Eqn.(5.1), we compute the information rate of the MIR design (I_{MIR_5}, I_{MIR_7}, $I_{MIR_{10}}$) and the MMSE design (I_{MMSE_5}, I_{MMSE_7}, $I_{MMSE_{10}}$) for these three different channels, respectively, and we can see the improvements of the information rate which are shown in the Figure 5.1-Figure 5.3. Figure 5.1 shows the improvement of the information rate when the transmitted data block length $M = 5$. Figure 5.2 and Figure 5.3 also show the information rate performance when the $M = 7$ and $M = 10$, respectively. Table 5.1 shows the values of the information rate in details and make a comparison of the information rate between the maximum information rate design and MMSE design of different channels under different values of SNRs. The results were obtained by averaging the MSEs over 500 channels.

From Figure 5.1-Figure 5.3 and Table 5.1, we can obtain that when the transmitted symbol block length is 5, the average improvement of the information rate between maximum information rate design and MMSE design over different SNRs is around 0.2318 $bit/symbol$, while if the block length increases to 7, the improvement increases to 0.2658 $bit/symbol$, and for $M = 10$, it increases to 0.2799 $bit/symbol$. We can observe that the im-

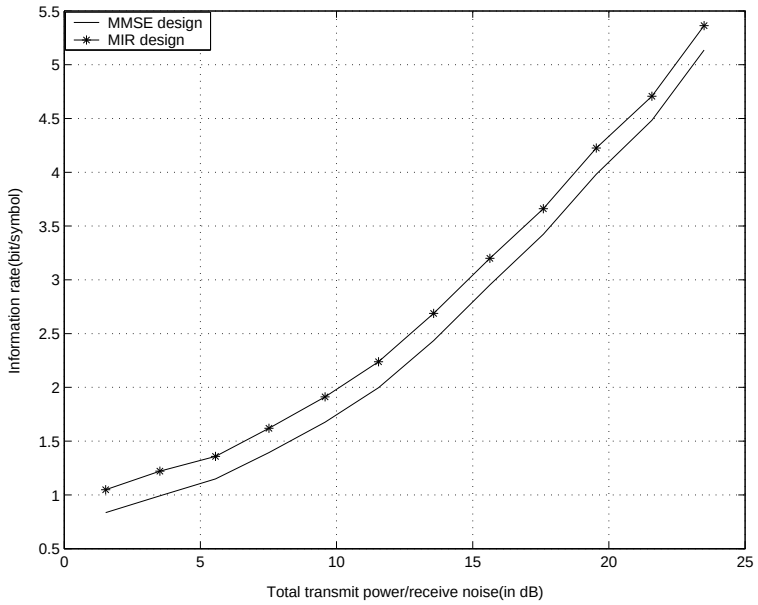

Figure 5.1: Information Rate Performance of MIR Design and MMSE Design With $M = 5$

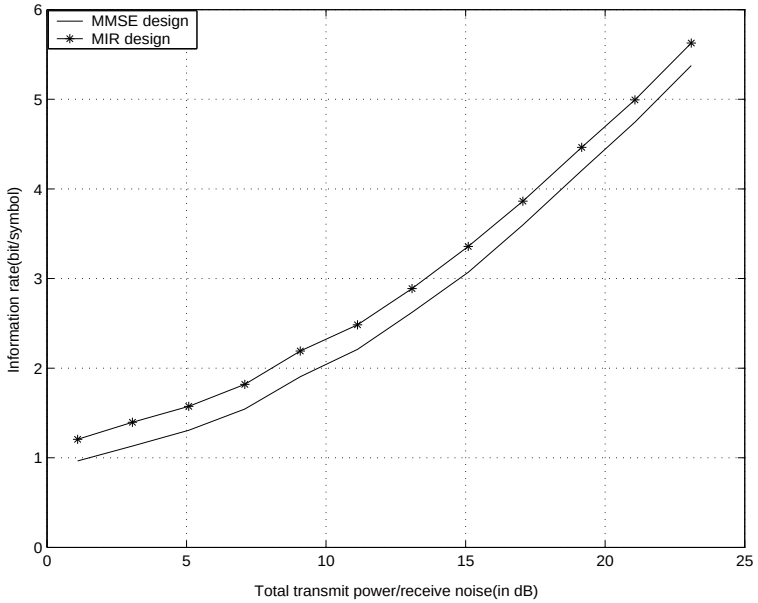

Figure 5.2: Information Rate Performance of MIR Design and MMSE Design With $M = 7$

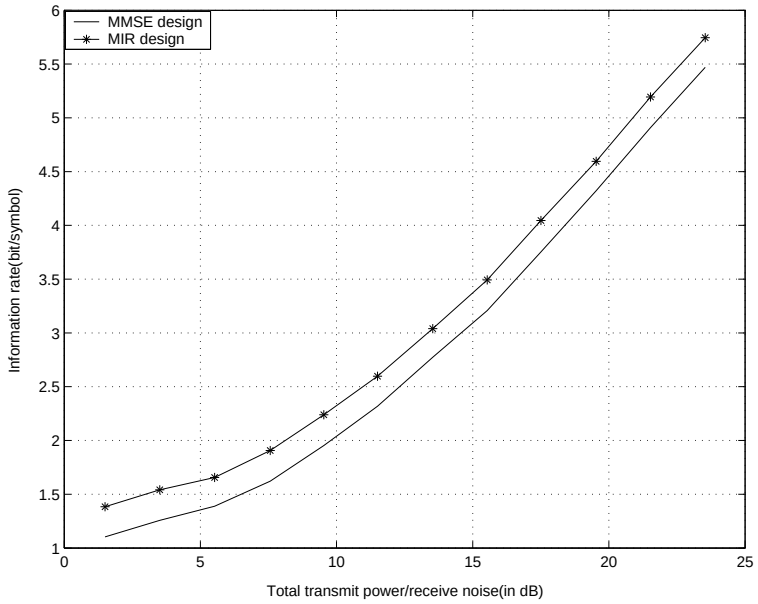

Figure 5.3: Information Rate Performance of MIR Design and MMSE Design With $M = 10$

provement of the information rate between MIR design and MMSE design is increasing when the transmitted data block length increases. The increasing of the transmitted data block length M can be considered as increasing the number of subchannels while we multiply the transmitted data block with the $M \times M$ precoder matrix $\mathbf{F}$. It means the data can be transmitted from the transmitter through more subchannels to the receiver if we increase M. Therefore, this can be the reason why our performance improves as M increases.

Secondly, we consider two FIR channels a_1 and a_2 with tap coefficients $a_1 : \{1, 0.5348+0.4494j, 0.3701j, -0.0515+0.0389j\}$, $a_2 : \{-0.0667-0.1824j, 0.3194-0.1801j, 0.4687+0.0399j, 0.0258+0.2870j\}$, respectively. These two FIR channels are generated by us. The channel order is three and the trans-

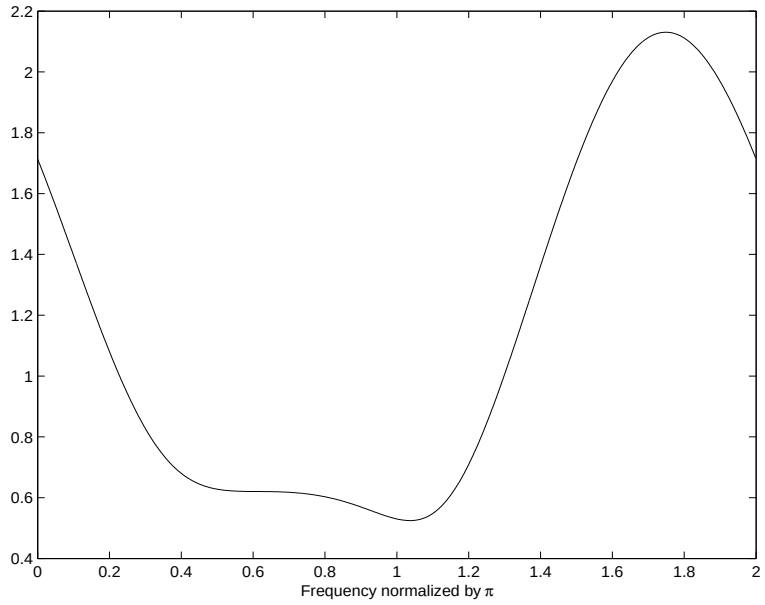

Figure 5.4: Frequency Response of Channel a_1

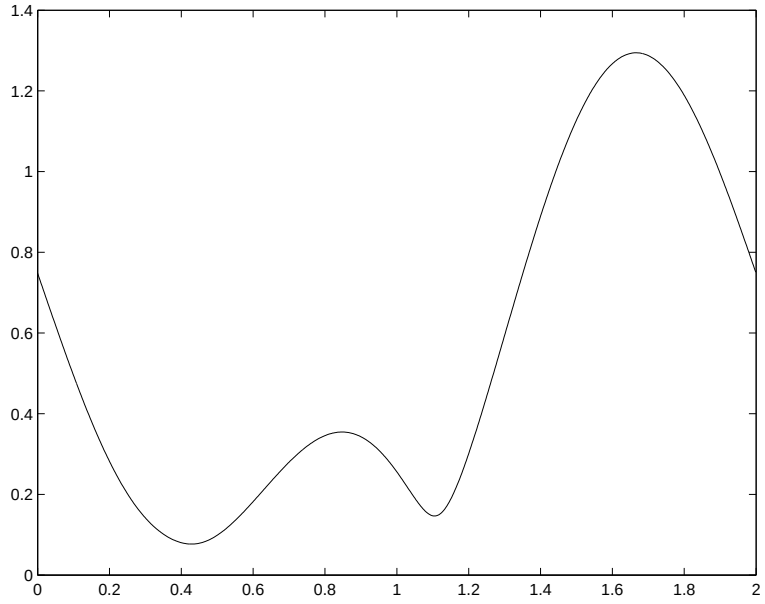

Figure 5.5: Frequency Response of Channel a_2

Table 5.2: Comparison of Information Rate between MIR Design and MMSE Design Using Channels a_1 and a_2

SNR(dB)	$I_{MMSE_{a_1}}$	$I_{MIR_{a_1}}$	$I_{MMSE_{a_2}}$	$I_{MIR_{a_2}}$
2	1.3203	1.4923	1.1093	1.5620
4	1.6529	1.8249	1.1646	1.6173
6	2.0740	2.2460	1.2467	1.6994
8	2.5664	2.7384	1.3737	1.8263
10	3.0975	3.2695	1.5487	2.0014
12	3.6839	3.8559	1.7931	2.2458
14	4.2754	4.4474	2.1071	2.5598
16	4.9050	5.0770	2.4893	2.9420
18	5.5356	5.7076	2.9469	3.3996
20	6.1841	6.3561	3.4712	3.9239
22	6.8578	7.0298	4.0355	4.4882
24	7.5084	7.6804	4.6252	5.0779

mitted data block length is $M = 7$. We just choose these two FIR channels as the examples to testify the results of our design. For channel a_1, the ratio of the largest to the smallest frequency response is around 4, and for channel a_2, its frequency response range is around 13 which means it is more frequency selective than channel a_1. More frequency selective means the coherent bandwidth (bandwidth of channel) becomes smaller compared to the transmitted signal bandwidth, it will distort the signal and eventually affect the detection of symbol. Thus, the information rate performance is influenced. The frequency responses of these two channels are shown in Figure 5.4 and Figure 5.5, respectively. Figure 5.6 and Figure 5.7 present the information rate performances of MIR design and MMSE design of these two channels. Table 5.2 also shows the data of the information rate in details. From Figure 5.6, Figure 5.7 and Table 5.2, we can observe that when we use channel a_1, the improvement of the information rate between MIR design and MMSE design over different SNRs is around 0.1720 $bit/symbol$. It is much smaller than

the one when we use channel a_2 which is 0.4527 $bit/symbol$. In addition, the information rate increases from 1.4923 $bit/symbol$ to 7.6804 $bit/symbol$ for the MIR design using channel a_1 and it increases from 1.5620 $bit/symbol$ to 5.0779 $bit/symbol$ for the MIR design using channel a_2 within the same SNR region. Therefore, we can conclude that as the channel becomes more frequency selective, the improvement of the information rate will be more obvious. Moreover, the information rate increases much faster for channel a_1 than it does for channel a_2. As we know, the information rate is an increasing function of $\mathbf{\Gamma}_f$ and $\mathbf{\Gamma}_f$ is a non-negative diagonal matrix. During the process of computing $\mathbf{\Gamma}_f$, the negative values will be replaced by zeros, hence, the corresponding subchannels will be discarded and will not be used to transmit the information. As the SNR increases, the values of the diagonal elements of $\mathbf{\Gamma}_f$ will also increase, thus more subchannels can be recovered and used to transmit the information. For channel a_1, the recovery speed is faster than channel a_2 because the channel a_1 is less frequency selective and has less affection on the distortion of the transmitted signal. Therefore, we can observe from the simulation results that the information rate increases much faster for channel a_1. Our designs are based on the time-invariant FIR channel. If the channel is time-varying, neither convolution nor frequency-domain multiplication can be used to calculate signal transmission through the channel.

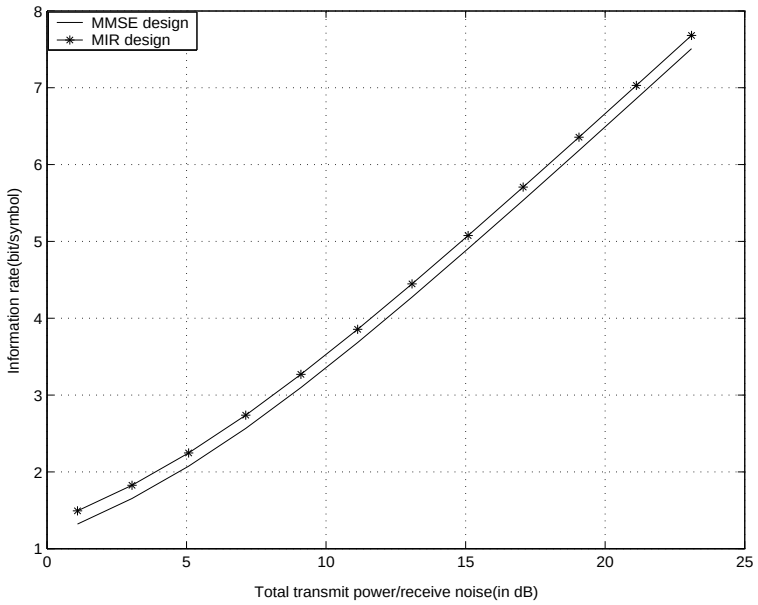

Figure 5.6: Information Rate Performance of MIR Design and MMSE Design Using Channel a_1

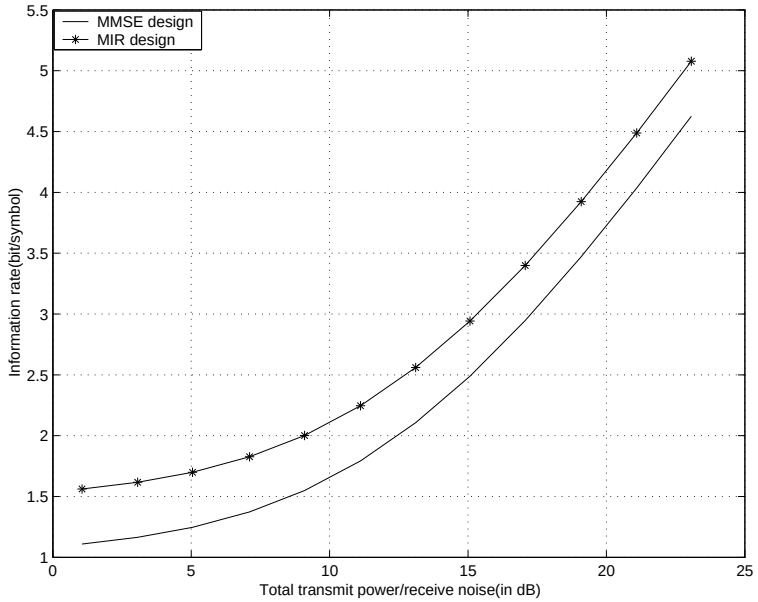

Figure 5.7: Information Rate Performance of MIR Design and MMSE Design Using Channel a_2

5.2.2 Mean-Squared Error Performance

If the weight matrix is set to $\mathbf{T} = \mathbf{Y}^{-\frac{1}{2}}$, then MMSE design is achieved. The following simulation results will compare the MSE performance of MMSE design and MIR design. Firstly, we consider two FIR channels with the transmitted symbol block size $M = 7$. The first is channel a_1 with four tap coefficients $\{1, 0.5348+0.4494j, 0.3701j, -0.0515+0.0389j\}$. The second one is a random generated channel. The complex valued taps of the channels are generated independently from a zero-mean Gaussian distribution with unit variance. We average over 500 random channel realizations to obtain our results. Figure 5.8 and Figure 5.9 compare the mean-squared error of the maximum information rate (MIR) design and the MMSE design according to different channels, respectively. It can be seen from both of the figures that the mean-squared error performance of MMSE design is better when compared to the MIR design. The improvement of the MSE is much more obvious when we use a randomly generated channel. From Figure 5.9, we can see the SNR gain for MMSE design over MIR design at the MSE of 0.2 is around 2.5 dB. It is larger than 1 dB for the fixed channel a_1 from Figure 5.8. Thus, we can say that the MMSE design doesn't deteriorate as much as MIR design when the channel becomes random. However, no matter which channel we use, the improvement of the mean-squared error between MMSE design and MIR design is considerable.

Secondly, we consider three randomly generated FIR channels with the transmitted data block size $M = 5, 7, 10$, respectively. Figure 5.10, Figure 5.9 and Figure 5.11 present the MSE performance of MMSE design and

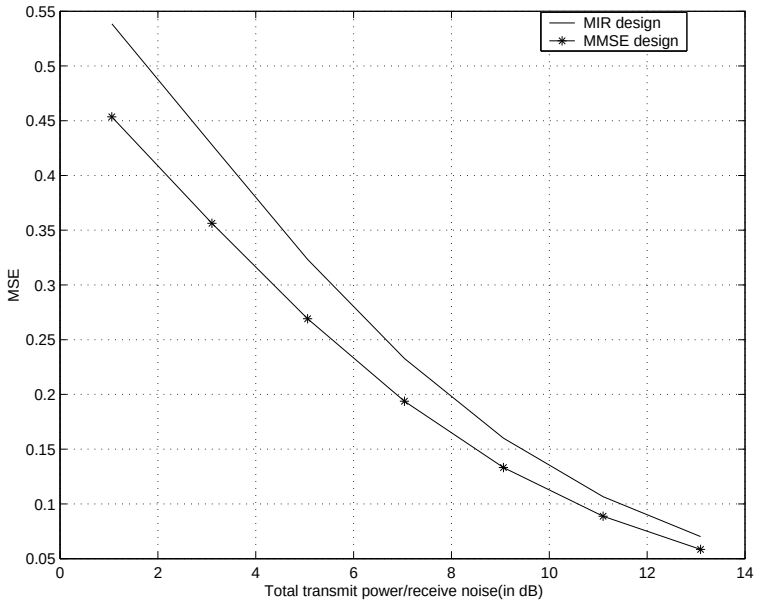

Figure 5.8: Mean-Squared Error Performance of MIR Design and MMSE Design for Channel a_1

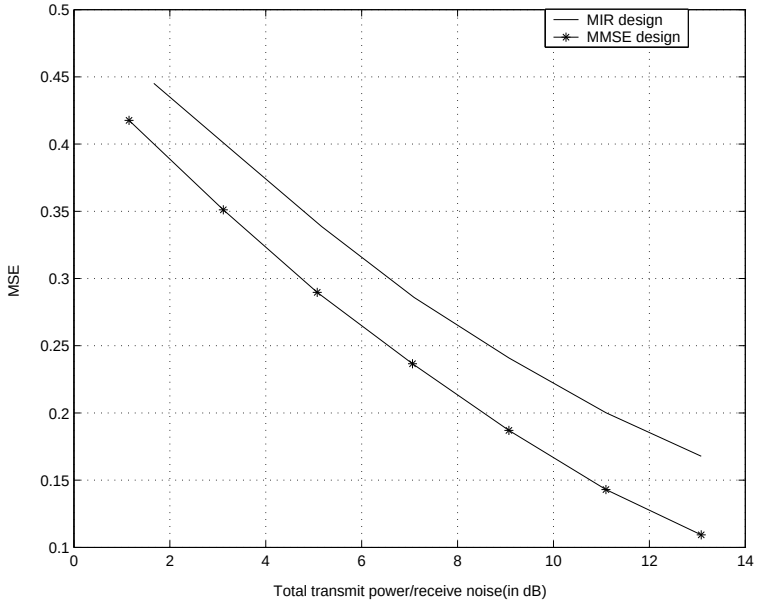

Figure 5.9: Mean-Squared Error Performance of MIR Design and MMSE Design for Randomly Generated Channel With $M = 7$

Table 5.3: Comparison of Mean-Squared Error between MMSE Design and MIR Design Using Randomly Generated Channels

SNR(dB)	E_{MMSE_5}	E_{MIR_5}	E_{MMSE_7}	E_{MIR_7}	$E_{MMSE_{10}}$	$E_{MIR_{10}}$
1	0.4895	0.5175	0.4187	0.4464	0.3838	0.4117
3	0.4159	0.4568	0.3513	0.3943	0.3188	0.3586
5	0.3517	0.3974	0.2891	0.3377	0.2606	0.3101
7	0.2918	0.3359	0.2326	0.2844	0.2121	0.2643
9	0.2374	0.2906	0.1878	0.2417	0.1641	0.2168
11	0.1878	0.2446	0.1444	0.1988	0.1281	0.1809
13	0.1373	0.1989	0.1087	0.1650	0.0940	0.1474

MIR design according to these three channels. Table 5.3 shows the data of MSE of MMSE design (E_{MMSE_5}, E_{MMSE_7}, $E_{MMSE_{10}}$) and MIR design (E_{MIR_5}, E_{MIR_7}, $E_{MIR_{10}}$) of different transmitted data block sizes under different SNRs in details. The results were obtained by averaging the MSEs over 500 channels. From Figure 5.9-Figure 5.11 and Table 5.3, we can observe that the MSE performance improves as the size of transmitted data block increases. At the same SNR, the MSE of the channel with $M = 10$ is the smallest and the MSE of the channel with $M = 7$ is also smaller than the MSE of the channel with $M = 5$. The performance improvement can be attributed to the increase in transmit diversity and array gain with the increase in number of subchannels.

Therefore, generally we can conclude that for a perfect channel, the information rate performance of the MMSE design does not deteriorate too much comparing to the MIR design. We can see this from Figure 5.6. Thus, if the transmission information rate is not an important requirement but a good MSE performance is in great need, the MMSE design is an ideal choice. However, if the channel becomes more frequency selective, and the

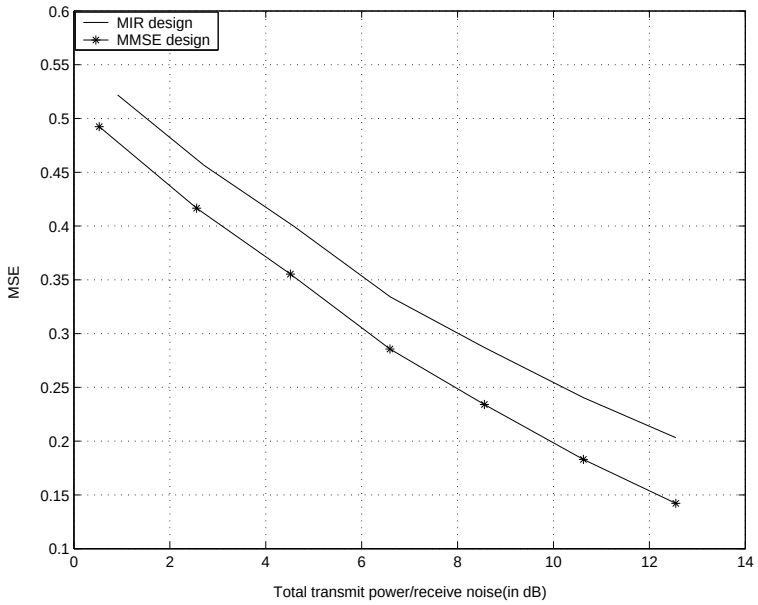

Figure 5.10: Mean-Squared Error Performance of MIR Design and MMSE Design for Randomly Generated Channel With $M = 5$

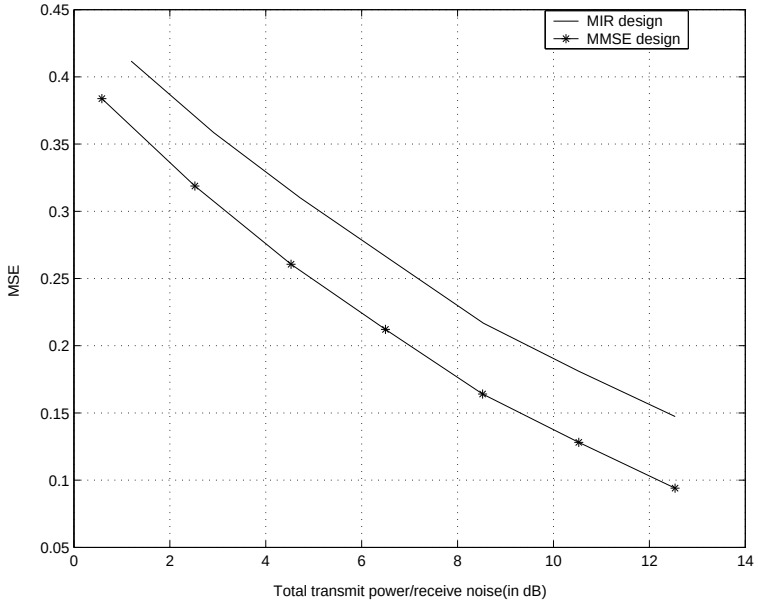

Figure 5.11: Mean-Squared Error Performance of MIR Design and MMSE Design for Randomly Generated Channel With $M = 10$

information rate performance is significant for us, the MIR design shall be presented and we can get a much better information rate performance. We can observe this from Figure 5.7. Maximizing the information rate is the only objective for MIR design, not for MMSE design. We will show the design which can maximize the information rate and minimize the bit error rate simultaneously later in our nonlinear part. Therefore, the MIR design and MMSE design are two optimal designs and from the simulation results we observe that we can obtain them through our weighted information rate design by choosing the weight matrix $\mathbf{T}$ accordingly.

5.2.3 Subchannel SNR Performance

For a multimedia application, where different types of information need to be transmitted simultaneously on different subchannels, we need to apply the QoS based design to have subchannels with different SNRs to ensure the successful transmission [24]. We consider an FIR channel and we transmit $M = 3$ independent symbol streams. The channel is generated randomly. The complex valued taps of the channels are generated independently from a zero-mean Gaussian distribution with unit variance. Each channel realization is then normalized so that the impulse response has unit norm. We can define the relative SNR matrix $\mathbf{Q}$ as following

$$\mathbf{Q} = \begin{bmatrix} \frac{1}{2} & 0 & 0 \\ 0 & \frac{1}{3} & 0 \\ 0 & 0 & \frac{1}{6} \end{bmatrix} \tag{5.7}$$

The matrix $\mathbf{Q}$ shows the relative SNR of every subchannel. It presents the interrelation of the SNR of each subchannel. We can see that the first subchannel requires the highest SNR of all the subchannels and the second subchannel requires more SNR than the third subchannel but less SNR than the first subchannel. Figure 5.12 illustrates the performance of the QoS based design, which indeed guarantees that the SNR of subchannel 1 is 2 dB higher than subchannel 2 and is 4.5 dB higher than subchannel 3. This meets our pre-requirements described in matrix $\mathbf{Q}$. From Figure 5.13, we can observe the relations of subchannel SNRs according to matrix $\mathbf{Q}$ more clearly where the SNR of the first subchannel is 1.5 times of the second subchannel and is 3 times of the third subchannel. Our results are obtained by averaging over 5,000 channel realizations. The optimal linear precoder and decoder are optimized for each channel realization. Figure 5.14 shows the subchannel SNRs of MMSE design. For MMSE design, we have known from Section 5.2.1 that the corresponding subchannels will be discarded due to the negative values of $\mathbf{\Gamma}_f$. Therefore, we can see from Figure 5.14 that subchannel 5 has been discarded. However, if we use QoS based design, we can make use of these five subchannels according to different subchannel SNR requirements without discarding any subchannels.

5.3 Performances of Nonlinear Schemes

In this section, we will make comparisons of the information rate and bit error rate performances between two DFE based optimal designs, such as

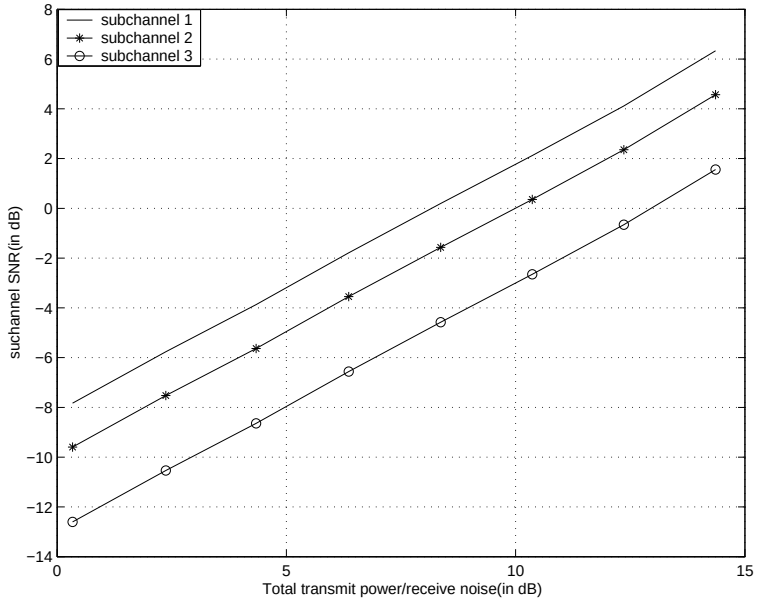

Figure 5.12: Subchannel SNR Performance of QoS Based Design(in dB)

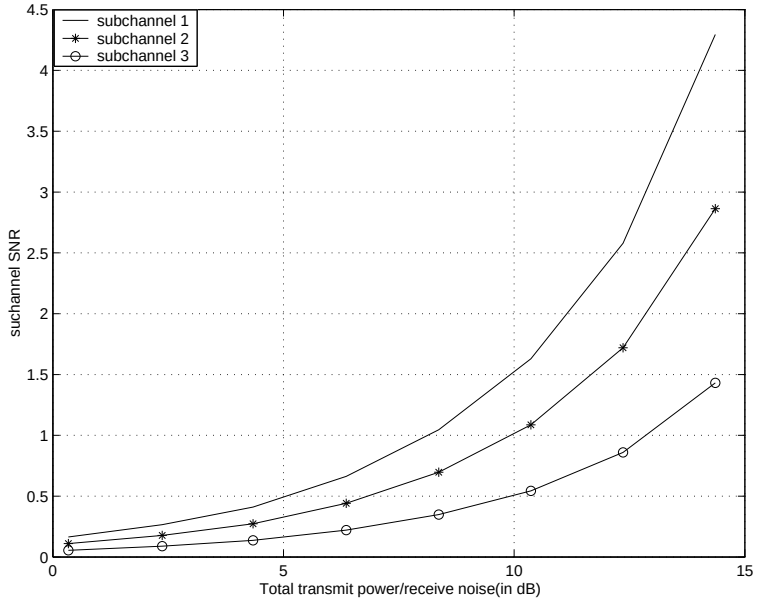

Figure 5.13: Subchannel SNR Performance of QoS Based Design

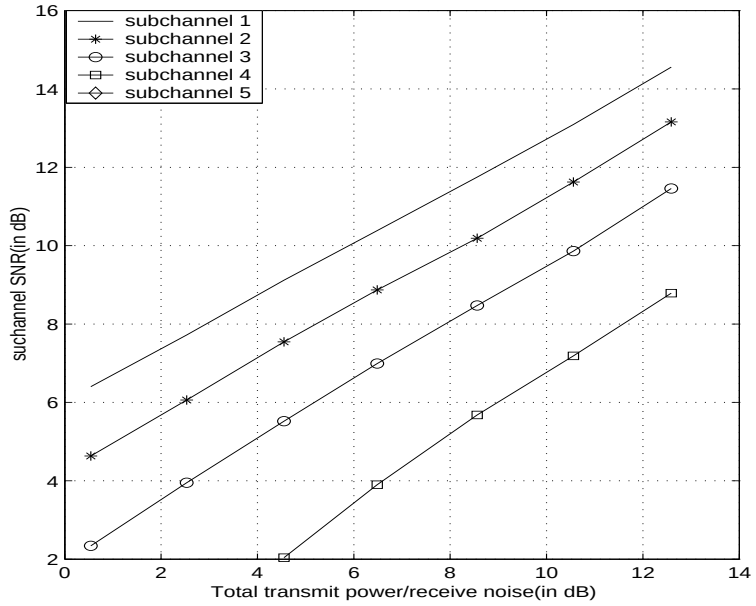

Figure 5.14: Subchannel SNR Performance of MMSE Design

minimum mean-squared error (MMSE-DFE) design and minimum bit error rate (MBER-DFE) design. The MBER-DFE design which is presented by us in Chapter 4 have good performances of information rate and bit error rate. It can maximize the information rate and minimize the bit error rate simultaneously. And we will show these results in details in the following subsections. We have the general form of the precoder matrix $\mathbf{F}$ as in Chapter 3, where $\mathbf{F} = \mathbf{X}\mathbf{\Gamma}_f$ and $\mathbf{\Gamma}_f$ is expressed as

$$\mathbf{\Gamma}_f = \left(\sqrt{\frac{p_0 + tr(\mathbf{Y}^{-1})}{tr(\mathbf{Y}^{-\frac{1}{2}})} \mathbf{Y}^{-\frac{1}{2}} - \mathbf{Y}^{-1}} \right)_+ \tag{5.8}$$

for the MMSE-DFE design. And for the MBER-DFE design, the $\mathbf{\Gamma}_f$ can be expressed as

$$\mathbf{\Gamma}_f = \left(\sqrt{\frac{p_0 + tr(\mathbf{Y}^{-1})}{M}} \mathbf{I} - \mathbf{Y}^{-1} \right)_+ \tag{5.9}$$

Moreover, the general form of decoder matrix $\mathbf{G}$ is expressed as in Chapter 4, where $\mathbf{G} \triangleq \mathbf{\Gamma}_g \mathbf{Y}^{-1} \mathbf{X}^H \mathbf{H}^H \mathbf{R}_{ww}^{-1}$, and for the MMSE-DFE design and MBER-DFE design, the $\mathbf{\Gamma}_g$ is shown as

$$\mathbf{\Gamma}_g = \mathbf{\Gamma}_f (\mathbf{Y}^{-1} + \mathbf{\Gamma}_f^2)^{-1} \tag{5.10}$$

5.3.1 Information Rate Performance

We consider two FIR channels: a_1 and a_2, and compute the information rate of the MMSE-DFE design and our MBER-DFE design, respectively. The transmitted symbol block size is $M = 7$. The tap coefficients of the channel a_1 and channel a_2 are $\{1, 0.5348 + 0.4494j, 0.3701j, -0.0515 + 0.0389j\}$ and $\{-0.0667 - 0.1824j,\ 0.3194 - 0.1801j,\ 0.4687 + 0.0399j, 0.0258 + 0.2870j\}$, respectively. The curves in Figure 5.15 and Figure 5.16 compare the information rates of the MMSE-DFE and MBER-DFE designs. We can deduce that the information rate of the MBER-DFE design outperforms the MMSE-DFE design. This is because for the MBER-DFE design we use Lagrangian method subject to the transmit power constraint to optimize the information rate and obtain a optimum precoder. The improvement of the information rates between the MBER-DFE design and MMSE-DFE design is around 0.2 *bit/symbol* when we use channel a_1. For channel a_2, the improvement

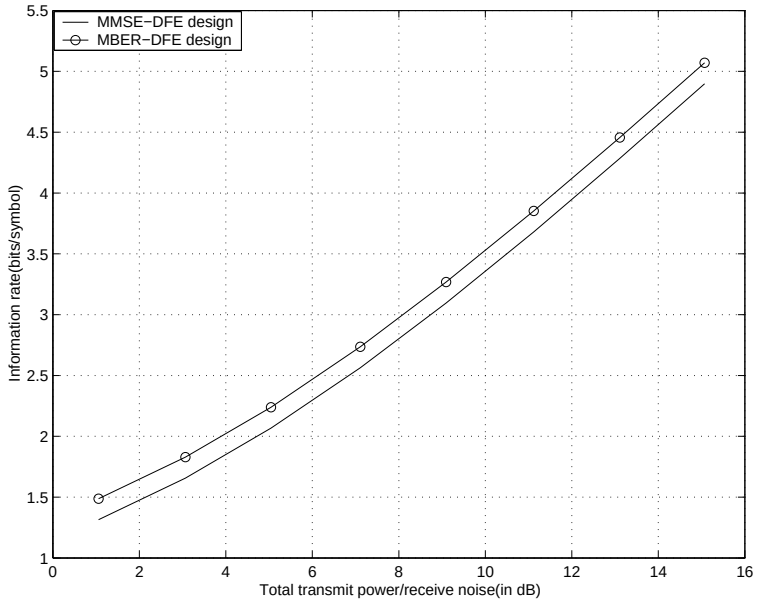

Figure 5.15: Information Rate Performance of MBER-DFE and ZF-DFE and MMSE-DFE Designs Using Channel a_1

is around 0.5 *bit/symbol* between MBER-DFE design and MMSE-DFE design. The improvement of the information rate will be more obvious when the channel becomes more frequency selective. Also, we can observe from Figure 5.15 and Figure 5.16 that the information rate increases much faster when we use channel a_1. This coincides with the previous simulation results that we obtain in the linear designs.

5.3.2 Bit Error Rate Performance

In order to compare the bit error rate performance, we consider several different channels which have different qualities and characteristics in order to allow us to analyze and show the performance improvement of the bit error

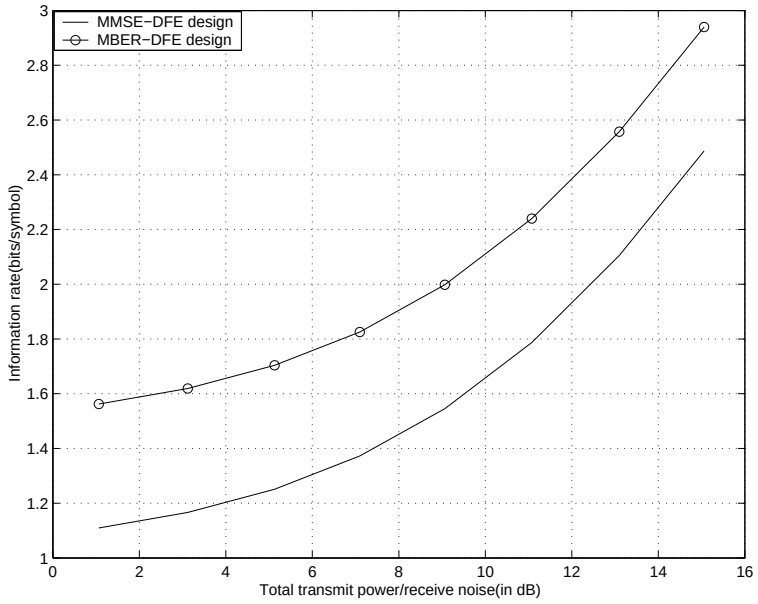

Figure 5.16: Information Rate Performance of MBER-DFE and ZF-DFE and MMSE-DFE Designs Using Channel a_2

rate between the MMSE-DFE design and our MBER-DFE design. In the following simulations, we will make the transmitted symbol block size $M = 32$. We will examine the BER performances using different FIR channels which have different tap coefficients. The model can provide some insight into our proposed MBER-DFE design.

Example 1: In this example, we examine the BER performance of the MMSE-DFE design and MBER-DFE design when the data blocks are transmitted over the channel a_1 with four tap coefficients $a_1 : \{1, 0.5348 + 0.4494j, 0.3701j, -0.0515 + 0.0389j\}$. The frequency response of channel a_1 is shown in Figure 5.4. Using the first channel a_1, Figure 5.17 compares the BERs of the MMSE-DFE and the MBER-DFE designs. We can observe that the bit error rate performance of MBER-DFE is better than the

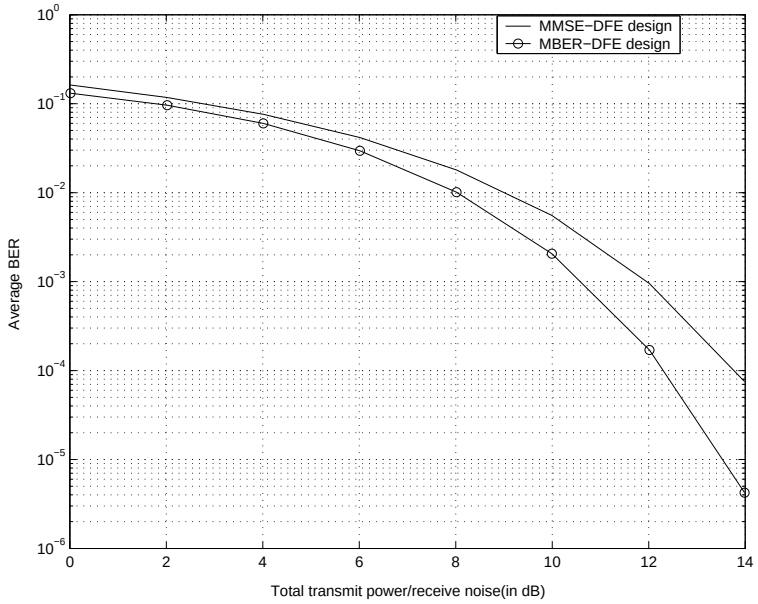

Figure 5.17: Bit Error Rate Performance of MBER-DFE and MMSE-DFE Designs for Channel a_1

MMSE-DFE design because we not only adopt MMSE criterion to minimize the BER but also choose the DFT matrix as the unitary matrix to ensure P_e to be a convex function and parameterize the precoder matrix. The DFT matrix in our MBER-DFE design is obtained from the eigenvalue decomposition of the channel matrix $\mathbf{H}$. It is different from the unitary matrix in MMSE-DFE design which is chosen as the identity matrix. The SNR gain for the MBER-DFE over MMSE-DFE at the BER of 10^{-4} is about 1.5 dB.

Example 2: We consider another third order FIR channel a_2, which have the tap coefficients as $a_2 : \{-0.0667 - 0.1824j,\ 0.3194 - 0.1801j, 0.4687 + 0.0399j, 0.0258 + 0.2870j\}$ and the frequency response of a_2 is shown in Figure 5.5. From Figure 5.5, we can observe that the range of frequency response of channel a_2 is around 13. Thus, it is much more frequency selective

than channel a_1. Figure 5.18 shows the BER curves of the MMSE-DFE and MBER-DFE designs. The SNR gain for the MBER-DFE over MMSE-DFE at the BER of 10^{-3} is around 4 dB. Comparing to Figure 5.17, the BER performance in Figure 5.18 becomes worse. It is because the channel becomes more frequency selective and the coherent bandwidth becomes smaller compared to the transmitted signal bandwidth. Then the signal will be distorted during transmission and the detection of symbol will also be affected. Thus, it will influence the BER performance. But we can see that our MBER-DFE design still outperforms the MMSE-DFE design. To explain the performance advantage of our MBER-DFE design, we recall from Chapter 4 that in order to minimize the BER, we need to maximize the matrix **GHF**, and we also note that our MBER-DFE design can make matrix **GHF** have equal diagonal elements while maximizing it. However, the MMSE-DFE design do not result in the product **GHF** has equal diagonal elements. This leads to different BER performances.

Example 3: In this example, we will consider a channel a_3 with tap coefficients $a_3 : \{0.6121, -0.5331 - 0.4481j, 0.369j, 0.0513 - 0.0388j\}$, and the channel order is $L = 3$. The frequency response of this channel is shown in Figure 5.19. From Figure 5.19, we can see that the ratio of the largest to the smallest frequency responses is around 8.75. It is more frequency selective than channel a_1 in Example 1, but it is less frequency selective than channel a_2 in example 2. Figure 5.20 shows the BER performance of the MMSE-DFE design and our MBER-DFE design. Similar to the previous examples, the MBER-DFE design shows clearly superior performance. The SNR gain of

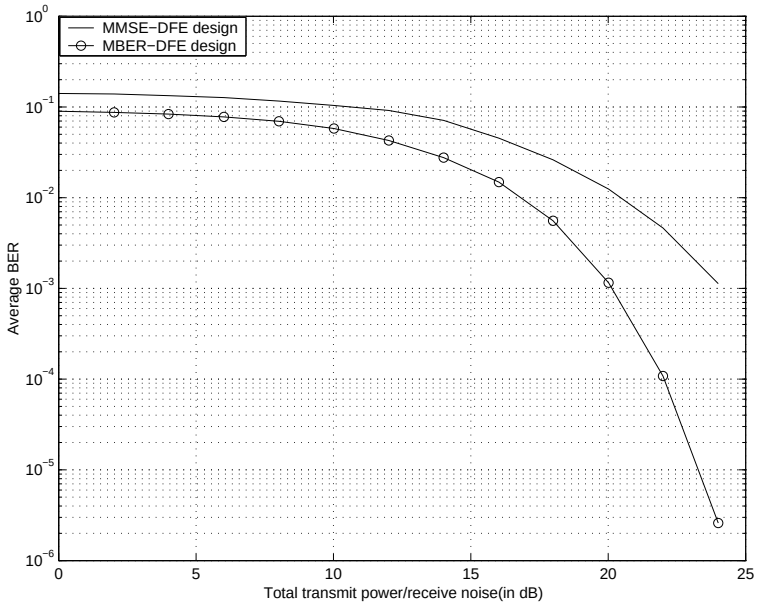

Figure 5.18: Bit Error Rate Performance of MBER-DFE and MMSE-DFE Designs for Channel a_2

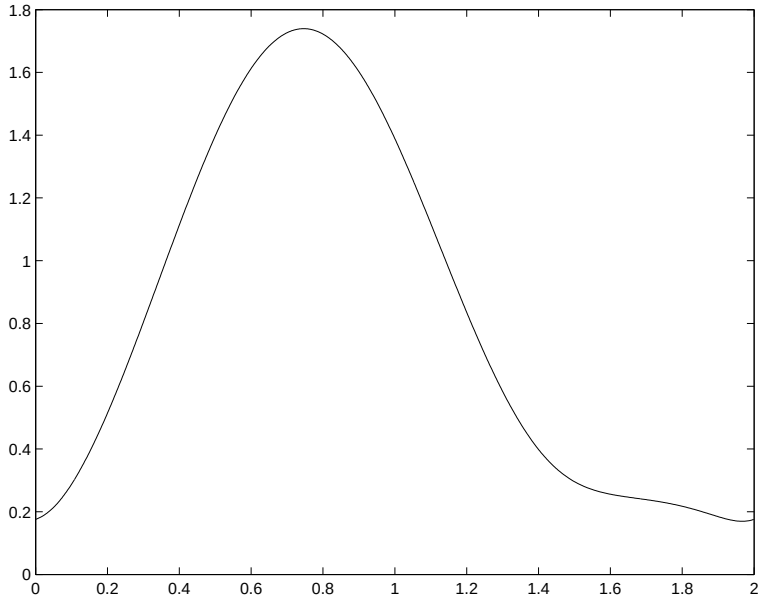

Figure 5.19: Frequency Response of Channel a_3

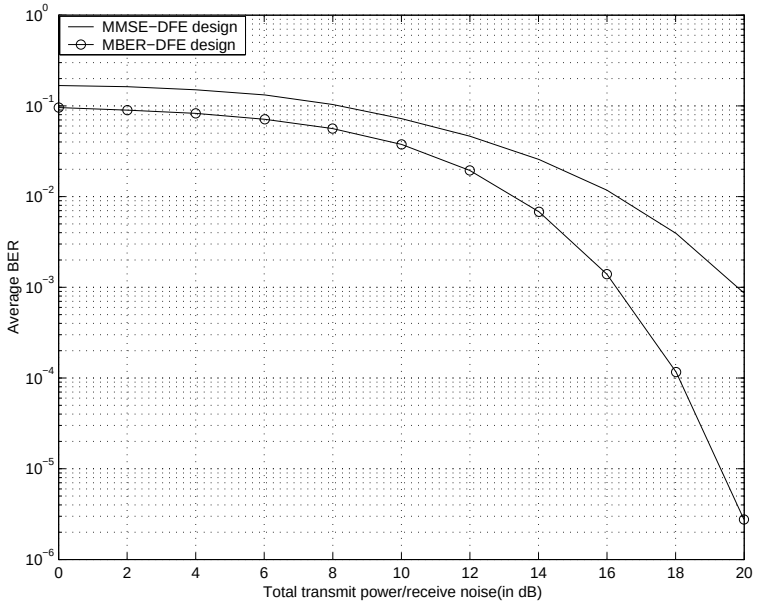

Figure 5.20: Bit Error Rate Performance of MBER-DFE and MMSE-DFE Designs for Channel a_3

the MBER-DFE design over MMSE-DFE design at the BER of 10^{-3} is about 3.7 dB in this case.

Example 4: In the previous examples, we examined the BER performances of various designs using three different FIR channels, which have different frequency selectivities, respectively. Now, we examine the average BER performance of the MMSE-DFE design and our MBER-DFE design over a class of randomly generated FIR channels. The transmitted symbol block size M is also equal to 32. The complex valued taps of the channels are generated independently from a zero-mean Gaussian distribution with unit variance. The channel order L is 3. The BER performance curves for MMSE-DFE and MBER-DFE over 5,000 channel realizations from this class are shown in Figure 5.21. These curves illustrate that the SNR gains

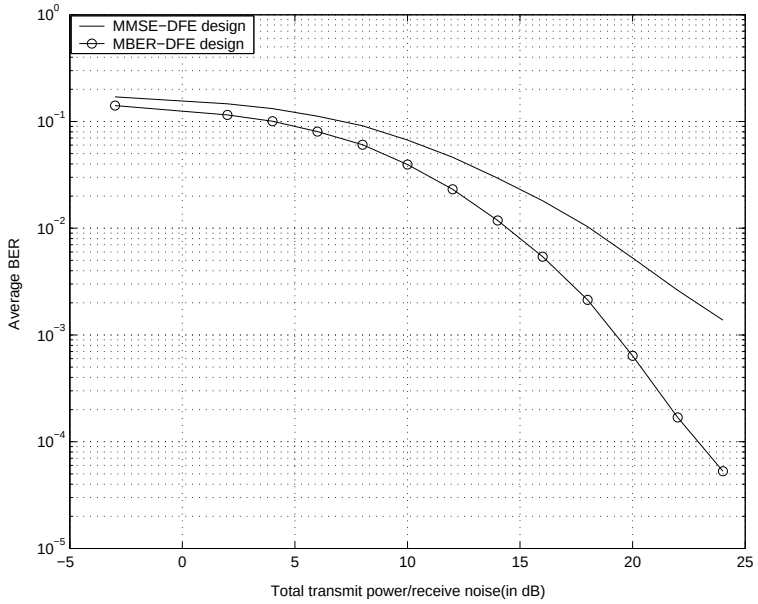

Figure 5.21: Bit Error Rate Performance of MBER-DFE and MMSE-DFE Designs for Randomly Generated Channel

of our MBER-DFE design over the MMSE-DFE design remain significant. We can see at the BER of 10^{-2} the SNR gain of our MBER-DFE over the MMSE-DFE is around 3.5 dB.

5.4 Summary

In this chapter, we have presented the simulation results of our various designs. Firstly, for linear schemes, it showed that we can obtain the maximum information rate design, minimum mean-squared error design and QoS based design by choosing the weight matrix $\mathbf{T}$ appropriately. From the simulation results we can see, our weighted information rate criterion generalized the linear precoder and decoder designs. Secondly, for nonlinear schemes, we

presented the information rate performance of our MBER-DFE design and the improvement of the information rate is apparent. We also compared the bit error rate performance of MBER-DFE and MMSE-DFE over different channels. The results indicate that our MBER-DFE design always has better BER performance, regardless of the channel frequency selectivity. And the more frequency selective the channel performed, the more obvious the SNR gain we observed of MBER-DFE design. In the next chapter, we will conclude our work in this thesis and discuss the future direction in this field.

Chapter 6

Conclusions and Future Work

6.1 Conclusions

In this thesis, we introduced the trends on wireless communications. Also, the concepts of channel coding, equalization and precoding techniques were presented. In order to have an ISI-free transmission, we could choose CP or ZP transmission method. In this thesis, we adopted the CP method to eliminate the ISI. We described the system model of linear and DFE-based nonlinear precoder and decoder and presented different kinds of designs. We also assumed that the channel state information was available at the transceiver end and the transmitted symbol and the noise were whitened and statistically independent. Information rate, mean-squared error and bit error rate performances for FIR channels were compared and summarized. Numerical results have also proved the improvements of our designs.

For linear precoder and decoder designs, we introduced a new criterion of weighted information rate. By maximizing the weighted information rate subject to the transmit power constraint, we could attain a general equation of the precoder matrix $\mathbf{\Gamma}_f$, which could be expressed by the weight matrix $\mathbf{T}$. It is a generalization of linear precoder and decoder design, from which we could obtain MMSE design, maximum information rate design and QoS based design by appropriately choosing the weight matrix $\mathbf{T}$. They could minimize the mean-squared error, maximize the information rate and deal with subchannels' relative SNRs, respectively. Simulation results confirmed the performance of the information rate of the MIR design. And we could also conclude that when the channel becomes more frequency selective, the information performance of MIR design over MMSE design becomes more obvious. In addition, the MSE performance of MMSE design was better than the MIR design and the difference becomes more obvious when the channel size increases. The SNR gain of the MMSE design over MIR design is considerable. Table 6.1 summarized the precoders and decoders of linear designs.

Table 6.1: Linear Precoders and Decoders

Designs	Precoder	Decoder
MIR	$\mathbf{\Gamma}_f = \left(\sqrt{\frac{p_0+tr(\mathbf{Y}^{-1})}{M}}\mathbf{I} - \mathbf{Y}^{-1}\right)_+$	$\mathbf{\Gamma}_g = \mathbf{\Gamma}_f^{-1}$ $\mathbf{\Gamma}_g = \mathbf{\Gamma}_f^H(\mathbf{Y}^{-1} + \mathbf{\Gamma}_f\mathbf{\Gamma}_f^H)^{-1}$
MMSE	$\mathbf{\Gamma}_f = \left(\sqrt{\frac{p_0+tr(\mathbf{Y}^{-1})}{tr(\mathbf{Y}^{-\frac{1}{2}})}\mathbf{Y}^{-\frac{1}{2}} - \mathbf{Y}^{-1}}\right)_+$	$\mathbf{\Gamma}_g = \mathbf{\Gamma}_f^H(\mathbf{Y}^{-1} + \mathbf{\Gamma}_f\mathbf{\Gamma}_f^H)^{-1}$
QoS Based	$\mathbf{\Gamma}_f = \left(\sqrt{\frac{p_0\mathbf{Q}\mathbf{Y}^{-1}}{tr(\mathbf{Y}^{-1}\mathbf{Q})}}\right)_+$	$\mathbf{\Gamma}_g = \mathbf{\Gamma}_f^H(\mathbf{Y}^{-1} + \mathbf{\Gamma}_f\mathbf{\Gamma}_f^H)^{-1}$

For DFE-based nonlinear precoder and decoder designs, we used La-

grangian method subject to the transmit power constraint to make the eigenvectors of the precoder matrix $\mathbf{F}$ match to the eigenvectors of the circulant channel matrix $\mathbf{H}$ in order to achieve the optimum information rate. The improvement of the information rates of our MIR-DFE design is more obvious when we use a more frequency selective channel which is consistent with the results of linear schemes. In addition, we also presented a new MBER-DFE design which could maximize the information rate and minimize the bit error rate concurrently. Firstly, using the MIR criterion, we obtained a design of MIR precoder, which can maximize the information rate. Then, the minimum BER was obtained by observing that the expression of BER was a convex function of the magnitude of the diagonal elements of the equalizer. A lower bound for the BER was derived. Using the MMSE criterion, we obtained a design of MMSE decoder that minimizes the lower bound, which could be called MBER decoder. It was parameterized by a unitary matrix and was obtained from special choice of the unitary matrix. In our thesis, we choose DFT matrix as the unitary matrix. In conclusion, it uses the $\mathbf{\Gamma}_f$ which can ensure that the information rate is maximized and adopts MMSE criterion and DFT matrix in order to obtain the minimum bit error rate. Simulation results proved that under the condition of channel a_1, whose range of frequency response is around 4, the SNR gain for our MBER-DFE over MMSE-DFE at the BER of 10^{-4} is about 1.5 dB. Subsequently, when the channel becomes more frequency selective, the SNR gain becomes more significant. When we use a randomly generated channel, the SNR gain at the BER of 10^{-2} becomes 3.5 dB.

6.2 Future Work

The nonlinear optimal design obtained in this thesis is for a transmission system with decision-feedback equalization and cyclic prefixed transmission method, white uncoded data, white noise and a known channel. The future work can be extended to various other schemes as the following:

1. We can use the zero padding transmission method instead of the cyclic prefixed method to eliminate the inter-block interference. In our chapter 2, we have introduced the principles of cyclic prefixed and zero padding transmission methods which are used to get rid of the IBI and the channel matrices of them have been presented. Comparing to cyclic prefixed method, zero padding can guarantee the symbol recovery and assures the FIR equalization of FIR channels regardless of the channel zero locations. It is more flexible than cyclic prefixed method because it can trade off equalization complexity with symbol detectability. Therefore, adopting zero padding transmission method in our designs can be one of our future work.

2. In our optimal designs, we assumed the noise to be whitened in order to simplify the analysis. Thus, the autocorrelation matrix of the noise is $\mathbf{R}_{ww} = \sigma^2\mathbf{I}$. In the future work, we can consider the colored noise instead of the white noise. We can use filters on the noise signals to alter the balance of frequency components so that the noise is no longer "white" but has some other qualities. In this case, the noise becomes a little more predictable than white noise, because we know that certain

frequencies will be more prominent. Thus, this can be another research topic in the future work.

3. We assume the channel state information is known at both the precoder and decoder sides in our work. In such scenario, our optimal precoder and decoder can appropriately take advantage of the channel state information and make use of the resources at best. However, we can extend our work to the channel which is imprecisely known at the precoder. In this case, the channel estimation technique is needed. We can use the precoding and decoding criterions in conjunction with different channel estimation methods to obtain the optimal designs and analyze the performances of information rate, mean-squared error and bit error rate. We need to do a lot research work in this field in the future.

4. Currently, we are using precoding and decoding techniques and restrict them to single-input, single-output (SISO) block transmission systems. However, consideration of how should we extend our designs to a multi-input, multi-output (MIMO) system will also become a future research topic.

Bibliography

[1] T. S. Rappaport, *Wireless Communications Principles and Practice, second Edition*, Prentice Hall, 2002.

[2] S. G. Wilson, *Digital Modulation and Coding,* Prentice Hall, 1998.

[3] S. S. Chan, T. N. Davidson and K. M. Wong, "Asymptotically Minimum Bit Error Rate Block Precoders For Minimum Mean Square Error Equalization," *IEEE Sensor Array and Multichannel Signal Processing Workshop Proceedings*, pp.140-144, Aug. 2002.

[4] J. A. C. Bringham, "Multicarrier Modulation for Data Transmission: An Idea Whose Time Has Come", *IEEE Commun. Mag.*, vol.28, pp.5-14, May 1990.

[5] J. S. Chow, J. C. Tu and J. M. Cioffi, "Performance Evaluation of A Multichannel Transceiver System For ADSL and VHDSL Services," *IEEE J. Select. Areas Commun.*, vol.9, pp.909-919, Aug. 1991.

[6] A. Scaglione, G. B. Giannakis and S. Barbarrossa, " Redundant-Filterbank Precoders and Equalizers Part II: Blind Channel Estimation,

Synchronization and Direct Equalization," *IEEE Trans. Signal Processing*, vol.47, pp.2007-2022, Jul. 1999.

[7] A. Scaglione, S. Barbarossa and G. B. Giannakis, "Filterbank Transceivers Optimizing Information Rate in Block Transmissions Over Dispersive Channels," *IEEE Trans. Inform. Theory*, vol.45, pp.1019-1032, Apr. 1999.

[8] A. Ruiz, J. M. Cioffi and S. Kastuia, "Discrete Multiple Tone Modulation With Coset Coding For The Spectrally Shaped Channel," *IEEE Trans. Commun.*, vol.40, pp.1012-1029, Jun. 1992.

[9] T. Wiegand, N. J. Fliege, "Orthogonal Multiple Carrier Data Transmission," *Eur. Trans. Telecommun.*, vol.3, pp.35-44, May 1992.

[10] A. Scaglione, G. B. Giannakis and S. Barbarrossa, "Redundant-Filterbank Precoders and Equalizers Part I: Unification and Optimal Designs," *IEEE Trans. Signal Processing*, vol.47, pp.1988-2006, Jul. 1999.

[11] J. Proakis, "Adaptive Equalization For TDMA Digital Mobile Radio," *IEEE Trans. Vehicular Technology*, vol.40, pp.333-341, May 1991.

[12] Z. Wang and G. B. Giannakis, "Wireless Multicarrier Communications," *IEEE Signal Processing Mag.*, pp.29-48, May 2002.

[13] G. B. Giannakis, "Filterbank For Blind Channel Identification and Equalization," *IEEE Signal Processing Letter*, vol.4, pp.184-187, Jun. 1997.

[14] T. Cover and J. Thomas, *Elements of Information Theory*, New York: Wiley, 1991.

[15] G. J. Foschini, "Layered Space-time Architecture For Wireless Communication in A Fading Environment When Using Multielement Antennas," *Bell Labs, Tech. J.*, vol.1, pp.41-59, 1996.

[16] T. L. Marzetta and B. M. Hochwald, "Capacity of A Mobile Multiple-antenna Communication Link in Rayleigh Flat Fading," *IEEE Trans. Inform. Theory*, vol.45, pp.139-157, Jan. 1999.

[17] A. Naguib, V. Tarokh, N. Seshadri and A. R. Calderbank, "A Space-time Coding Modem For High-data-rate Wireless Communication," *IEEE J. Select Areas Commun.*, vol.16, pp.1459-1478, Oct. 1998.

[18] G. G. Raleigh and J, M. Cioffi, "Spatio-temporal Coding For Wireless Communications," *IEEE Trans. Commun.*, vol.46, pp.357-366, Mar. 1998.

[19] A. Stamoulis, G. B. Giannakis and A. Scaglione, "Self-recovering Transceivers For Block Transmissions: Filterbank Precoders and Decision-Feedback Equalizers," *IEEE Signal Processing Workshop on Signal Processing Advances in Wireless Communications, SPAWC'99*, pp.243-246, May 1999.

[20] G. G. Raleigh and V. K. Jones, "Multivariate Modulation and Coding For Wireless Communication," *IEEE J. Select Areas Commun.*, vol.17, pp.851-866, May 1999.

[21] J. G. Proakis, *Digital Communications, fourth Edition*, McGraw Hill, 2001.

[22] A. Stamoulis, Wei Tang and G. B. Giannakis, "Information Rate Mixiimizing FIR Transceivers: Filterbank Precoders and Decision-Feedback Equalizers For Block Transmissions Over Dispersive Channels," *IEEE Global Telecommunications Conference, 1999. GLOBECOM'99*, vol.4, pp.2142-2146, 1999.

[23] Yulin Liu and Qicong Peng, "A New Method of Joint Filterbank Precoders and Decision Feedback Equalizers Optimization Over Dispersive Channels," *EUROCON'2001, Trends in Commun., International Conference on*, vol.2, pp.528-531, Jul. 2001.

[24] H. Sampath, P. Stoica and A. Paulraj, "Generalized Linear Precoder and Decoder Design For MIMO Channels Using the Weighted MMSE Criterion," *IEEE Trans. Commun.*, vol.49, pp.2198-2206, Dec. 2001.

[25] V. Tarokh, A. Naguib, N. Seshadri and A. R. Calderbank, "Combined Array Processing and Space-time Coding," *IEEE Trans. Inform. Theory.*, vol.45, pp.1121-1128, May 1999.

[26] S. Barbarossa and A. Scaglione, "Theoretical Bounds On the Estimation And Prediction of Multipath Time-varying Channels," *in Proc. Int. Conf. Acoust. Speech, Signal Process., Istanbul, Turkey*, Jun. 2000.

[27] A. Scaglione, P. Stoica, S. Barbarossa, G. B. Giannakis and H. Sampath, "Optimal Designs for Space-time Linear Precoders and Decoders," *IEEE Trans. Signal Processing*, vol.50, pp.1051-1064, May 2002.

[28] A. Mertins, "MMSE Design of Redundant FIR Precoders For Arbitrary Channel Lengths," *IEEE Trans. Signal Processing*, vol.51, pp.2402-2409, Sep. 2003.

[29] G. J. Foschini and M. J. Gans, "On Limits of Wireless Communications in A Fading Multipath Environment When Using Multiple Antennas," *Wireless Pers. Commun.*, vol.6, pp.311-335, Mar. 1998.

[30] Yanwu Ding, T. N. Davidson, Zhiquan Luo and K. M. Wong, "Minimum BER Block Precoders For Zero-Forcing Equalization," *IEEE Trans. Signal Processing*, vol.51, pp.2410-2423, Sep. 2003.

[31] J. M. Cioffi, G. P. Dudevoir, M. V. Eyuboglu and G. D. Forney, "MMSE Decision-Feedback Equalizers and Coding-Part I: Equalization Results," *IEEE Trans. Commun.*, vol.43, pp.2582-2594, Oct. 1995.

[32] A. Stamoulis, G. B. Giannakis and A. Scaglione, "Block FIR Decision-Feedback Equalizers for Filterbank Precoded Transmissions With Blind Channel Estimation Capabilities," *IEEE Trans. Commun.*, vol.49, pp.69-83, Jan. 2001.

[33] N. Al-Dhahir and J. M. Cioffi, "Block Transmission Over Dispersive Channels: Transmit Filter Optimization and Realization, And MMSE-DFE Receiver Performance," *IEEE Trans. Inform. Theory*, vol.42, pp.137-160, Jan. 1996.

[34] Yuanpei Lin, See May Phoong, "BER Minimized OFDM Systems with Channel Independent Precoders," *IEEE Trans. Signal Processing*, vol.51, pp.2369-2380, Sep. 2003.

[35] J. S. Chow, J. C. Tu and J. M. Cioffi, "A discrete multitone transceiver system for HDSL applications," *IEEE J. Select. Areas Commun.*, pp.895-908, Aug. 1991.

[36] G. D. Forney, Jr. and M. V. Eyuboglu, "Combined Equalization and Coding Using Precoding," *IEEE Commun. Mag.*, pp.25-34, Dec. 1991.

[37] J. Yang and S. Roy, "On Joint Transmitter and Receiver Optimization for Multiple-Input-Multiple-Output (MIMO) Transmission Systems," *IEEE Trans. Inform. Theory*, vol.42, pp.3221-3231, Sep. 1994.

[38] S. Kasturia, J. T. Aslanis and J. M. Cioffi, "Vector Coding for Partial Response Channels," *IEEE Trans. Inform. Theory*, vol.36, pp.741-761, July 1990.

[39] B. Muquet, Z. D. Wang, G. B. Giannakis, M. Courville and P. Duhamel, "Cyclic Prefixing or Zero Padding for Wireless Multicarrier Transmissions," *IEEE Trans. Commun.*, vol.50, pp.2136-2148, Dec. 2002.

[40] A. Goldsmith and S. G. Chua, "Adaptive coded modulation for fading channels," *IEEE Trans. Commun.*, vol.46, pp.595-602, May 1998.

Appendix A

Proof of Jensen's Inequality

Here we introduce and prove Jensen's inequality.

Jensen's inequality is expressed as: If f is a convex function on the interval $[a, b]$, then

$$f\Big(\sum_{k=1}^{n} \lambda_k x_k\Big) \leq \sum_{k=1}^{n} \lambda_k f(x_k) \tag{A.1}$$

where $0 \leq \lambda_k \leq 1$, $\lambda_1 + \lambda_2 + ... + \lambda_n = 1$ and each $x_k \in [a, b]$. If f is a concave function, the inequality is reversed.

There is another formulation of Jensen's inequality used in probability.

Let X be some random variable, and let $f(x)$ be a convex function(defined at least on a segment containing the range of X). Then the expected value of $f(x)$ is at least the value of f at the mean of X:

$$E\Big(f(x)\Big) \geq f\Big(E(x)\Big) \tag{A.2}$$

Proof: We prove the equivalent formulation. Let X be some random variable, and let $f(x)$ be a convex function(defined at least on a segment containing the range of X).

Let $c = E(X)$. Since $f(x)$ is convex, there exists a supporting line for $f(x)$ at c:

$$\varphi(x) = \alpha(x - c) + f(c) \tag{A.3}$$

for some α, and $\varphi(x) \leq f(x)$. Then

$$E\Big(f(X)\Big) \geq E\Big(\varphi(X)\Big) = E\Big(\alpha(X - c)\Big) + f(c) = f(c) \tag{A.4}$$

as claimed.

Appendix B

Proof of Lemma 1 in [30]

Since $\mathbf{V}$ is a unitary matrix, we can get $tr(\mathbf{V}^H\mathbf{E}\mathbf{V}) = tr(\mathbf{A})$. In addition, the diagonal elements of $\mathbf{E}$ and $\mathbf{V}^H\mathbf{E}\mathbf{V}$ are non-negative because $\mathbf{E}$ is positive semidefinite. We know that for a sequence of length N with non-negative numbers $\{x_i\}_{i=1}^N$, which $\sum_{i=1}^N x_i = y$, the sequence which maximize the minimum value of x_i is $x_i = y/N$. Applying this result to the left hand side of Eqn.(B.1) and observing that the constraint on $\mathbf{V}$ may restrict the values that the diagonal elements of $\mathbf{V}^H\mathbf{E}\mathbf{V}$ can take on, we have

$$\max_{\mathbf{V}\mathbf{V}^H=\mathbf{I}} \min[\mathbf{V}^H\mathbf{E}\mathbf{V}]_{mm} = tr(\mathbf{E})/M \tag{B.1}$$

Let $\mathbf{V} = \mathbf{\Phi}\mathbf{L}$, where $\mathbf{L}$ is also a unitary matrix. Then we have

$$[\mathbf{V}^H\mathbf{E}\mathbf{V}]_{mm} = [\mathbf{L}^H\mathbf{T}\mathbf{L}]_{mm} = \sum_{i=1}^{M} t_i |l_{mi}|^2 \tag{B.2}$$

where t_i is the i^{th} diagonal element of $\mathbf{T}$ and l_{mi} is the $(m,i)^{th}$ element of $\mathbf{L}$. If $\mathbf{L}$ is chosen to be the normalized DFT matrix, then since the magnitude of each element of the DFT matrix is equal to $|l_{mi}|^2 = 1/M$, we have that

$$[\mathbf{V}^H\mathbf{E}\mathbf{V}]_{mm} = \sum_{i=1}^{M} t_i \frac{1}{M} = \frac{tr(\mathbf{E})}{M}, \quad \text{for all } 1 \leq m \leq M \tag{B.3}$$

and hence the proof.

Appendix C

Proof of Eqn.(3.37)

Referring to the Eqn.(3.36) in Chapter 3, we can obtain the Lagrangian equation which maximizing the weighted information rate subject to the transmit power constraint as following

$$\mathcal{L} = \frac{t_{ii}}{M} \sum_{i=1}^{M} \log_2(1 + y_{ii}|\gamma_{f,ii}|^2) - \mu(\sum_{i=1}^{M} |\gamma_{f,ii}|^2 - p_0) \tag{C.1}$$

We differentiate Eqn.(C.1) with respect to $|\gamma_{f,ii}|^2$ and let the result equal to zero and can obtain

$$\frac{y_{ii}t_{ii}}{M} \cdot \frac{1}{1 + y_{ii}|\gamma_{f,ii}|^2} \cdot \log_2 e - \mu = 0 \tag{C.2}$$

$$\Rightarrow \frac{\mu M}{y_{ii}t_{ii} \log_2 e} = \frac{1}{1 + y_{ii}|\gamma_{f,ii}|^2} \tag{C.3}$$

$$\Rightarrow y_{ii}|\gamma_{f,ii}|^2 = \frac{y_{ii}t_{ii}\log_2 e}{\mu M} - 1 \tag{C.4}$$

$$\Rightarrow |\gamma_{f,ii}|^2 = \frac{t_{ii}\log_2 e}{\mu M} - y_{ii}^{-1} \tag{C.5}$$

and hence the proof is concluded.

Appendix D

Proof of Eqn.(4.14)

Referring to Eqn.(4.12) in Chapter 4, we can obtain the following Lagrangian equation which maximize the information rate subject to the transmit power constraint as following

$$\mathcal{L} = \frac{1}{M}\sum_{i=1}^{M}\log_2(1 + y_{ii}|\gamma_{f,ii}|^2) + \mu(p_0 - \sum_{i=1}^{M}|\gamma_{f,ii}|^2) \tag{D.1}$$

Therefore, making use of the properties of logarithm, we differentiate Eqn.(D.1) with respect to $|\gamma_{f,ii}|$ and let the result equal to zero. We can obtain the following expressions

$$\frac{\partial\mathcal{L}}{\partial|\gamma_{f,ii}|} = 0 = \frac{1}{M}\cdot\frac{2y_{ii}|\gamma_{f,ii}|\log_2 e}{1 + y_{ii}|\gamma_{f,ii}|^2} - 2\mu|\gamma_{f,ii}| \tag{D.2}$$

$$\Rightarrow 2\mu|\gamma_{f,ii}| = \frac{1}{M}\cdot\frac{2y_{ii}|\gamma_{f,ii}|\log_2 e}{1 + y_{ii}|\gamma_{f,ii}|^2} \tag{D.3}$$

$$\Rightarrow \mu = \frac{1}{M} \cdot \frac{y_{ii} \log_2 e}{1 + y_{ii}|\gamma_{f,ii}|^2} \tag{D.4}$$

$$\Rightarrow \mu = \frac{1}{M} \cdot \frac{y_{ii} \log_2 e}{1 + y_{ii}|\gamma_{f,ii}|^2} \tag{D.5}$$

$$\Rightarrow |\gamma_{f,ii}|^2 = \frac{\log_2 e}{\mu M} - y_{ii}^{-1} \tag{D.6}$$

We substitute Eqn.(D.6) into the equation of transmit power which is defined in Eqn.(4.11) and can obtain

$$\sum_{i=1}^{M} |\gamma_{f,ii}|^2 = p_0 = \sum_{i=1}^{M} \left(\frac{\log_2 e}{\mu M} - y_{ii}^{-1} \right) \tag{D.7}$$

$$\Rightarrow \frac{\log_2 e}{\mu M} tr(\mathbf{I}) - tr(\mathbf{Y}^{-1}) = p_0 \tag{D.8}$$

Since $\mathbf{I}$ is a $M \times M$ identity matrix, $tr(\mathbf{I}) = M$, thus Eqn.(D.8) can be written as

$$\frac{\log_2 e}{\mu} - tr(\mathbf{Y}^{-1}) = p_0 \tag{D.9}$$

$$\Rightarrow \mu = \frac{\log_2 e}{p_0 + tr(\mathbf{Y}^{-1})} \tag{D.10}$$

and hence the proof is concluded.